# Quality Assurance of 3D prints

## The development of a low cost test & Investigating the influence of temperature and humidity on print quality

by

D. Drexhage

to obtain the degree of Master of Science
at the Delft University of Technology.

Student numbers: 4224760
Supervisors: Prof. ir. Jenny Dankelman
Prof. ir. René Delfos

TU Delft

# Contents

**List of Figures** 1

**List of Tables** 2

**Abbreviations** 3

**Symbols** 5

**1 Introduction** 7

1.1 Surgical care in low and middle-income countries . . . 7
1.1.1 Increase in non-communicable diseases . . . 7
1.1.2 Limited access to surgical care . . . 7
1.1.3 Production in high-income countries . . . 8
1.2 Solving the problem of access to affordable surgical care in LMICs . . . 8
1.2.1 The potential of 3D printing . . . 8
1.3 Objectives . . . 9

**2 Design a home-made test** 10

2.1 Context and Requirements . . . 10
2.1.1 Individual . . . 11
2.1.2 Physical Environment . . . 11
2.1.3 Systems and structures . . . 14
2.1.4 Technical . . . 15
2.1.5 Requirements . . . 16
2.2 State of the art . . . 17
2.2.1 Non-Destructive Testing . . . 17
2.2.2 Destructive Testing . . . 19

2.3 Designing the Test . . . 23
2.3.1 Frame . . . 24
2.3.2 Actuator . . . 25
2.3.3 Strain measurement . . . 25
2.3.4 Load measurement . . . 26
2.3.5 Building the set-up . . . 26
2.4 Validating the test . . . 28
2.4.1 Method . . . 28
2.4.2 Results . . . 29
2.4.3 Discussion . . . 31
2.4.4 Conclusion . . . 31
2.5 Discussion . . . 32
2.5.1 Context-specific validation . . . 32
2.5.2 Cost-benefit consideration . . . 32
2.5.3 Multiple mechanical properties . . . 32
2.5.4 The actual print . . . 33

**3 Influence of Temperature and Humidity 34**
3.1 Influence of increasing temperature and relative humidity on print quality during storage of filament and 3D-printing on the final print quality . . . 35
3.1.1 Method . . . 36
3.1.2 Results . . . 37
3.1.3 Conclusion . . . 43
3.2 Influence of increasing temperature and relative humidity on print quality during storage of the final print prior to and while testing the print quality . . . 44
3.2.1 Method . . . 44
3.2.2 Results . . . 45
3.2.3 Conclusion . . . 48
3.3 Discussion . . . 48

**4 Discussion 49**
4.1 Limitations . . . 49
4.2 Recommendations . . . 50

**A Building the test 51**
A.1 Part list . . . 51
A.2 Tool list . . . 52
A.3 Assembly . . . 52
A.3.1 3D printing . . . 52
A.3.2 Drilling the holes . . . 52
A.3.3 Lower bar . . . 54
A.3.4 Middle bar . . . 55
A.3.5 Assembly . . . 56
A.4 Electronics . . . 57
A.5 Software . . . 58
A.5.1 Installing the software . . . 58
A.5.2 Installing software packages . . . 59
A.5.3 Writing the code . . . 60

**B Fused deposition modeling 67**
B.1 Fused deposition modeling technique . . . 67
B.1.1 The print process . . . 67
B.1.2 Dimensional deviations . . . 67
B.1.3 Printing with support . . . 67
B.2 Bond Formation . . . 68

**C What should be tested? 73**
C.1 Compare with existing products . . . . . 73
C.2 New design . . . . . 74
C.3 Probability and consequences of failure with corresponding risk . . . . . 76

**Bibliography 78**

# List of Figures


2.1 A possible tensile test using weights to apply force and a ruler to measure elongation . . . . . 20
2.2 Tensile test using a bucket which can be filled with water to apply force and a gauge to measure elongation . . . . . 20
2.3 A possible bending test using a bucket which can be filled with water to apply force and a gauge to measure elongation . . . . . 20
2.4 A possible impact test using a pendulum to apply force . . . . . 21
2.5 A possible fatigue test, testing fatigue impact properties using a motor for rotation . . . . . 21
2.6 A possible fatigue test, testing fatigue bending properties using a motor for rotation . . . . . 21
2.7 Low-cost tensile test designed by Schindler and Veidt . . . . . 22
2.8 Low-cost tensile test and creep designed by Momoh et al. . . . . 22
2.9 The Open-Pull test designed by Hermann . . . . . 23
2.10 The test set-up designed by Amend Jr and Lipson . . . . . 23
2.11 Aperture-adjustment knob from the catalog of the Kijenzi print lab [5]. . . . . 24
2.12 Bed net connector from the catalog of the Kijenzi print lab [5]. . . . . 24
2.13 Aluminium beam for frame . . . . . 24
2.14 Different load cells for load measurement . . . . . 26
2.15 The test set-up . . . . . 27
2.16 Dimensions of the test specimen for bending according to ASTM D790. . . . . 28
2.17 Average $F_{max}$ of the specimens tested with different test set-ups. . . . . 30
2.18 Average maximum bending strength of the specimens tested with different test set-ups. . . . . 30
2.19 Average Elastic Modulus of the specimens tested with different test set-ups. . . . . 31
2.20 Simultaneously print the intended product and the test strip . . . . . 33

3.1 Dimensions of the test specimen for bending according to ASTM D790. . . . . 36
3.2 Adhesion to the build plate at $20^oC$ and a relative humidity of 70% . . . . . 38
3.3 Adhesion to the build plate at $35^oC$ and a relative humidity of 70% . . . . . 38
3.4 Adhesion to the build plate at $40^oC$ and a relative humidity of 70% . . . . . 38
3.5 Adhesion to the build plate at $20^oC$ and a relative humidity of 50, 70 and 90% . . . . . 38
3.6 Adhesion to the build plate at $35^oC$ and a relative humidity of 50, 70 and 90% . . . . . 38
3.7 Adhesion to the build plate at $40^oC$ and a relative humidity of 50, 70 and 90% . . . . . 38
3.8 Adhesion to the build plate compared to absolute humidity (g $H_2O$/kg air) . . . . . 39
3.9 Average weight of the specimens produced with material stored for 24 hours at these absolute humidity conditions. . . . . 40
3.10 $F_{max}$ of the specimen for different storage conditions. . . . . 41
3.11 Bending strength of the specimen for different storage conditions. . . . . 42
3.12 Elastic modulus of the specimen for different storage conditions. . . . . 43
3.13 $F_{max}$ of specimens manufactured at several specific humidity and temperature conditions for different testing conditions. . . . . 46
3.14 Bending strength of specimens manufactured at several specific humidity and temperature conditions for different testing conditions. . . . . 47
3.15 Elastic modulus of specimens manufactured at several specific humidity and temperature conditions for different testing conditions. . . . . 47

A.1 Schematics Electronics . . . . . 57

B.1 Schematic visualization of the fused deposition modeling setup. . . . . 68
B.2 The FDM printed product . . . . . 69

# List of Tables


2.1 Overview of existing test set-ups . . . 23
2.2 Options for frame . . . 24
2.3 Options for strain measurement . . . 25
2.4 Constant printer settings used for creating the specimen sets. . . . 28
2.5 Specimen batches created for different tests. . . . 29
2.6 t-score $F_{max}$ comparing the home-made test set-up and the conventional Zwick/Roell test . . . 30
2.7 t-score maximum bending strength comparing the home-made test set-up and the conventional Zwick-Roell test . . . 30
2.8 t-score elastic modulus comparing the home-made test set-up and the conventional Zwick/Roell test . . . 31

3.1 Temperatures and relative humidity at which the filament is stored 24 hours before printing and at which the print is created. . . . 36
3.2 Constant printer settings used for creating the specimen sets. . . . 37
3.3 'Dry' and wet weight, with corresponding estimated Glass Transition Temperature (Tg) for the wet specimen. . . . 45

A.1 Part list . . . 51
A.2 Tool list . . . 52

B.1 Viscosity values for ABS P400 . . . 72

C.1 The likelihood and consequences of failure . . . 76
C.2 Risk factor . . . 77

# Abbreviations

**3DP** 3D Printing
**ABS** Acrylonitrile Butadiene Styrene
**AM** Additive Manufacturing
**ANOVA** Analysis of Variance
**ASTM** American Society for Testing and Material
**BJ** Binder Jetting
**BoP** Bottom of the Pyramid
**CDs** communicable diseases
**CIJ** Continuous Inkjet
**DALYS** Disability-Adjusted Life Years
**DED** Direct Energy Deposition
**DMLS** Direct Metal Laser Sintering
**DOD** Drop On Demand
**EBAM** Electron Beam Additive Manufacturing
**EBM** Electron Beam Melting
**FDM** fused deposition modeling
**FEA** Finite Element Analysis
**FEM** Finite Element Method
**GBD** Global Burden of Disease
**GPD** gross domestic product
**HICs** high-income countries
**IHME** Institute for Health Metrics and Evaluation
**ISO** international organization for standardization
**LENS** laser engineered net shaping
**LMICs** low- and middle-income countries
**LOM** laminated object manufacturing
**LPS** liquid-phase sintering
**Mw** Molecular Weight
**ME** material extrusion
**MJ** material jetting
**mLS** metal laser sintering
**MTRH** Moi Teaching and Referral Hospital
**NCDs** non-communicable diseases
**NPJ** Nanoparticle Jetting
**PA** Polyamide/Nylon
**PA(12)** Polyamide/Nylon
**PBF** Powder Bed Fusion
**PEEK** Polyether Ether Ketone

**PET** Polyethylene
**PETG** Glycol Modified Polyethylene
**PLA** Polylactic Acid
**PLGA** Poly(Lactide-Co-Glycolide)
**pLS** Polymer Laser Sintering
**PP** Polypropylene
**PS** Polystyrene
**QA** quality assurance
**RH** Relative Humidity
**SL** Sheet Lamination
**SLA** Stereolithography
**SLM** Selective Laser Melting
**SLS** Selective Laser Sintering
**SSA** Sub-Saharan Africa
**Tg** Glass Transition Temperature
**UC** Ultrasonic Consolidation
**UTS** Ultimate Tensile Strength
**VOC** Volatile Organice Carbon
**VP** Vat Photopolymerization
**WHO** World Health Organization
**YLD** Years Lost due to Disability
**YLL** Years of Life Lost

# Symbols

| | |
|---|---|
| $A$ | Cross-Sectional Area |
| $c$ | Specific Heat |
| $D_N$ | Nozzle Diameter |
| $\delta$ | Mid-Span Deflection |
| $\epsilon$ | Strain |
| $\dot{\epsilon}$ | Strain Rate |
| $\epsilon_f$ | Ductility, strain till fracture |
| $E$ | Tensile / Young's Modulus |
| $E_f$ | Flexural Modulus |
| $\eta$ | Viscosity |
| $F$ | Applied Force / Fracture Force |
| $g$ | Gravitational Constant |
| $\Gamma$ | Surface Tension Coefficient |
| $h$ | Convection with the Air (and Conduction with the Foundation) |
| $H_L$ | Layer Thickness |
| $\Delta h$ | Height Difference |
| $I$ | Moment of Inertia |
| $k$ | Conduction Through the Filament |
| $K$ | Shear Modulus |
| $L$ | Length |
| $L_0$ | Initial Length |
| $m$ | Mass / Constant / Slope of Load-Displacement Curve |
| $M$ | Applied Moment |
| $P$ | Perimeter |
| $r$ | Radius |
| $r_0$ | Initial Radius |
| $S$ | Cross-Sectional Area |
| $\sigma$ | Stress |
| $\sigma_{max}$ | Maximum Stress |
| $\sigma_t$ | Tensile Stress / Strength |
| $\sigma_y$ | Yield Strength |
| $t$ | Time |
| $T$ | Temperature |
| $T_\infty$ | Temperature of Environment |
| $T_N$ | Nozzle/Extrusion Temperature |
| $\frac{d\theta}{dt}$ | Dimensionless Neck Growth with Time |
| $\frac{d\theta}{dT}$ | Dimensionless Neck Growth with Temperature |
| $U$ | Impact Energy |
| $v$ | Velocity |
| $V$ | Volume |
| $V_E$ | Extrusion Velocity |
| $V_F$ | Filling Velocity |
| $\omega$ | Road Width |
| $W_s$ | Work of Surface Tension |
| $W_v$ | Work of Viscous Forces |
| $y$ | Half-Length of Neck |
| $y_m$ | Maximal Distance From Neutral Axis |
| $Z_c$ | Elastic Section Modulus |

# Abstract

Low- and middle-income countries are facing a growing burden of non-communicable diseases, which require surgical interventions. However, the lack of (functioning) medical equipment is hindering access to surgical care in these countries. 3D printing has the potential to provide a solution to this problem, but ensuring the quality of 3D-printed medical products is a challenge that needs to be addressed.
The objectives of this master thesis are twofold:

1. To design a low-cost and easy-to-use test that can be used in low- and middle-income countries to ensure the quality of 3D printed parts.
   *Method:* First of all the requirements for the test method were drafted, thereafter existing test methods were looked for and a test set-up was designed and built. The test set-up was hereafter validated, comparing it to the conventional Zwick/Roell test. In order to do so, an Ultimaker 2Go 3D printer was used to create PLA specimens. The dimensions of the specimen are set according to the ASTM D790 standard. Three different batches of PLA specimens were created. These batches were divided in two and tested for their bending properties with both the homemade test set-up and the conventional Zwick/Roell test.
   *Results:* The majority (8/9) of the test results obtained from both the homemade test set-up and the Zwick/Roell test set-up exhibit no significant difference. However, the t-score for the $F_{max}$ measured with specimen batch 1 between the homemade test and Zwick/Roell test showed a significant difference. All the results measured with the homemade test set-up showed a higher value than the results measured with the Zwick/Roell test set-up, indicating the possibility that the homemade test set-up is wrongly calibrated at the beginning. Therefore, calibrating the load cell might result in lower results and a non-significant difference between all the results measured by the homemade test set-up and the Zwick/Roell test set-up.
   *Conclusion:* Depending on the desired level of accuracy for the measurement of bending properties, the homemade test set-up appears to be a viable alternative to the Zwick/Roell test.

2. To investigate the effect of temperature and relative humidity on the quality of fused deposition modeling (FDM) printed parts.
   *Method:* The influence of a temperature of $20^oC$, $35^oC$, and $40^oC$ at a relative humidity of 50%, 70%, and 90% (resulting in 9 different conditions) was investigated for two situations; (1) during storage of the print material 24 hours prior to and during printing, and (2) during storage of the final print 24 hours prior to and during testing of the print.
   Situation 1: 24 hours prior to printing, the print material (PLA filament) was stored at one of the above-mentioned conditions. Hereafter, specimen batches were created using an Ultimaker 2Go printer at the same conditions as at which the material was stored. An Espec humidity oven is used to control the temperature and humidity of the environment. For each condition, two batches of 7 specimens were created. Hereafter, the prints were stored at room temperature and ± 40% RH for a maximum of 5 days. The specimens were hereafter tested for their bending properties using a Zwick/Roell test.
   Situation 2; Different print batches of PLA were created similar to situation 1. 24 hours prior to testing, the final print was stored at one of the 9 above-mentioned conditions. Directly hereafter, the specimen batches were tested for their bending properties using a Zwick/Roell test.
   *Results:* $F_{max}$, max bending strength, and elastic modulus all decrease when printed or tested at increased temperature and relative humidity. Increasing relative humidity especially seems to have a negative influence on the bending properties at a higher temperature. Additionally, the study found that increased %RH and temperature results in under extrusion, a lower weight, and poor surface quality.
   *Conclusion:* Increasing %RH and increasing temperature during (1) the printing process and (2) during storage before testing has a negative impact on the bending properties of the 3D printed specimen.

# 1 Introduction

## 1.1. Surgical care in low and middle-income countries

Access to proper healthcare is a fundamental right for all individuals worldwide, irrespective of their geographical location or socio-economic status. Unfortunately, the quality of healthcare worldwide varies significantly between low- and middle-income countries (LMICs) and high-income countries (HICs).

### 1.1.1. Increase in non-communicable diseases

In LMICs, under-nutrition and communicable diseases (CDs) such as diarrhea, malaria, and HIV/AIDS have long been recognized as the leading causes of premature death or disability. In response, many NGO's and governments have focused on reducing the burden of CDs, resulting in significant improvements in mortality and morbidity rates [6, 7]. However, over the same period, there has been an increase in non-communicable diseases (NCDs) such as cancer and cardiovascular diseases, which is expected to rise further in the coming years. For example, it is projected that the number of deaths caused by NCDs in Sub-Saharan Africa (SSA) will increase from 59% in 2002 to 69% in 2030 [8]. Furthermore, the number of injuries (caused by, e.g. traffic accidents, forces of nature, or interpersonal violence) in LMICs are also on the rise. The increase in NCDs and injuries has created an increased need for surgical care in the world's poorest regions, highlighting the importance of equitable access to surgical services [9].

### 1.1.2. Limited access to surgical care

Despite the increasing need for surgical care in LMICs, the distribution of surgical services worldwide is heavily skewed towards high-income countries. Approximately 60% of the surgeries worldwide are performed in rich countries, where only 15% of the world's population lives. In contrast, only 3.5% of the surgeries take place in LMICs where 35% of the world population lives [6]. According to Debas et al. [10], 9 out of 10 people in LMICs lack access to basic surgical care, affecting 2 billion individuals. From this group, 1.5 million people unnecessarily die each year from conditions that are surgically treatable or preventable.

The lack of (functioning) surgical equipment is one of the major causes of limited access to surgical care. For example, a study carried out by the Institute for Health Metrics and Evaluation [11] showed that Kenyan facilities carried on average only 77% of the equipment listed as necessary by the World Health Organization (WHO). This situation is even worse in rural areas, where the percentage of available necessary equipment is even lower. Even when the appropriate equipment is available, many hospitals struggle to keep the equipment working. In 1997, the WHO estimated that 70% of medical equipment coming from HICs did not work in hospitals in LMICs [12]. Although this percentage has significantly reduced over time, approximately 40% of medical equipment remains out of service in hospitals in LMICs [13–15].

### 1.1.3. Production in high-income countries

Another challenge that LMICs are facing is the fact that research, development, and production of medical devices are primarily performed in and for HICs economies [16, 17]. This creates several problems for LMICs in terms of access, affordability, and suitability of medical devices.

#### Transportation challenges in LMICs

Transportation of medical equipment and supplies is often difficult in LMICs due to high costs, lack of infrastructure, and slow and unreliable delivery.
Importing goods into Sub-Saharan Africa, for example, can be up to three times more expensive and take six times longer than importing into high-income countries. [18–21].
Additionally, complex transport arrangements involving trucks, boats, and bicycles can increase transportation costs. The poor transportation infrastructure also leads to slow supply chains, significant risk of damage or loss, and limited availability of surgical instruments and functional hospital equipment [15, 22–24].

#### Contextual design challenges in LMICs

Most medical devices are designed for use in HICs with stable electricity grids, clean water supply, and proper temperature- and air-regulation systems. However, in LMICs, electricity grids are often unstable, clean water supply is uncertain, and the air is often dusty, humid, and higher in temperature. Therefore, much of the medical equipment may not be suitable for low resource settings where robust and affordable equipment is needed [25].

#### Maintenance challenges in LMICs

Installation, preventive and corrective maintenance services, and user training programs for medical equipment are often lacking in LMICs [26, 27]. When the equipment finally reaches its destination, it becomes harder to maintain, and the delivery of spare parts is costly and slow [28]. According to Perry and Malkin [15], on average, 38.3% of hospital equipment in LMICs is out of service, with 27% of this equipment needing only spare parts to repair. Due to the inefficient supply chain, repairs remain out of reach.

The poor access to affordable surgical care in LMICs has a direct influence on mortality and the quality of life, affecting people of all ages. Approximately 85% of the young patients (up to age 18) in Africa have a surgically treatable disorder by the age of 15 and suffer for a prolonged portion of their lifetimes due to a surgically avertable condition. [29]. The lack of surgical resources has a huge impact on economic wealth, it significantly reduces employment opportunities, and about 25 million households worldwide are pushed into poverty due to the high costs of surgical care Bhatia and Ramadurai [30].

## 1.2. Solving the problem of access to affordable surgical care in LMICs

Improving equipment resources is one way to improve surgical care in LMICs. Ideally, surgical instruments should be produced locally in LMICs to avoid high import fees, slow supply chains, and stimulate local economies [31]. Another possible solution is to locally produce spare parts to make maintenance easier.

### 1.2.1. The potential of 3D printing

One potential solution to increase the availability of (functioning) medical equipment is the use of 3D printing technology. 3D printers have become more accessible and affordable in recent years, and FDM printers show great potential for LMICs. 3D printers can be used at any location where electricity is available, allowing for local production and repair of equipment, and avoiding expensive and inefficient supply chains. Additionally, 3D printing enables rapid design changes and improvements

for user environments. For 3D printing to improve the availability of surgical equipment in LMICs, it must be economically viable, able to print a broad range of products, and produce high-quality printed products [22, 30, 32]. However, quality assurance (QA) remains a common problem for 3D printing in medical applications where the mechanical properties of printed parts are critical to human life.

## 1.3. Objectives

LMICs are facing a growing burden of non-communicable diseases NCDs, which require surgical interventions. However, the lack of (functioning) medical equipment is hindering access to surgical care in these countries. 3D printing has the potential to provide a solution to this problem, but ensuring the quality of 3D-printed medical products is a challenge that needs to be addressed.

The research question that guides this study is: How can the quality of FDM printed medical products be assured in LMICs, and what is the effect of temperature and relative humidity on the quality of these products? The objectives of this master thesis are twofold:

(a) To design a low-cost and easy-to-use test that can be used in LMICs to ensure the quality of FDM printed parts.

(b) To investigate the effect of temperature and relative humidity on the quality of FDM printed parts.

In order to design a suitable test, the context for which the test is designed and the belonging test requirements are defined in section 2.1. When the requirements are formulated, already existing tests are evaluated for their applicability in section 2.2. Hereafter a test set-up is designed in section 2.3, after which the test is evaluated in section 2.4.

In order to test the influence of temperature and humidity on the quality of the 3D printed parts, a test set-up is built, and test specimens are created and tested. Section 3.1 evaluates the influence of varying temperatures and humidity levels during both storage of filament and printing on the bending properties of the print. Section 3.2 evaluates the influence of varying temperatures and humidity levels during storage of the final print 24 hours prior to testing the bending properties of the print.

# 2

# Design a home-made test

## 2.1. Context and Requirements

In order to develop an appropriate QA test for LMICs, it is crucial to understand the context in which the test will be implemented. Kenya is chosen as a case study due to the writer's internship experience at Moi Teaching and Referral Hospital in Kenya, previous research on 3D printing in Kenya, and the connections and knowledge of the local context held by TU Delft. To comprehensively analyze the context and identify context-specific requirements, the framework for holistic contextual design for low-resource settings developed by Aranda-Jan et al. [33] is utilized. This framework comprises four main contextual categories and sub-categories:

- Individual
  - Socio-cultural
- Physical environment
  - Infrastructure
  - Geographical / Environmental
- Systems and structures
  - Institutional
  - Economic
  - Public Health
- Technical
  - Technology
  - Industrial

Based on the analysis of the context for which the test is intended, specific requirements for the test are identified.

### 2.1.1. Individual

**Socio-cultural**

In designing a suitable QA test for LMICs, it is crucial to consider the socio-cultural context of the potential end-users who will operate the test. The culture, knowledge, attitudes, and behavior of individuals can significantly influence their user experience [34–36].

Computer Knowledge
Access to computers is limited in LMICs compared to HICs. Limited computer skills in Sub-Saharan Africa can hinder the implementation of new computer-driven technology [37]. Although there has been an increase in computer usage among Kenyan students over the years, a survey conducted by Mingaine [38] in 2013 revealed that Kenya still struggles to obtain qualified ICT teachers in secondary schools.// The QA test is designed for 3D printer operators, who require basic computer skills to operate the printer software. While the Kenyan population in general has limited computer knowledge, it is reasonable to assume that the end-users for whom the QA test will be created have a basic understanding of how to operate a computer, download files and programs, and run programs on their computer.

*While working with computers in LMICs might be less obvious than in HICs, the test is designed for 3D printer operators who are more likely to have access to and knowledge of computers. Therefore, it is assumed that the test set-up can use a computer and that the operator has some basic computer skills.*

Eagerness to Learn
It is important to understand how new technology might be received by the end-users. Introducing an extra QA test might complicate their work, which can discourage people from actually using it. However, from previous experiences, local Kenyan people are eager to learn and interested in new technologies [39]. Therefore, it is assumed that introducing an extra QA step that requires the usage of (new) technologies would not be an obstacle.

*Experience learns that local Kenyan people are eager to learn and interested in new technologies. Therefore, it is assumed that introducing an extra QA-step which requires the usage of (new) technologies would not be an obstacle.*

Disassemble and reassemble
During the author's internship at the bio-mechanical engineering department at the MTR Hospital in Eldoret (Kenya), it was noted that the engineers preferred to work with devices that they could easily disassemble and reassemble, enabling them to easily replace damaged components. Similarly, Hille [39] noticed that locals would prefer to buy a partly assembled device so that they could learn and understand the device during the assembly process. Thus, the QA test set-up should be easily assembled, disassembled, and reassembled to enable the operators to learn and understand the test set-up.

*The test set-up should not be fully assembled, but instead should be easy to assemble, disassemble and reassemble to enable the operators to learn and understand the test set-up.*

Step-by-step instruction manual
The Kenyan education system heavily focuses on step-by-step problem-solving. Therefore, many students are used to working with step-by-step instruction manuals and require such manuals to properly operate electronic equipment. As such, it is essential to provide a step-by-step manual for the installation and usage of the QA test.

*A step-by-step instruction manual for the installation and usage of the test should be provided.*

### 2.1.2. Physical Environment

**Infrastructure**

The physical environment plays a crucial role in the successful implementation of any new device. This section discusses the relevant factors related to the physical environment, specifically infrastruc-

ture and transportation options, for the design of a low-cost and functional medical device test setup in Kenya.

Transportation Options
In order to design a low-cost and well-functioning test set-up, it is essential that local end-users can build and maintain the set-up. Therefore, it is important to know what parts are locally available, or if not locally available, how long it takes to import the goods. Also, the reliability of the supply chain is important. When a failing part is not locally available, takes long to import, or is likely to get damaged during transportation it will greatly delay the repair of the test set-up.
While Kenya is highly investing in infrastructure, in 2011 infrastructure deficits still contributed to about 30% of the productivity handicap faced by Kenyan firms. [40]

Several channels are available for importing goods, including intercontinental transportation by air or sea, and transportation in and to neighboring countries by trucks or trains.

*The port*
Kenya has a big advantage compared to neighbouring landlocked countries since it is located at sea. The port of Mombasa is the second-largest port in Sub-Saharan Africa after Durban in terms of tonnage and containers handled [41]. However, it is uncertain whether this will continue to be one of the primary ports. Mombasa is having significant capacity constraints [40]. According to Lamarque [42], there are several stakeholders who benefit from delays in unloading, clearing, and transportation. It is therefore questionable whether these inefficiencies will be resolved in the foreseeable future.

*The airport*
Another channel through which goods can be imported is via air. Jomo Kenyatta Airport in Nairobi is Kenya's largest airport and the sixth busiest airport in Africa [43]. Beyond its role as an international hub, Kenya has a domestic air transport market that is the fourth-largest in Sub-Saharan Africa (following South Africa, Nigeria, and Mozambique) [40]. The efficiency at the Jomo Kenyatta Airport however, is not optimal and needs to be further improved [44–46].

*Road*
When goods arrive at (air)ports, these goods are further transported via road or railway. Roads are the main means of transport for people and freight in Kenya and remain the only access means to rural areas [41]. The roads are highly concentrated around the South-West of Kenya. The other parts of the country are nevertheless, connected to this area by some big roads. The quality of the condition of these roads, however, varies from good to poor. And although it might be relatively easy to get to other parts of the country, getting to the more rural areas will require transport via dust roads, which are usually in worse conditions. [40]. Furthermore, Kenya's infrastructure networks are largely isolated from those of its neighbouring countries, and while there are some transport links with Uganda and Sudan, road connections to Ethiopia, Tanzania, and Somalia are limited and of very low quality [41].

*Railway*
Kenya's railway from Mombasa to Nairobi continuing into Uganda has been greatly improved over the past couple of years. This provides additional transportation capacity from and to Uganda.

*There are several ways to import goods to Kenya, over sea, via air, road or railway. However, import costs are high, efficiency in customs clearance is limited and parts might get damaged during transportation. Therefore, it would be preferable to design a test which uses components which are easy to obtain locally.*

Access to Electricity
Although electricity is commonly available in many HICs, Sub-Saharan African countries often struggle with a stable grid. In 2018, only 47.7% of Sub-Saharan Africans had access to electricity, with Kenya performing better at 75%. However, rural Kenyan areas have a lower percentage of access, with 71.7% [47, 48]. Power outages in Kenya are frequent, with an average of 22.5 outages annually, totaling 216.3 hours without electricity Taneja [49]. Access to electricity is essential for 3D printing, therefore, it can be assumed that the end-users have electricity. However, the QA test must be designed to withstand power outages and surges. It's important to ensure the test does not take too long, increasing the risk of interruption due to power outages.

*We assume that the QA-test can use electricity, since 3D printers also need electricity. However, the grid might be unstable and power outages are experienced frequently. Therefore it is preferred that the test should not take too long and the set-up should be able to withstand power outages and surges.*

Mobile and Computer
Mobile phone users have increased worldwide, with developing countries surpassing developed countries. In Kenya, mobile phone coverage is high at 86.2%, while computer ownership is much lower at 18.2%, with only 7.4% of households having internet connectivity. Households with computers tend to have higher education levels, and computer ownership is higher in urban areas than in rural areas [40]. While there are ways to operate 3D printers without computers [50–52], probably most operators use a computer. However, some may not be very skilled in computer usage.

*A clear instruction manual is essential, and the usage of complicated programs should be limited.*

**Internet**

The amount of internet users in Kenya is very high (87.2%). However, it is still costly, and Fab Labs in rural areas face challenges with providing high-speed, reliable internet connection [53]s. While most fab-labs have some internet access, it's preferable to limit the need for internet usage as much as possible.

*The need for internet usage should be limited as much as possible.*

**Geographical/Environmental**

The environment is an important factor to consider, as the test may function differently in different environments. For instance, temperature and humidity may influence the quality of the prints, and the test must be able to determine when temperature/humidity has significantly influenced the print's quality. Temperature greatly influences the cooling behavior of the print, neck growth, and mechanical properties of the final print.

Local temperature
Temperature can have a great influence on the quality of the final prints. The cooling behaviour of the prints determines how the product solidifies. Neck growth, the process of the deposited layers binding to each other, depends on the thermal energy. The neck growth greatly influences the mechanical properties of the final print [54–56]. Furthermore, temperature has a great influence on warp deformation [57, 58]. Temperature fluctuations can result in great inconsistency in the final product. Therefore, the quality assurance test should be able to detect inconsistencies in the quality as a result of temperature fluctuations. Furthermore, the test itself should be reliable in the different operating temperatures.

The temperature in Kenya can fluctuate greatly depending on place and time during the year, but also during the day. In Kisumu for example, where the 3D-print company Kijenzi is based, the temperature in January fluctuates on average between 15,7 and 31,3 $^{o}$C. When moving more to Garissa, located more in the east of the country, the average high temperature during the yearly almost never drops below 35$^{o}$C, while in the warmest months almost reaching 40$^{o}$C. When moving to Nyahururu (located

north of Nairobi), the lowest temperature in January is on average below $8^oC$ [59, 60].

*When designing the test, it must be taken into account that the test should be able to;*

- *Operate and be reliable in temperatures ranging between $0^o C$ - $40^o C$,*
- *Distinguish whether (extreme) temperature fluctuations have influenced the quality of the 3D print, before, during and after the printing process.*

Relative humidity
Humidity can have a great influence on the quality of the prints. Several papers have been written about filament placed in a humid environment before and the impact this had on the print quality. [59, 60]. Similar to temperature, the humidity in Kenya can fluctuate greatly depending on place and time during the year. In Kisumu for example, where the 3D company Kijenzi is based, the humidity percentage fluctuates between 50% on average in January and 70% on average in May. When moving more to Lodwar, located in the north of the country, the lowest average humidity during the year drops to almost 40% in January. In Marsabit (also located in the north of the country) however, the average humidity in January is around 78% which goes up to even 89% average humidity around November/December [59].

*When designing the test, it must be taken into account that the test should be able to;*

- *Operate and be reliable in relative humidity ranging between 40% - 90%,*
- *Distinguish whether (extreme) fluctuations in humidity have influenced the quality of the 3D print, before, during and after the printing process.*

*The test set-up should be able to function under several circumstances, in temperatures ranging from $0^o C$ to $40^o C$, and also at humidity ranging from 40% to 90%. Except for being able to operate at these different temperatures, the test should also be reliable at these different temperatures and be able to demonstrate if temperature or humidity has influenced the quality of the print.*

### 2.1.3. Systems and structures

**Economic**

The gross domestic product (GPD) per capita in Kenya has grown significantly over the last decade. In 2019 the average GPD per capita in SSA was around $1.585,-. With around $1.816,- GPD per capita, Kenya performs better than the average countries in SSA. Worldwide however, the average GPD per capita is around $11.428,- meaning that Kenya is still seriously lacking behind the rest of the world [61]. In 2014 Kenya shifted from a low-income country to a lower-middle-income country. This still means that the population has limited resources to spend. Furthermore, in 2015, 36.1% of the population in Kenya was living below the poverty line [62]. This means that the price of 3D manufactured parts will be essential, whenever manufactured parts are too expensive it will be impossible to sell.
Current 3D printers are getting cheaper and a good FDM printer is soon available for around $200. Assuming that a print lab has a number of 3D printers on hand, it seems reasonable to assume that a similar budget should be available for the test setup.

*Although Kenya's economy appears to perform better than neighbouring countries, Kenya is still a lower-middle income country and the majority of the population has limited resources to spend. Therefore, price is key. A price of ≤ $200.- is deemed to be reasonable.*

**Public Health**

A main objective of the Kenyan 3D print lab in Kijenzi is to print spare parts for broken medical equipment. The Kenyan health sector is divided into the private and public sector. Many Kenyans who are able to spend money on healthcare choose to go to private clinics. However, public health spending is still accountable for around 46% of total health expenditures. The public health sector is essential for those with low income or without income at all [63, 64].
While prices need to be kept low, to keep public healthcare affordable/free, the Kenyan government

sets strict rules for medical equipment to ensure safety. Therefore, medical devices often need to be thoroughly tested and comply with strict rules. Since many different medical devices need to be tested for different mechanical properties (e.g. bending or tensile strength) it is preferred to design one test which can test multiple mechanical properties.

*To keep public healthcare available for those with low income or without income at all, medical equipment needs to be affordable, while quality must be guaranteed to ensure safe treatment. Therefore, it is essential to design a low-cost test that can test a broad range of mechanical properties.*

### 2.1.4. Technical

**Technology**

While the test is designed in the Netherlands, one should keep sight on the local technological limitations and possibilities in LMICs, in this case in Kenya. Where some technical components might be readily available or easy to maintain here, it might be difficult or very costly to obtain or very costly in other regions of the world.

Affordability
One of the most important aspects is the test to be affordable. While cost is an important aspect all around the world, LMICs are less wealthy, requiring products to be sold at a lower price, which that costs must be lower in order to set-up a financially healthy business. Therefore, price is key for the creation of the test. When designing the test it is essential to understand whether the needed parts are locally available, or whether these have to be imported at possibly high costs. When the test is automated, smart choices have to be made regarding the required software, microprocessors, and motors, such that it is possible to keep the cost as low as possible.

*When designing an automated test, software, microprocessors, and motors should be low-price/ open source and locally available to avoid high transport costs.*

Availability of repair tools, spares, and replacement parts
When the test is designed as robust as possible, it is never possible to guarantee that the test will never get damaged. For durability terms, but also to keep the cost as low as possible for the end-user, it should be easy to repair and have a long lifetime. Therefore it is important to know what kind of repairs can be easily done locally. When a 3D printer operator is located at a fablab, it can be assumed that quite a lot of tools are accessible. The fablab in Nairobi for example, is able to 3D print, but also offers CNC-milling, precision milling, vinyl cutting, and other technologies [65]. However, probably not every 3D printer operator will have access to such technologies. During my internship at Moi Teaching and Referral Hospital (MTRH), there were several workshops where equipment could be fixed. In these workshops all basic tools such as screwdrivers, hammers, and soldering irons were available, but more advanced technology was missing.

*Since not every 3D printer operator will have access to advanced tools, it should be possible to easily install, run and repair the test set-up with simple tools.*

In his research on 3D printers, Hille Ris Lambers explored the availability of 3D-printer parts, in which he came to three insights that should be kept in mind during the design of the QA-test;

- *"It is possible to locally source recycled stepper motors and fans,*
- *12V components are locally easier acquirable than 24V components,*
- *The Kenyan webshop Jumia is a good reference for finding accessible materials and components."*

Provision of training for the usage and maintenance
In the ideal situation, the QA-test would be available and usable for every 3D printer operator, independent of the place where the potential user is located. Therefore, it should be possible to instruct

and train the potential end-user on how to initially set up, use, operate, and maintain the test without the need to physically provide training.

*Instruction and training for the initial test set-up, the usage, and maintenance should be accessible and understandable everywhere around the world.*

**Industrial**

Before the test is designed, it is recommended to do a quick scan to know if there are already high-quality alternatives available. Which eliminates the need for a newly designed test set-up.
The Kenyan Bureau of Standards (KEBS) provides laboratory facilities meant for the examination and testing of commodities /materials. While it is possible to test a broad range of material properties at these labs, the labs are located in Nairobi, which limits the possibility to produce locally. Furthermore, renting the laboratory for every needed test will be expensive and so this is not a good alternative. There are a few big companies that produce mechanical testing equipment, one of them is SGS, which has several offices in Kenya. However, the testing equipment which SGS produces is expensive and therefore not suitable for small local 3D printer operators.

### 2.1.5. Requirements

Based on the context for which the QA-test is designed, several requirements have been drawn up, these requirements are listed below;

- Affordable; ≤ $200
- Robust; able to withstand power outages and surges,
- If electrical, testing time should be limited to account for potential power outages,
- Use locally available parts,
- No or limited internet usage needed,
- Open source software,
- Function at a temperature range of 0 - 40 $^{o}$C and relative humidity of 40 - 90 %,
- Easy to assemble, install, operate, and maintain,
- Easy to operate with limited computer skills,
- Step-by-step user manual,
- Able to distinguish whether temperate or humidity has influenced the print quality,
- Able to distinguish whether the formation of a fracture surface has occurred,
- Able to test all kinds of shapes
- Able to test multiple material properties.

Since the test set-up is designed for 3D-printer operators, it is assumed that the following resources are available;

- Electricity
- (Limited) internet connection
- Computer
- Stepper motors
- 12V components
- Items from the Kenyan webshop Jumia

## 2.2. State of the art

In order to design a new test, it is essential to (1) know whether a suitable test does not yet exist and (2) get valuable input/ideas from existing tests. Therefor, several tests are compared and evaluated on their eligibility.

### 2.2.1. Non-Destructive Testing

For economical reasons it would be most desirable to design a non-destructive test. If it would be possible to test the 3D-printed part for its mechanical properties without destroying or irreversible changing the mechanical properties of the part, meaning it could still be sold after testing. When testing for mechanical properties however, the part is often exposed to (high) forces in order to define whether it can withstand these forces. Although it might be possible that the part does not fail due to these forces, it is still hard to guarantee that plastic deformation has not started at all or that these forces have not caused small material changes which are not visible to the naked eye. There are however non-destructive tests which are nowadays already used for material property testing.

#### Visual Inspection

Visual inspection is the most basic type of non-destructive testing. If the observer knows what he/she should be looking for, it is a relatively quick process and the main advantage of visual inspection is that no (expensive) measurement tools are required. For FDM, visual testing can be used to observe whether warping or cracking or have occurred. Using measurement tools, such as a ruler and a magnifying glass, dimensional deviations can be detected. Also variations in colour are notified when the printed object is visually inspected. Visual inspection however, does not guarantee that the mechanical properties of the printed part are sufficient.

#### Penetrate Testing

Liquid penetrate testing is a testing method to detect flaws at the surface of the material. Normally, the material surface is cleaned, after which the liquid penetrate is sprayed onto the surface. Hereafter, the liquid penetrate is removed and an developer is applied, which reveals where the liquid penetrate has been left behind, showing flaws at the surface. While this is a simple technique, it works only on relatively non-porous surface materials and is therefor not applicable for the most common used materials in FDM such as Polylactic Acid (PLA) and Acrylonitrile Butadiene Styrene (ABS) [66].

#### Weight

One of the most simple testing methods is to weight the test part and look whether significant deviations in the expected weight are measured. Therefor it should be possible to place the test object on a weighting scale. Although it is a very simple measurement technique, deviations in (expected) weight do not indicate what caused these weight fluctuations and it is therefor often hard to determine the effect of the weight fluctuation on the mechanical properties of the part.

#### Ultrasonic Testing

In most ultrasonic testing techniques, short pulses of ultrasound are sent into the material and detected after passing through the structure. The propagation and reflection of the sound waves provides information about flaws in the material. While it is possible to manually perform ultrasonic testing, the signal amplitude depends on the thickness of the coupling fluid layer, which depends on the pressure applied. Therefor, the operator has to be skilled to get a reliable result [67]. Furthermore, scanning parts with contours of varying thickness require additional programming to account for shape changes [68].
While this technique might be well applicable to solid materials, with limited complexity, the advantage of 3D printing is the freedom to create complex shapes and the possibility to print with certain

infill percentages, deliberately creating voids. Therefor, ultrasonic testing is not an appropriate testing method for 3D printed materials.

#### Acoustic Emission Testing

This test methods measures the radiation of acoustic (elastic) waves in the test material, that occurs when the materials undergoes irreversible changes in its internal structure, such as matrix micro cracking, fiber-matrix debonding, localized delamination, or fiber pullout and breakage. The method is often used for continuous surveillance of load-bearing structures and is therefor not a suitable testing method in order to predict the performance of a FDM manufactured part. Another drawback of this kind of material testing is that it requires a great skill to correlate the acoustic emission data to specific types of damage mechanisms [69, 70]. According to Barile et al. ABS printed parts printed at higher extrusion temperatures produce more acoustic signals than parts produced at lower extrusion temperature. This is caused by the fact that the specimens printed at higher extrusion temperatures are more compact [71].

#### Radiographic Testing

Radiographic testing uses a source of X-rays or gamma rays, these rays are sent through the object which is tested. A film behind the object absorbs the radiation which passes through the object. Radiography however is relatively expensive and requires skilled operators for the technique and interpretation [72],therefor it is not suited.

#### Thermography

Thermography often uses *Infrared Testing* to detect the presence of defects. The thermal conductivity of a material changes due to defects, resulting in difference in the electromagnetic radiation the object emits. This radiation can be detected and measured with infrared imagers. The instrumentation needed for these kinds of testing are very sensitive and expensive and require highly skilled inspectors to run the instruments [69]. Therefor, this is not a suitable testing method.

#### Shearography

Shearography is an optical measurement technique used to detect disbonds, delaminations, wrinkles, porosity, impact and other damages. By illuminating the surface area of the test object, an interference pattern is created, hereafter a small load is applied, which will cause the material to deform. A nonuniform material quality will change the interference pattern and enable the operator to detect flaws. A disadvantage of shearography is that characterization of defect types other than delamination is extremely difficult [69, 73] and therefor not an ideal test.

#### Electromagnetic Testing

Electromagnetic testing uses magnetism and electricity to detect and evaluate the material. It is used to detect flaws in the material such as fractures and corrosion. There are several electromagnetic testing techniques [69].

##### Eddy Current Testing, Remote Field Testing and Alternating Current Field Measurement

Eddy current testing, remote field testing and alternating current field measurements are quite similar; flaws in the test part, such as voids, cracks and changes in grain size influence the (electro)magnetic field. These changes in the (electro)magnetic field are measured [70] to detect the defects in the material.

Magnetic Particle Inspection and Magnetic Flux Leakage
The principle of magnetic particle inspection and magnetic flux leakage is similar. The test part is magnetized, when there is a discontinuity, such as a crack or flaw, the magnetic flux is broken, which causes a leakage of the flux. The difference between the two techniques is that magnetic particle inspection uses small magnetic particles in order to detect flux leakage, while magnetic flux leakage uses a sensor to detect the magnetic fields [70, 74].

While all these testing methods are ingenious and can detect flaws in the material, all of the above mentioned techniques are designed for metals (some even require the material to be ferromagnetic). While it is possible to print with ferromagnetic material, this material is much more costly than the available polymers and the required printers are too expensive. Therefor, electromagnetic testing is not a suitable testing method for the FDM produced parts.

In conclusion, many non-destructive testing techniques are not applicable because of their expensive character and complexity. This is not the only reason, most of the described techniques above detect flaws in the material such as voids and cracks. Fused deposition modeling will always (often even deliberately by choosing a lower infill percentage than 100%) produce a product which contains more voids than injection molding. The described non-destructive methods are designed to detect one/several defects, but most techniques will probably be unable to make a distinction between the voids which are created deliberately and voids which have arisen due to flaws in the manufacturing process. The high amount of voids present in FDM manufactured parts will probably give very noisy results in most of the above described non-destructive testing methods. Visual inspection and measuring the weight of the test object however, are simple tests which are readily available for low resource settings. Many 3D printing labs already use visual inspection to validate the print, measuring the weight might be a suitable additional validation step. For both tests however, it is questionable how reliable the results are. Therefor, solely using these tests is probably insufficient for proper quality assurance.

### 2.2.2. Destructive Testing

While it would be preferable to test everything non-destructively, the non-destructive testing methods are not sufficient to determine whether the mechanical properties of the FDM manufactured part meet the requirements. Therefore, it is inevitable to use destructive testing as validation of the produced parts. There are several destructive testing techniques, which measure different mechanical properties. For example tensile, compressive and bending properties can be tested, but also the load capacity against shearing, fatigue and creep properties and the impact resistance can be tested.

#### Tensile test

Tensile properties indicate how the material will react to forces being applied in tension. There is a broad variety of expensive, high quality tests available. It is however relatively simple to build a test set-up with limited resources to test the tensile properties of a certain piece. In order to test the tensile properties of a test piece, the applied force and the corresponding elongation of the material have to be measured.

It would be possible to add weights as a force and use a ruler to measure the corresponding elongation, as displayed in figure 2.1.

While it is possible to add small weights, the increase in force won't be continuous, but step-wise. Another possibility is to use a bucket and fill it with water at a specific speed, this will result in a more continuous increase in force. Instead of rulers, many other measuring devices can be used, such as a gauge measuring displacement. This possible test set-up is drawn in figure 2.2.

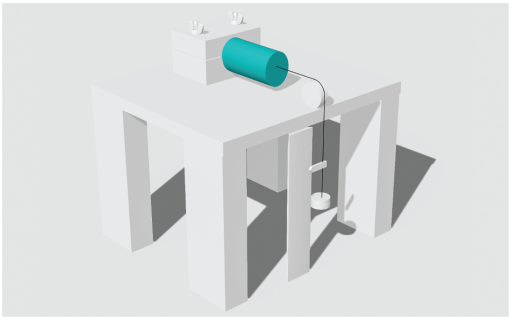

Figure 2.1: A possible tensile test using weights to apply force and a ruler to measure elongation

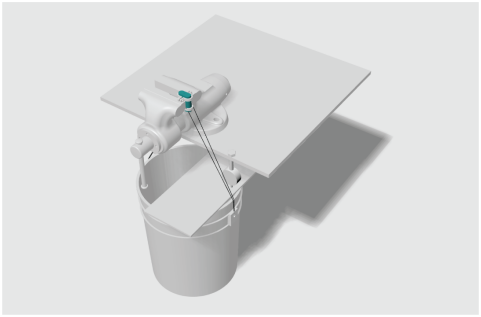

Figure 2.2: Tensile test using a bucket which can be filled with water to apply force and a gauge to measure elongation

#### Compressive test

Compressive properties indicate how a material will react to compressing forces which tend to reduce the size of the part. According to Ahn et al. the compressive strength of FDM material is higher than the tensile strength. Furthermore, tensile strength highly depends on the FDM building direction and so, when designing a part for FDM, one should be aware that the tensile loaded area tends to fail easier than the compression loaded area [75]. It is therefor more likely that when performing mechanical tests on FDM parts, tensile properties will be tested instead of compressive properties. There are however several low-cost tests that can be designed. For example, similar to the tensile test in figure 2.2, a tensile test with a bucket to apply force and a gauge to measure compression can be used.

#### Bending test

The bending or flexural properties of a material indicate how the material will react to bending forces. Similar to tensile tests, there is a broad variety of expensive, high quality tests available, but it is relatively simple to build a simple bending test with limited resources.

The support for the test piece has to be different, but it should be possible to use a bucket to apply force and a gauge to measure displacement. A similar test set-up to figure 2.2 would result in the bending test set-up displayed in figure 2.3.

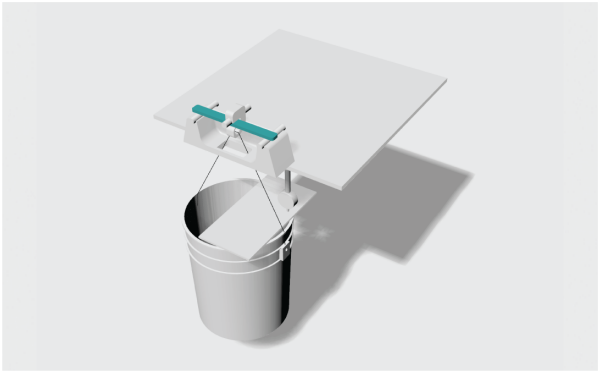

Figure 2.3: A possible bending test using a bucket which can be filled with water to apply force and a gauge to measure elongation

#### Impact test

Two classic impact tests are the IZOD and Charpy tests, both these tests use a pendulum. This is a test which is relatively simple to build. A weight is attached to the pendulum and the pendulum is dropped

from an initial height. Comparing the initial height of the pendulum before and after impact, enables the user to calculate the impact energy required to break the specimen. A drawing of a potential test set-up is shown in figure 2.4.

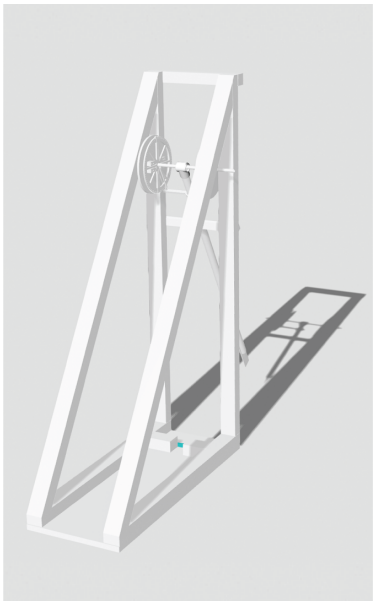

Figure 2.4: A possible impact test using a pendulum to apply force

**Fatigue Test**

There are several fatigue tests, which measure different material properties. All fatigue tests are based on applying the same type of force multiple times. It is for example possible to measure the resistance to multiple impact forces. A possible test set-up to test impact fatigue properties is drawn in figure 2.5. This test set up uses a weight attached to the pendulum and a motor for rotation. A similar test set-up could be used to test bending fatigue properties, as shown in figure 2.6.

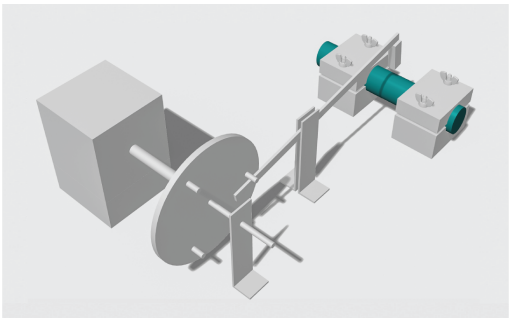

Figure 2.5: A possible fatigue test, testing fatigue impact properties using a motor for rotation

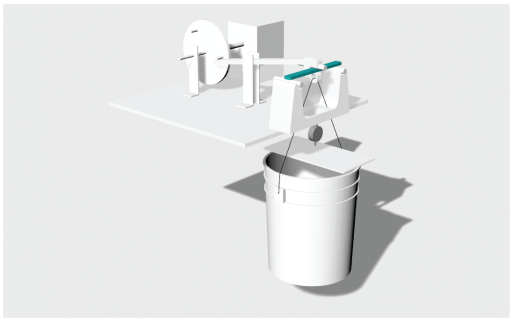

Figure 2.6: A possible fatigue test, testing fatigue bending properties using a motor for rotation

In conclusion, while all drawn tests above can be made with limited resources, it is the question whether they work properly. All test configurations can only test one specific material property; either tensile, compressive, bending or fatigue properties. It would be ideal to build one test set-up which, with a simple press on the button, could measure multiple material properties. Most commercial testing machines are able to test all kinds of material properties, by just changing the grips on the test. There are several high quality manufacturers which offer mechanical testing equipment. For example the

Zwick/Roell test, MTS Bionix test and Instron mechanical test set-ups. These mechanical tests are however very costly and therefor not suitable for print labs in LMICs.

Schindler and Veidt [1] designed a low-cost tensile test, with the assumption that many testing locations do have a Charpy pendulum available. An alternative clamping device is designed as shown in figure 2.7. During a test, the pendulum hammer hits the center of the pivot (D). The impact imposes a movement on the arms that contains a component of relative rotation centred at the pivot. Therewith the forked ends of the arms (A) move apart from each other, stretching the small tensile specimen (B) that is spanned between them.

Another tensile (and creep) testing machine was designed by Momoh et al. [2]. The testing machine consists out of a main frame, a load application system (including a lever, load hanger, dead weight and single strand roller chain) and a strain measuring system (including a dial gauge and pointer) as shown in figure 2.8.

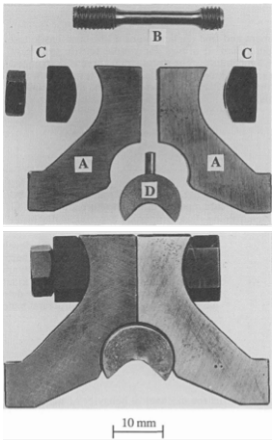


Figure 2.7: Alternative clamping device for tensile testing designed by Schindler and Veidt, consisting of (A) two arms, (B) the tensile specimen, (C) cylindrical shoulders and (D) a central pivot.

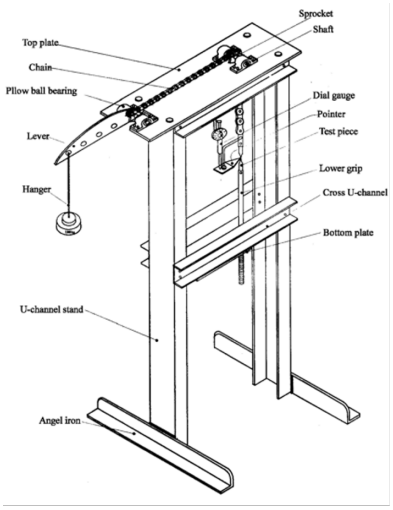


Figure 2.8: The tensile and creep testing machine designed by Momoh et al.

Another testing machine is the so called 'Open-Pull' testing machine from Hermann [3]. This test set-up is shown in figure 2.9. The testing machine consists out of a main frame from wood, load is applied using two stepper motors. The applied load is measured with a load cell and strain is measured optically using a camera.

Amend Jr and Lipson [4] also designed a test device as shown in figure 2.10. The test-up exists out of a metal frame. Load is applied using geared servo motors and the applied load is measured using a load cell. The displacement is measured by the "clicks" of the motor encoder.

All test set-ups have advantages and disadvantages. An overview of the tests with their properties is given in table 2.1. As shown, the two non-actuated tests designed by Schindler and Veidt and Momoh et al. are the lowest in price. These tests are not suitable for testing other properties than tensile (and creep) testing. Using the mechanical tests designed by Hermann and Amend Jr and Lipson, however, it should be relatively simple to slightly adjust the test set-up to test for multiple mechanical properties. When testing for more mechanical properties, it should be considered to build only one slightly more expensive test.

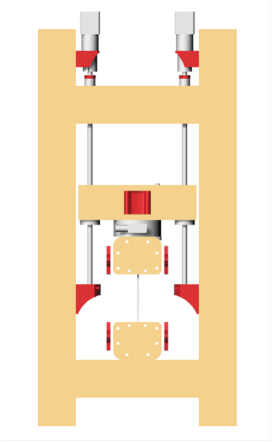

Figure 2.9: The Open-Pull test designed by Hermann

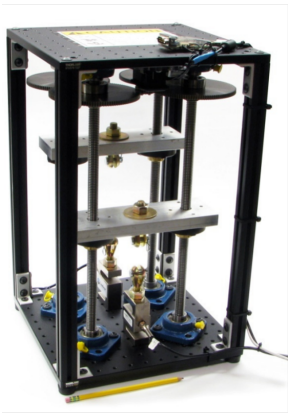

Figure 2.10: The test set-up designed by Amend Jr and Lipson

Table 2.1: Overview of existing test set-ups. * = estimated price

| | **Schindler and Veidt** | **Momoh et al.** | **Hermann** | **Amend Jr and Lipson** |
|---|---|---|---|---|
| **Test properties:** | | | | |
| **Mechanical property tested** | Tensile | Tensile and creep | Tensile (relatively easy to change) | Tensile (relatively easy to change) |
| **Price** | $150,-* | $150,-* | $350.- | $2.205,- |
| **Frame** | Charpy Pendulum | Metal U-shaped beams | Wooden frame | Metal frame |
| **Actuator** | Weight in Pendulum | Weight (hanger) on lever | Two stepper motors | Servo motor |
| **Strain measurement** | Ruler | Dial gauge | Camera | Motor 'clicks' |
| **Load measurement** | Weight | Weight | Flat load cell | S-shaped load cell |
| **Software** | - | - | Arduino (Open source) | Matlab (Expensive) |
| **Availability of step-by-step instruction for:** | | | | |
| **Building the test set-up** | No | No | No | Yes |
| **Building the electronics** | - | - | Yes | No |
| **Using the software** | - | - | Yes | No |
| **Using the test set-up** | No | No | No | Yes |
| **Independent of electricity** | Yes | Yes | No | No |
| **Independent of software** | Yes | Yes | No | No |
| **Easy to change the applied load** | Yes | Yes | Yes | Yes |
| **Able to test different shaped specimens** | No | No | Requires small adjustment | Requires small adjustment |
| **Able to test different mechanical properties** | No | No | Requires small adjustment | Requires small adjustment |
| **Usage of locally available parts** | No | Yes | Yes | No |

## 2.3. Designing the Test

Since FDM enables the operator to produce a broad variety of parts, parts for many different purposes can be produced, ranging from spare parts for medical equipment, to tools such as surgical knifes, to prosthesis to non-medical equipment. All these objects will be used differently, and will have other forces to endure. A leg prosthesis will probably endure mostly frequent compressive forces, but the Kijenzi printing lab also prints aperture-adjustment knobs which will primarily be exposed to torsion forces and bed net connectors which will mainly be exposed to bending forces.

It is therefor essential to design a test which can test several mechanical properties. One can build several test set-ups which are independent of electricity (as described in chapter 2.2.2). A disadvantage of these tests is that for every mechanical property a different test set-up needs to be created and val-

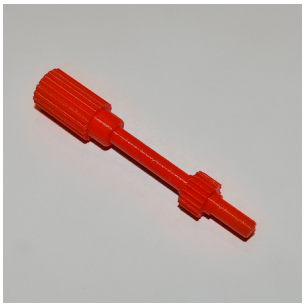

Figure 2.11: Aperture-adjustment knob from the catalog of the Kijenzi print lab [5].

Figure 2.12: Bed net connector from the catalog of the Kijenzi print lab [5].

idated. Therefor, it is better to create a test which resembles the commercial testing machines, but is more affordable. The test designed by Hermann is a relatively affordable test, which uses open source software. But test requires several adjustments.

### 2.3.1. Frame

There are several options for building a frame. First of all one can choose to make the frame from different materials such as wood or metal. Momoh et al.[2] use metal U-shaped beams for the frame, Amend Jr and Lipson[4] use different kinds of metal beams to make the test set-up. Many 3D printers are nowadays build using aluminium profiles which have a tapped lead and slots for nuts (see figure 2.13).

Figure 2.13: Aluminium beam for frame

The advantages and disadvantages of the different potential beams to build the frame are listed in table 2.2.

Table 2.2: Options for frame

| | **Wood** | **U-Shaped steel profile** | **Aluminium construction profile** |
|---|---|---|---|
| **Advantages** | Easy to work with<br>Relatively Cheap | Strong | Easy to connect<br>Resistant to corrosion<br>Possible to buy in the correct length<br>Light weighted |
| **Disadvantages** | Might deform due to temperature & humidity<br>Tooling is required for connecting | Costly<br>Might need soldering | Costs more than wood |

Since the test has to be able to be able to operate at varying environmental conditions (under varying

temperature and humidity), it is wise to choose a metal frame since would can start warping, deform or tear when exposed to different temperatures and humidity. Using the aluminium construction profiles enables the end-user to build the frame, without the need for soldering and with minimal required drilling. Aluminium does not corrode and is a lightweight metal and so it is the ideal material for a desktop test set-up. Furthermore, these aluminium bars are available on the website Jumia, which according to the Kijenzi print lab is a site often used in Kenya to order products. On this site, it is possible to order the beams in varying lengths, due to which sawing to the required size is unnecessary. Furthermore, these beams are relatively inexpensive (in total < $20,-). Overall, these beams seem to be a great option

### 2.3.2. Actuator

There are several possibilities for actuating the test set-up, either manual, by applying a load or using a motor. Amend Jr and Lipson use a servo motor, while Hermann uses stepper motors. When manually applying load, it is hard to ensure a constant strain increase. Many experiments are based either on a constant increase of strain. Although it is not required for quality assurance, it does enable the operator to later maybe compare the test results by test results generated by someone else. Furthermore, manually applying load is often less precise. When for example using weight, often the weight is increased step-wise, due to which limited data points are gathered. Therefor, it might be preferred to use a motor as actuator.

Since many Arduino projects use stepper motors, it is possible to locally source recycled stepper motors and the displacement caused by a stepper motor is easy to measure in terms of the amount of steps (see chapter 2.3.3, this seems the obvious choice for an actuator.

### 2.3.3. Strain measurement

Strain can be measured using many different measurement techniques, such as (digital) rulers, (digital) dial gauges, camera's/optics and the motor used. All have got different advantages and disadvantages. The different strain measurements are compared for affordability, intuitive usage, accuracy, easy to couple to applied load and the necessary of software. This comparison is shown in table 2.3.

Table 2.3: Options for strain measurement

| | **Analogue Ruler** | **Digital Ruler** | **Analogue Dial Gauge** | **Digital Dial Gauge** | **Camera** | **Stepper Motor** |
|---|---|---|---|---|---|---|
| **Affordable** | + | - | + | - | - - | + + |
| **Intuitive** | + + | + | + + | + | - - | - |
| **Accurate** | - - | + | - - | + | + | + |
| **Easy coupling to applied load** | - | - | - | - | - | + |
| **Does not require software** | + | - | + | - | - | - |

Although at first sight the ruler and dial gauge seem a very suited option for strain measurement, the precision of the strain measurement comes closely to the ruler or dial gauge chosen. Using an analogue ruler or dial gauge makes it hard to constantly measure the strain and couple the strain to the applied force. Using a digital ruler or dial gauge increases the cost-price and extra software is needed for these measurements, which makes it less intuitive.

When already using stepper motors as actuators for the test set-up however, no additional costs are required to use these same stepper motors to measure strain. Since affordability is the most important test requirement, the stepper motor seems the best option. The stepper motor will already be controlled using software, therefor measuring the strain via software of the stepper motor should not be a giant barrier.

### 2.3.4. Load measurement

Since it is chosen not to apply the load in the form of weights, the applied needs to be measured. The most convenient way to measure the applied load is to use load cells. There are several load cells which can be used. They can be flat rectangular (2.14, left), flat rounded (2.14, middle) or S-shaped (2.14, right).

Figure 2.14: Different load cells for load measurement. Images are obtained from AliExpress

### 2.3.5. Building the set-up

Hereafter a design for the test set-up is made and the set-up is build. Appendix A describes how the test is build. This Appendix contains the part list to build the test set-up, a list of required tools for assembly, a step-by-step assembly instruction, an overview of the electronic set-up and a step-by-step user manual on how to set-up the software.

The total part list required to build this test set-up adds up to around $160,-. The real cost could in theory be even lower, by using recycled stepper motors, which are possible to source locally according to Hille Ris Lambers [39]. Nonetheless, the designed test is much cheaper than the test designed by Amend Jr and Lipson and around halve of the price of the test designed by Hermann. Although it costs more than the non-actuated tests, this test is able to test several mechanical properties, and so it is not necessary to build several test set-ups. When the end-user wants to test for other mechanical properties, the only thing which needs to be changed are the clamps. The different clamps can be 3D printed, enabling the print lab to easily create different test set-ups.

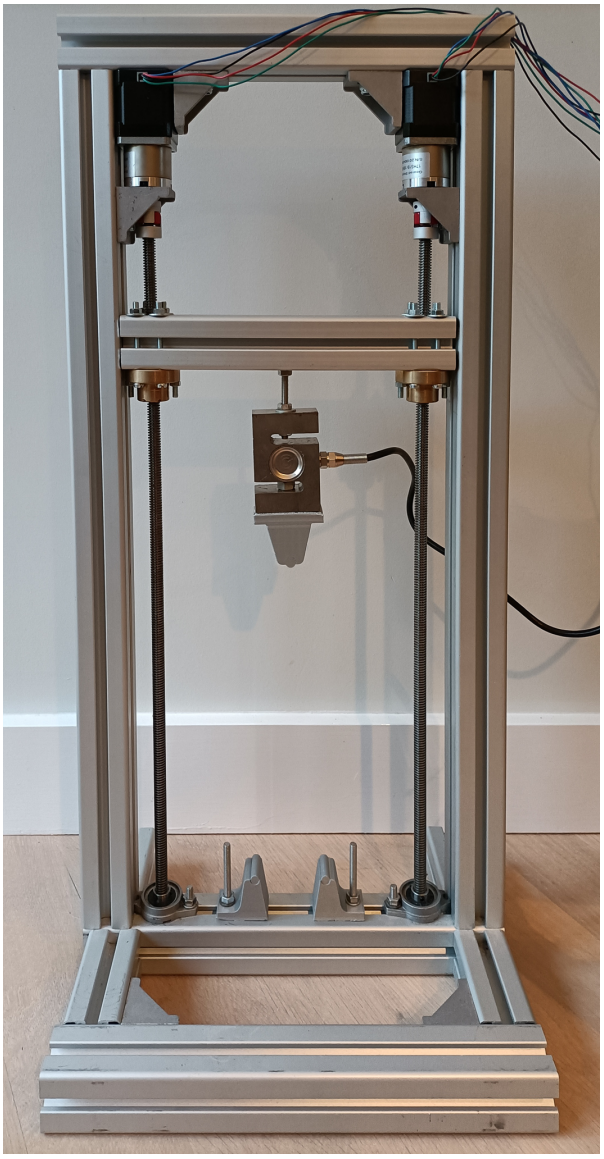

Figure 2.15: The test set-up

The test set-up is shown in figure 2.15. While the test is build and the total cost is reasonable, it has to be validated to determine whether the reliability for quality assurance. In the next section the test is validated.

## 2.4. Validating the test

In order to validate the homemade test set-up, the bending properties of a number of specimens were measured using both the homemade test set-up and a conventional Zwick-Roell test set-up. The null hypothesis of this study assumes that there is no significant difference between the mean bending properties of the specimens tested with the homemade test set-up and those tested with the Zwick-Roell test set-up.

### 2.4.1. Method

To validate the test set-up, several print sets were created using silver metallic PLA from the Ultimaker brand and tested using both the homemade test setup and the conventional Zwick/Roell test set-up. The geometry of the 3D printed specimens was modeled in Rhinoceros, saved as an STL file, and opened in the open-source software Cura, which was used to generate the G-code file and control the printer parameters. The dimensions of the small bending specimens used in this study were based on the dimensions recommended in ASTM D790. The dimensions used to create the small bending specimens are shown in figure 2.16.

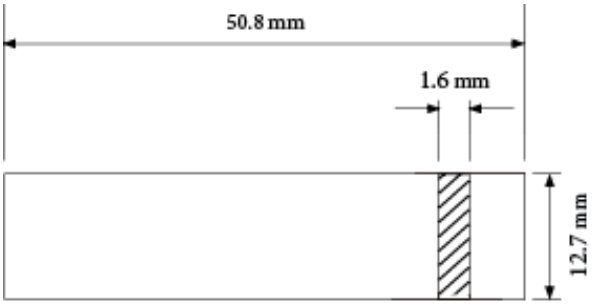


Figure 2.16: Dimensions of the test specimen for bending according to ASTM D790.

The specimens were printed using an Ultimaker 2Go printer, which is known for its reliability. The printer was equipped with a heating bed and blue Ultimaker tape was applied to the build plate before printing. All print batches were created using identical printer parameters, as outlined in table 2.4.

Table 2.4: Constant printer settings used for creating the specimen sets.

| | |
|---|---|
| **Printer** | Ultimaker 2Go |
| **Material** | Ultimaker Silver Metallic PLA |
| **Nozzle diameter (mm)** | 0.4 |
| **Layer thickness** | 0.15 |
| **Build Plate Adhesion** | Brim |
| **Extruder Temperature ($^o$C)** | 200 |
| **Build Plate Temperature ($^o$C)** | 60 |
| **Infill Pattern** | Lines |
| **Air Gap** | 0 |
| **Print Speed (mm/s)** | 60 |
| **Infill Percentage (%)** | 100 |
| **Build Orientation** | Flat |

Three specimen batches were created under varying temperature and Relative Humidity (RH) conditions, by placing the print material in an Espec humidity oven 24 hours prior to printing. Each specimen batch consisted of 28 specimens printed in 4 print sessions. The specimens were created using an Ultimaker 2Go printer which was placed in the Espec humidity oven for printing. After printing, the printed brim was removed, and the specimens were detached from each other. The prints were stored at room temperature and ± 40% RH for maximal 5 days and then conditioned for 24 hours at 20$^o$C and 50% RH before testing for their bending properties. Each specimen batch is split in two; one is tested

with the conventional Zwick/Roell test and the other with the homemade test-set up. The different print batches created are shown in table 2.5.

Table 2.5: Specimen batches created for different tests.

| Specimen batch | Storage & print conditions | $H_2O$ in the air (g) | Total # of specimens | # of specimens tested with home-made test | # of specimens tested with Zwick/Roell test |
|---|---|---|---|---|---|
| 1 | $20^oC$, 50 RH | 7.5 | 28 | 14 | 14 |
| 2 | $35^oC$, 50 RH | 17.5 | 28 | 14 | 14 |
| 3 | $40^oC$, 50 RH | 24.9 | 28 | 14 | 14 |

The difference in bending properties was statistically analyzed using a two-sample t-test with $\alpha = 0.05$, according to the formula:

$$t = \frac{\bar{x}_A + \bar{x}_B}{pooled\,standard\,deviation * \sqrt{\frac{1}{n_A} + \frac{1}{n_B}}} \tag{2.1}$$

With:
$\bar{x}_A$ = mean of the specimen group tested with the homemade test set-up.
$\bar{x}_B$ = mean of the specimen group tested with the conventional Zwick/Roell test.
$n_A$ = number of specimens in the group tested with the homemade test set-up.
$n_B$ = number of specimens in the group tested with the conventional Zwick/Roell test.

And

$$pooled\,standard\,deviation = \sqrt{\frac{(n_A - 1)s_A^2 + (n_B - 1)s_B^2}{n_A + n_B - 2}} \tag{2.2}$$

With:
$s_A$ = standard deviation of the specimen group tested with the homemade test set-up.
$s_B$ = standard deviation of the specimen group tested with the conventional Zwick/Roell test.

Where the Degrees of freedom are calculated according to:

$$DOF = n_A + n_B - 2 \tag{2.3}$$

The null hypothesis was that there is no significant difference between the means of the specimens tested with the homemade test and the means of the specimens tested with the conventional Zwick/Roell test for each specimen batch

### 2.4.2. Results

The degrees of freedom per batch are calculated according to formula 2.3, which results in 26. Using $\alpha$ = 0.05 and a two-tailed interval, t has to be higher than 2.056 to falsify the null hypothesis.

The average $F_{max}$ per specimen batch tested with the home-made and Zwick-Roell test is shown in figure 2.17. The corresponding t-values are displayed in table 2.6.

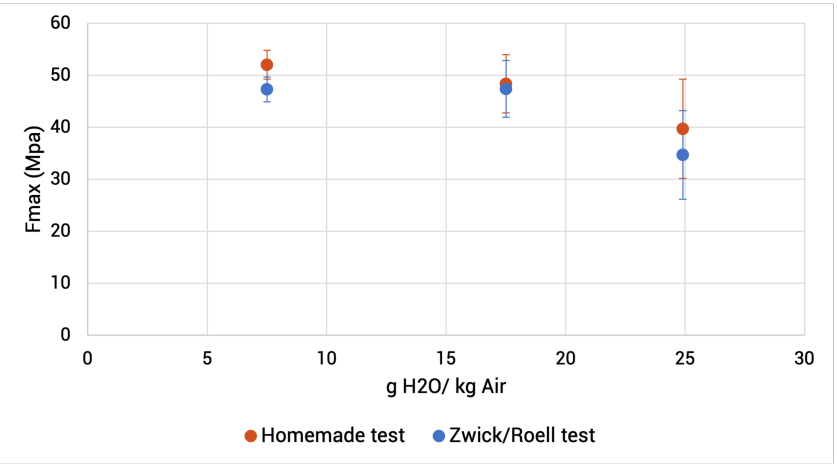


Figure 2.17: Average $F_{max}$ of the specimens tested with the conventional Zwick/Roell test and with the homemade test. The specimens are produced with material stored for 24 hours at 20, 35, and 40 degrees and 50% relative humidity and printed at the same conditions. This resembles an absolute humidity of 7.5, 17.5, and 24.9 g $H_2O$ in the air. Hereafter, the specimens are stored for 24 hours at 20 degrees and 50% relative humidity before testing. The error bars show the standard deviation.

Table 2.6: t-score $F_{max}$ comparing the home-made test set-up and the conventional Zwick/Roell test

| Specimen batch | t-score |
|---|---|
| 1 | 2.0 |
| 2 | 0.7 |
| 3 | 1.6 |

The average maximum bending strength per specimen batch tested with the homemade and Zwick/Roell test is shown in figure 2.18. The corresponding t-values are displayed in table 2.8.

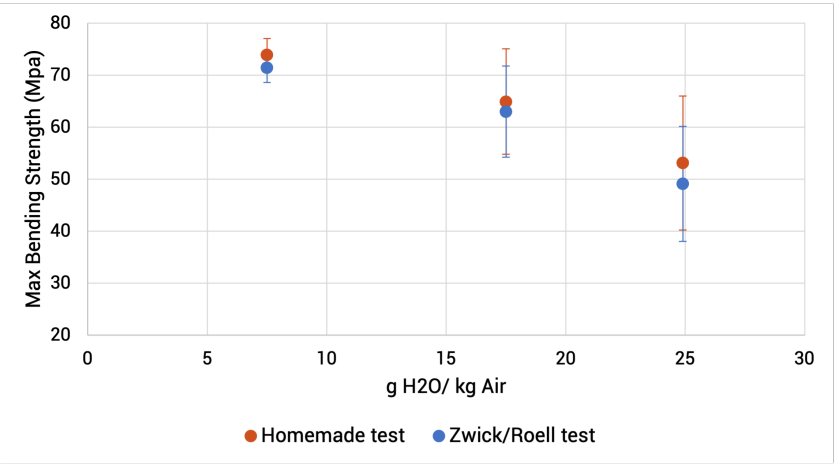


Figure 2.18: Average maximum bending strength of the specimens tested with the conventional Zwick/Roell test and with the homemade test. The specimens are produced with material stored for 24 hours at 20, 35, and 40 degrees and 50% relative humidity and printed at the same conditions. This resembles an absolute humidity of 7.5, 17.5, and 24.9 g $H_2O$ in the air. Hereafter, the specimens are stored for 24 hours at 20 degrees and 50% relative humidity before testing. The error bars show the standard deviation.

Table 2.7: t-score maximum bending strength comparing the home-made test set-up and the conventional Zwick-Roell test

| Specimen batch | t-score |
|---|---|
| 1 | 2.5 |
| 2 | 0.6 |
| 3 | 1.0 |

The average elastic modulus per specimen batch tested with the homemade and Zwick/Roell test is shown in figure 2.18. The corresponding t-values are displayed in table 2.8.

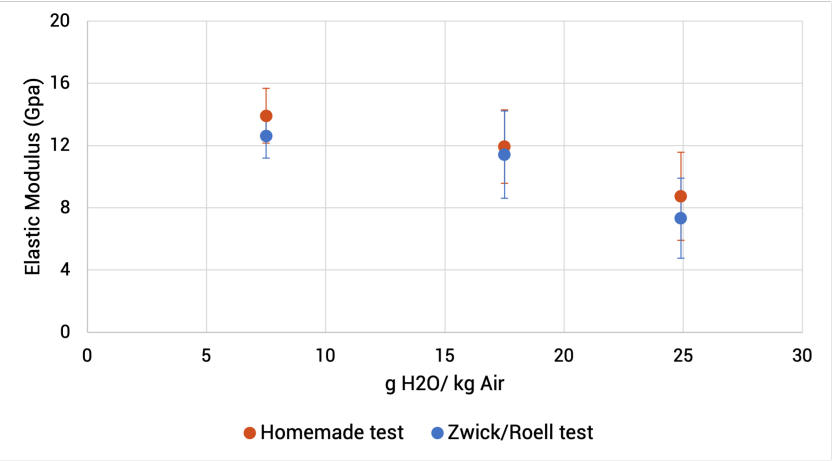


Figure 2.19: Average elastic modulus of the specimens tested with the conventional Zwick/Roell test and with the homemade test. The specimens are produced with material stored for 24 hours at 20, 35, and 40 degrees and 50% relative humidity and printed at the same conditions. This resembles an absolute humidity of 7.5, 17.5, and 24.9 g $H_2O$ in the air. Hereafter, the specimens are stored for 24 hours at 20 degrees and 50% relative humidity before testing. The error bars show the standard deviation.

Table 2.8: t-score elastic modulus comparing the home-made test set-up and the conventional Zwick/Roell test

| Specimen batch | t-score |
|---|---|
| 1 | 1.0 |
| 2 | 0.7 |
| 3 | 1.4 |

### 2.4.3. Discussion

The t-score for the $F_{max}$ measured with specimen batch 1 between the homemade test and Zwick/Roell test showed a significant difference. However, all the results measured with the homemade test set-up showed a higher value than the results measured with the Zwick/Roell test set-up, indicating the possibility that the homemade test set-up is wrongly calibrated at the beginning. Therefore, calibrating the load cell might result in lower results and a non-significant difference between all the results measured by the homemade test set-up and the Zwick/Roell test set-up.

### 2.4.4. Conclusion

The majority (8/9) of the test results obtained from both the homemade test set-up and the Zwick/Roell test set-up exhibit no significant difference. Thus, depending on the desired level of accuracy for the measurement of bending properties, the homemade test set-up appears to be a viable alternative to the Zwick/Roell test.

## 2.5. Discussion

The results of the comparison between the homemade test set-up and the conventional test in section 2.4 indicate that the vast majority of measured results show no significant difference, which is a positive finding. However, there are additional aspects that need to be validated to determine whether the homemade test set-up is suitable for validating FDM-produced parts in LMICs, as outlined in section 2.1.5.

### 2.5.1. Context-specific validation

The first step in validation is to have the test set up and run locally by potential end-users. The test is designed using locally procured parts, open-source software, and an elaborate step-by-step user instruction provided in Appendix A. However, it needs to be validated whether local end-users can locally obtain the components for the test, build and operate the test and whether the step-by-step instructions are effective, especially for local end-users with limited knowledge of the open-source software Arduino.

### 2.5.2. Cost-benefit consideration

The test set-up is designed to be low-cost and costs approximately $160, which is considered to be reasonable. However, there is currently no box to protect the electronics from humidity and dust, and a low-cost 3D-printed box may need to be added, slightly increasing the price. Also, no battery is implemented in the test set-up to reduce costs, but this may be added to make the test set-up more robust for power outages and continued testing when electricity is temporarily unavailable.

### 2.5.3. Multiple mechanical properties

The test set-up must be capable of testing multiple material properties, and while the measured bending properties tested by the homemade test set-up are compared to those measured with a conventional test, the test set-up should also be validated for testing different mechanical properties. Different clamps in the test set-up should be used to measure other mechanical properties, such as tensile and compressive properties and compare the outcomes to conventional test set-ups.

### 2.5.4. The actual print

The test set-up should eventually be used to validate locally FDM-printed products, which may not have standard test strip dimensions. It is difficult to predict the forces to which the printed product will be exposed and the forces that are most likely to cause failure. Therefore, certain produced parts will need to be exposed to test settings that simulate real usage, which will require tailor-made test set-ups. Appendix C provides guidance on what to design and test FDM-printed products for. After designing and testing for simulated use, the test set-up designed in this chapter can be used to ensure continuity in the quality of the produced product. However, the test is destructive, and the printed product cannot be used after testing. Additionally, larger, solid prints may produce a lot of waste during destructive testing. One possible solution is to simultaneously print a test strip next to the produced print, as shown in figure 2.20. It is assumed that poor print quality of the produced print will result in poor print quality of the test strip.

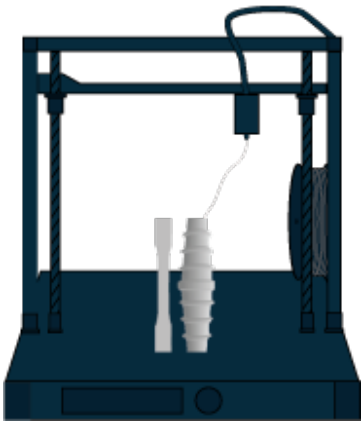

Figure 2.20: Simultaneously print the intended product and the test strip

# 3

# Influence of Temperature and Humidity

As described in section 2.1, the average temperature and humidity in Kenya can fluctuate enormously depending on the location, month in the year and time of the day.

Local print labs often do not control the environment and so temperature and relative humidity can fluctuate. These variations in environmental temperature and humidity might influence the final print quality, since temperature and humidity during storage and the print process might influence the print production. Varying environmental temperature and humidity during testing on the other hand, might give a misleading result about the final quality of the print. While storage of material before printing, printing and testing might occur at varying temperatures, the printed parts might also be stored and used at varying environmental conditions. When designing and printing several objects, it must be taken into account that the properties of the final product might be influenced by environmental conditions.

In order to properly print, test and use 3D printed objects, it is essential to know if and how temperature and humidity influences the printing process, the print quality and the test results.
There are several ways in which environmental temperature and humidity can influence the mechanical properties of the final print;

(a) When the filament is stored in humid and warm conditions, this might cause the filament to degrade, which influences the final quality of the print.

(b) Warm and humid conditions could influence the print process, causing the printer not to perform optimal, resulting in a poor print result.

(c) When testing the print quality under different circumstances, the test results might fluctuate due to these different circumstances instead of due to real differences in the prints.

(d) When the print is stored in humid and warm conditions, this could cause material changes to the print.

(e) When the print is used in extreme conditions, the print might perform different

Although research on the effect of temperature and humidity on the 3D printing process, or 3D printed parts is limited, there are several studies which have investigated the effect of temperature and humidity on PLA in general. The majority of the studies concluded that at higher temperature and humidity, the Molecular Weight (Mw) and Tg of PLA decreases and the overall degradation of PLA is accelerated [76–80].

In this research, the effect of increasing temperature and relative humidity on the bending properties of the final print is investigated during; (1) the short storage of print material (filament) prior to and during 3D printing, and (2) prior to and during testing.

## 3.1. Influence of increasing temperature and relative humidity on print quality during storage of filament and 3D-printing on the final print quality

Valerga et al. [76] studied the influence of humidity during storage of PLA filament on the final print properties. They stored PLA at a 25$^o$C at three different humidity levels for a week before printing. Storing the material at higher humidity levels, resulted in the formation of bubbles, which favor the propagation of cracks when forces are applied. Storing the PLA filament in dry conditions resulted in a stronger (but also more brittle) print.

The influence of storage conditions on PLA filament has not been further researched, but several researchers have looked into the effect of temperature and humidity on the degradation of PLA. Copinet et al. [81] stored PLA films under constant temperatures of 30, 45 and 60 $^o$C at relative humidity of 30, 50 and 100 %. Under these storage conditions, at higher temperature and higher relative humidity the weight-average Mw, Tg and elongation at break all reduced faster compared to lower temperature and humidity.

Blasi et al. [77] looked at the effect of water on Poly(Lactide-Co-Glycolide) (PLGA). When the material was placed in water at different temperatures (23, 30, 37 and 55 $^o$C), this resulted in a decrease in Tg of 15$^o$C independent of the storage temperature. Furthermore, PLGA was placed at different relative humidity's at 32-90%. After four days, equilibrium was reached and the moisture content in the PLGA was measured, ranging between 0.82 - 2.61% w/w compared to 0.30% w/w for the dry material. A linear correlation between Tg and moisture content was observed. The water responsible for the moisture content ranging between 0.3 - 2.6% w/w could be classified as non-freezable bound water, higher water contents formed a heterogeneous system and therefore did not cause further reduction of the Tg. Furthermore, a similar decrease in average molecular weight was observed when the PLGA was incubated in water as when placed a 90% relative humidity (at 37$^o$C).

Also Karamanlioglu and Alkan [80] sees that the degradation of PLA is temperature dependent. The tests performed by Karamanlioglu and Alkan are performed under milder conditions than the tests mentioned before. In this experiment, PLA was tested initially before the material was stored under constant conditions, hereafter the material was stored at (1) 20±2$^o$C and 40±10 % relative humidity for five years and at (2) 55$^o$C under dry conditions for a year after which it was stored for four years under the same conditions as in scenario (1). The PLA's tensile strength, young's modulus and strain at break decreased for both scenario's compared to the initial material properties. Storing the material at high temperature under dry conditions for a year prior to storage at room temperature and humidity leaded to a greater decline in these mechanical properties than when the samples where immediately stored at room temperature and humidity.

In short, the degradation of PLA is accelerated by high temperature and humidity. Most of the above mentioned studies however either test the material after exposing it to relatively high temperatures or relatively high humidity (even placing it in a water bath) or, when the conditions are milder, the material is stored under these conditions for a very long time. The temperature in Kenya varies between 0 - 40$^o$C, the relative humidity varies between of 40 - 90 %. Most printing labs store their filament in dry boxes at cool places. Therefore, the filament will only be exposed to higher temperatures and humidity levels only for a short period of time, with 40$^o$C and 90% relative humidity as the most extreme conditions. In these conditions however, the filament will probably also absorb water from the humid air. Furthermore, none of the above mentioned studies took into account the print process itself. Printing at higher temperatures often leads to better bond formation (see Appendix B) and so to better prints. It would be interesting to see whether print quality is influenced by printing at different temperature and humidity while material is stored for a relatively short time at similar conditions.

### 3.1.1. Method

In order to test whether the print quality is influenced by water uptake of the filament when stored (for a relatively short period) and printed under varying temperatures and humidity levels, several print sets are created. The material which is tested is silver metallic PLA of the Ultimaker brand. Before printing, the material is stored while placed onto the 3D printer for 24 hours under a specific temperature and relative humidity. Hereafter, the test strip is printed at the exact same temperature and relative humidity. An Espec humidity oven is used to control the temperature and humidity of the environment. The filament is stored and printed at $20^oC$, $35^oC$ and $40^oC$ at relative humidity of 50%, 70% and 90%. In the table 3.1 conditions under which the filament is stored 24 hours before printing and at which the print is created are shown.

Table 3.1: Temperatures and relative humidity at which the filament is stored 24 hours before printing and at which the print is created.

| **Temperature** ($^o$C) | **Relative Humidity** (%) | **Water content in air** (g $H_2O$/kg air) |
|---|---|---|
| 20 | 50 | 7.2 |
| | 70 | 10.1 |
| | 90 | 13.1 |
| 35 | 50 | 17.6 |
| | 70 | 25.0 |
| | 90 | 32.5 |
| 40 | 50 | 23.3 |
| | 70 | 33.2 |
| | 90 | 43.3 |

The geometry of the 3D printed specimens was modelled in Rhinoceros, saved as an STL file and opened in the open source software Cura. Cura software was used to generate the G-code file and to command and control the printer parameters. For the dimensions of the test specimens, the dimensions for the small specimen according to ASTM D790 are used. The dimensions used to create the small bending specimens are shown in figure 3.1.

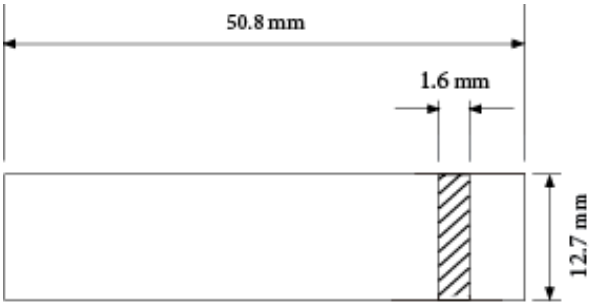


Figure 3.1: Dimensions of the test specimen for bending according to ASTM D790.

Per condition (temperature and relative humidity combination) two batches of 7 specimens were created. Ultimaker 2Go is the 3D printer used to created these specimens. Due to the small dimensions, the printer fits in the humidity oven. Furthermore, Ultimaker is known as a reliable 3D printer, therefore deviations caused by an unreliable printer are minimized. The Ultimaker 2Go printer is upgraded with a heating bed, which makes it possible to heat the build plate. Before printing, blue Ultimaker tape is applied to the build plate. Except for the humidity and temperature at which the filament is stored before printing and at which the printer is operated during printer, all printer parameters are similar for all the print batches. The constant print parameters used can be found in table 3.2.

Table 3.2: Constant printer settings used for creating the specimen sets.

| | |
|---|---|
| **Printer** | Ultimaker 2Go |
| **Material** | Ultimaker Silver Metallic PLA |
| **Nozzle diameter (mm)** | 0.4 |
| **Layer thickness** | 0.15 |
| **Build Plate Adhesion** | Brim |
| **Extruder Temperature ($^o$C)** | 200 |
| **Build Plate Temperature ($^o$C)** | 60 |
| **Infill Pattern** | Lines |
| **Air Gap** | 0 |
| **Print Speed (mm/s)** | 60 |
| **Infill Percentage (%)** | 100 |
| **Build Orientation** | Flat |

After printing, the print is removed from the build plate and a photo is made from the bottom of the print batch, which is used to analyse the adhesion to the build plate. The program ImageJ is used to measure the proportion of the surface area of good, medium or poor quality. The quality definitions are formulated as follows;

Good quality: The deposited material appears to have attached good to the build plate and the formation of air gaps within the raster is minimal.
Medium quality: The deposited material appears to have attached good to the build plate, but voids have formed within the raster.
Poor quality: Poor adhere to the build plate, resulting in a chaotic print pattern.

Hereafter, the printed brim is removed and the specimens are detached from each other and stored for at room temperature and ± 40% RH for maximal 5 days. 24 hours before testing, the specimens are placed in the Espec humidity oven at 20$^o$C and 50%. Hereafter, the specimens are one by one weighted. A precision scale of KERN with a deviation of 0.01 mg/0.1 is used to weigh the specimens. Directly after weighting, the specimens are tested for their bending properties using a Zwick//Roell testing machine.

### 3.1.2. Results

After conditioning the material for 24 hours at a specific temperature and humidity, the specimens are created. One thing, which can immediately be noted during printing is that at a higher temperature and humidity, the material becomes gum-like and adhesion to the build plate gets bad. Furthermore, at high temperature and humidity, the material feeder starts to hamper, which results in a sub-optimal material extrusion through the nozzle. The bad adhesion to the build plate and the failing material feed at higher temperature and humidity make it nearly impossible to print the batch of 40$^o$C and 90% humidity, therefore this batch is omitted.

#### Adhesion to buildplate

When printing at 20$^o$C and 70% RH, the printing process is smooth and the adhesion to the build plate and neck forming between the deposited material roads seems good (see figure 3.2), this gets worse when the temperature rises to example to example 35$^oC$ (see figure 3.3). It is clearly visible that the prints at 40$^o$C and 70% RH results in very poor adhesion to the build plate (see figure 3.4).

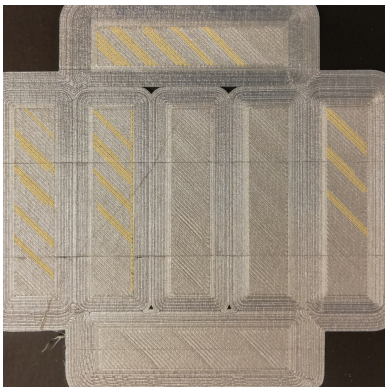

Figure 3.2: Bottom of print created at 20$^{o}$C and a relative humidity of 70% with print material conditioned at these same conditions 24 hours before printing. The yellow parts in the picture indicate medium print quality.

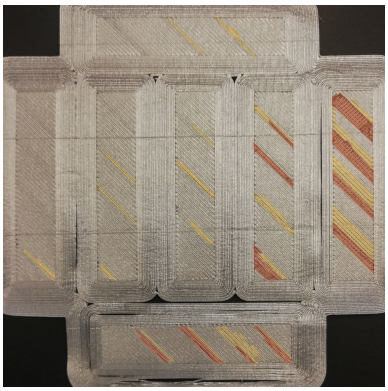

Figure 3.3: Bottom of print created at 35$^{o}$C and a relative humidity of 70% with print material conditioned at these same conditions 24 hours before printing. The yellow parts in the picture indicate medium print quality, the orange parts in the picture indicate poor print quality.

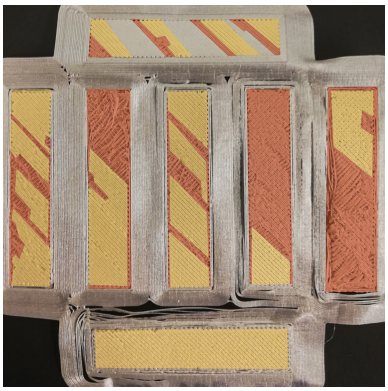

Figure 3.4: Bottom of print created at 40$^{o}$C and a relative humidity of 70% with print material conditioned at these same conditions 24 hours before printing. The yellow parts in the picture indicate medium print quality, the orange parts in the picture indicate poor print quality

Also for increasing relative humidity while keeping the temperature constant, the adhesion to the build plate and the the resulting surface quality decreases. Figures 3.5, 3.6 and 3.7 show the percentage of good, medium and poor quality for relative humidity of 50, 70 and 90% at 20, 35 and 40$^{o}$C.

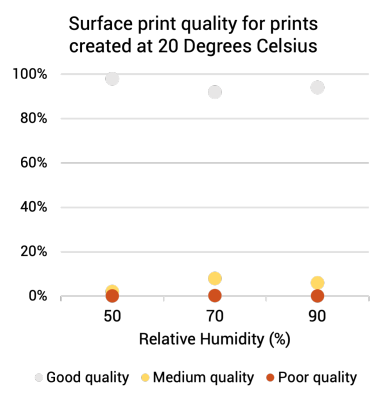


Figure 3.5: Bottom of print created at 20$^{o}$C and a relative humidity of 50, 70 and 90% with print material conditioned at these same conditions 24 hours before printing.

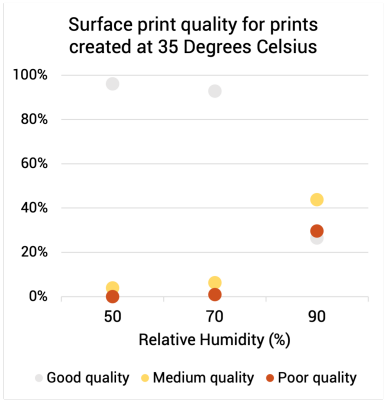


Figure 3.6: Bottom of print created at 35$^{o}$C and a relative humidity of 5-, 70 and 90% with print material conditioned at these same conditions 24 hours before printing.

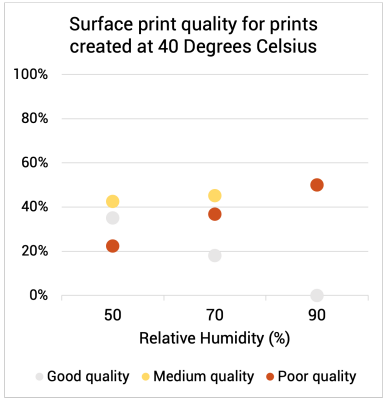


Figure 3.7: Bottom of print created at 40$^{o}$C and a relative humidity of 50, 70 and 90% with print material conditioned at these same conditions 24 hours before printing.

As clearly visible in figure 3.5, 3.6 and 3.7, an increasing relative humidity results in poorer print surface area, increasing relative humidity however has a far greater impact at higher temperature. When looking at the values in table 3.1, it is visible that the amount of water in the air is much higher at 40$^{o}$C and, while an increase in relative humidity from 50% to 90% at 20$^{o}$C means an absolute increase of ±6 g $H_2O$/ kg air, increasing the relative humidity at 40$^{o}$C from 50% to 90% means an absolute increase of ±20 g $H_2O$/ kg air.
When looking at the print adhesion to the build plate compared to the absolute humidity (see figure 3.8), however it is clear that absolute humidity is not the sole causes of poorer build plate adhesion. The graph does not show a linear progression, but a gross deterioration at around 23 g $H_2O$/kg air, which is measured at the highest print temperature of 40 $^{o}$C. Hereafter the measured surface improves significantly at the higher absolute humidity of around 25 $H_2O$/kg air, which is printed at a temperature of 35 degrees. While the difference in absolute humidity is small, the difference in surface quality is enormous. In the 3D print community, poor adhesion to the print bed due to higher humidity in combination with higher temperatures is also a well-known phenomenon, this phenomenon is described by many 3D printer operators [82, 83].

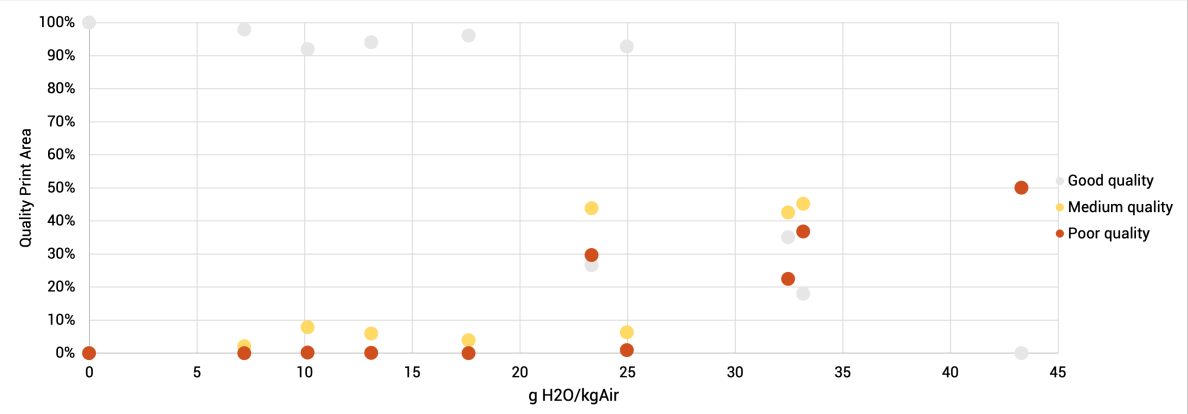


Figure 3.8: Adhesion to the build plate compared to absolute humidity (g $H_2O$/kg air with print material conditioned at these absolute humidity conditions 24 hours before printing.

**Under extrusion**

It is clear that storing the print material and printing at higher temperature and humidity has a negative effect on the adhesion to the build plate, another thing which was immediately noted is the hampering of the filament feeder. When the filament was placed at increased temperature and relative humidity 24 hours prior to printing, the filament feeder started hampering. Hampering of the feeder can be caused by several factors, such as a clogged nozzle or a dirty bowden tube which causes excessive friction. The nozzle and bowden tube are therefore frequently checked to ensure these factors did not cause the hampering of the feeder.

It appears that the hampering of the feeder is caused by changes in the filament after 24 hours of storage at relatively warm and humid conditions. As concluded by Valerga et al. [76] storing of PLA at high humidity levels results in the formation of bubbles. Also at several print community forums, the formation of air bubbles and extruder jams are reported. When the filament has absorbed water, the water will evaporate when it reaches the nozzle, resulting in bubbles. Small bubbles of steam can cause the extrusion to sputter and gives poor consistency, resulting in a less smooth surface. Larger steam bubbles can cause material oozing followed by no extrusion and in extreme cases the formation of bubbles can cause material jams [82, 84–87]. Hampering of the feeder and the formation of air bubbles might cause under extrusion which can be demonstrated by a reduced weight, therefore it is interesting to see whether the weight of the specimens changes. Figure 3.9 shows the average weight of the different species for the absolute humidity conditions under which they are produced and the material is stored 24 hours before printing. As clearly visible, the weight decreases significant when temperature and humidity is increased. At 20$^o$C and 50% RH (7.5 g $H_2O$/ kg air), the produced specimen weights around 1 gram, at 40$^o$C and 70% RH (34.9 g $H_2O$/ kg air) the produced specimen weights less than 0.85 gram, a difference of more than 15%.

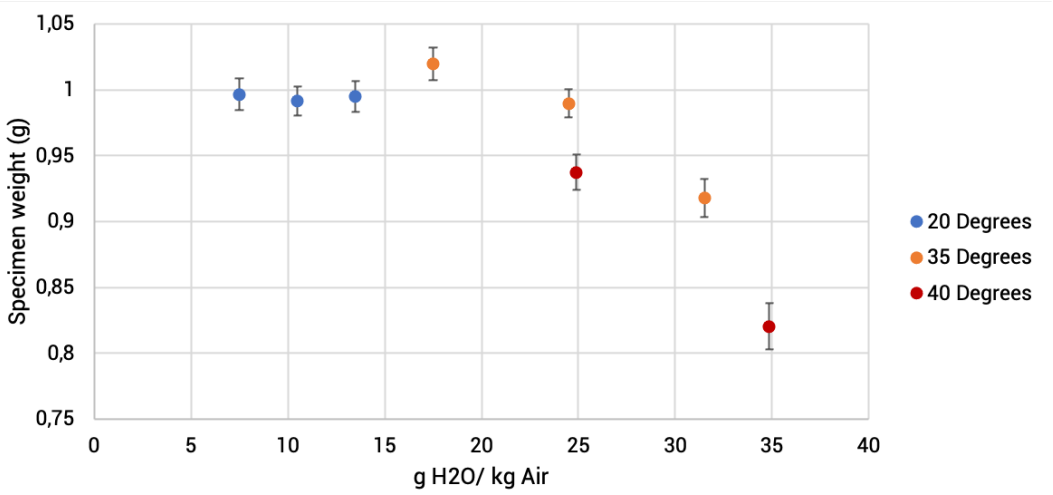


Figure 3.9: Average weight of the specimens produced with material stored for 24 hours at these absolute humidity conditions and produced under the same humidity conditions. The error bars show the standard deviation.

**Bending properties**

Judging on visual feedback and weight, the quality of the print is poorer when the material is placed at increased temperature and humidity 24 hours before printing, it is however the question whether this also shows in the mechanical properties. The bending properties of the specimen are measured using a Zwick/Roell testing machine.

$F_{max}$
The maximum force the specimens can withstand is shown in figure 3.10. As visible, the maximum force varies between 40 and 50N at a humidity between 7.5 and 31.5 g $H_2O$/ kg air, at temperature 20 and 35$^o$C. It seems that an increasing humidity at constant temperature (20 or 35$^o$C) leads to a lower $F_{max}$, but when looking at the absolute humidity in the air, the influence of increasing humidity at lower temperatures seems moderate. At a temperature of 40$^o$C however, the decrease in maximum force is substantial with increasing humidity. Also the increase in temperature of 35 to 40$^o$C, with similar absolute humidity (around 20 g $H_2O$/ kg air) seems to have a substantial decreasing effect on the $F_{max}$. When looking at the weight (x at the right axis in figure 3.10) it is visible that it cannot exactly predict the $F_{max}$, but the trend is similar. Weight can therefore function as a great indicator on the $F_{max}$ performance of the print.

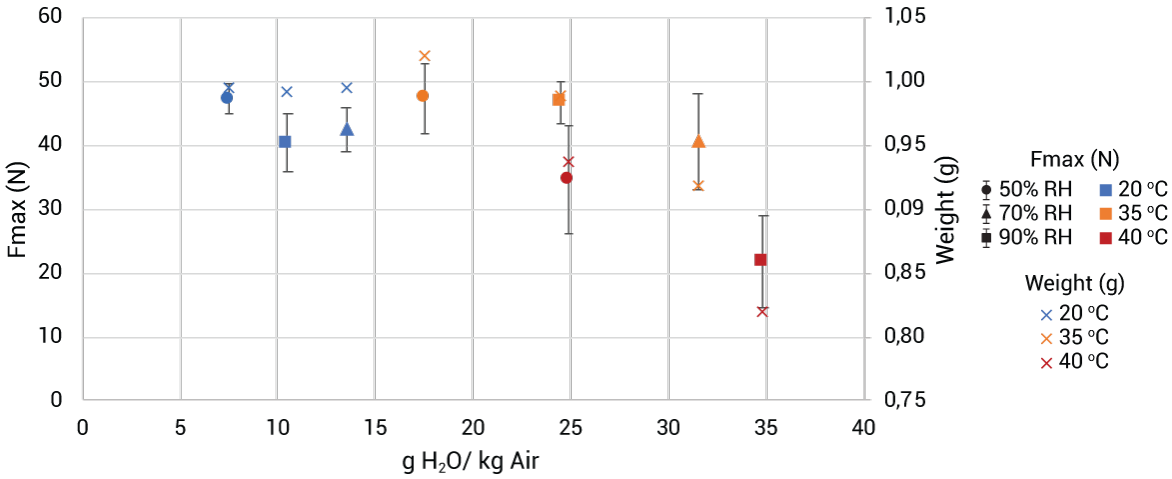


Figure 3.10: $F_{max}$ of the specimen for different storage conditions of the specimens produced with material stored for 24 hours at these absolute humidity conditions and produced under the same humidity conditions (left axis) compared to the corresponding weight (x) of the specimen (right axis). The error bars show the standard deviation.

*Bending Strength*

$F_{max}$ might be misleading, since the maximum force a specimen can withstand highly depends on the thickness of the specimen, therefore the bending strength is calculated, shown in figure 3.11. Since the dimensional deviations in the specimens are minimal, the difference in maximum bending strength at varying temperature and humidity is similar to $F_{max}$. As visible, the maximum bending strength varies between 75 and 55N at a humidity between 7.5 and 31.5 g $H_2O$/ kg air, at temperature 20 and $35^oC$. It seems that an increasing humidity at constant temperature (20 or $35^oC$) leads to a lower maximum bending strength, but when looking at the absolute humidity in the air, the influence of increasing humidity at lower temperatures seems moderate. At a temperature of $40^oC$ however, the decrease in maximum bending strength is substantial with increasing humidity. Also the increase in temperature of 35 to $40^oC$, with similar absolute humidity (around 20 g $H_2O$/ kg air) seems to have a substantial decreasing effect on the maximum bending strength. Another noteworthy result is that the standard deviation in bending strength increases in the specimen batches when temperature and humidity increases. In other words; the homogeneity within the batches produced at higher temperature and humidity is lower. Therefore, more specimen need to be tested for their mechanical properties and a higher safety margin should be taken into account when products are produced with material stored and prints made at higher temperature and humidity. When looking at figure 3.5, 3.6 and 3.7, it seems obvious that the standard deviation increases. In the same print batch at $20^oC$ and 70% RH the difference in print bed adhesion and surface quality is minimal between the specimen, while at $40^oC$ and 70% RH one specimen can completely be described as medium print surface quality, while another specimen exists for the vast majority out of poor surface quality and yet another specimen exists for more or less $1/3^{th}$ out of good surface quality, $1/3^{th}$ out of medium surface quality and $1/3^{th}$ out of medium quality. If the differences in surface quality between specimen within the same print are already this big, it can be expected that the differences in (surface) quality between different print batches are as least as big, if not bigger.

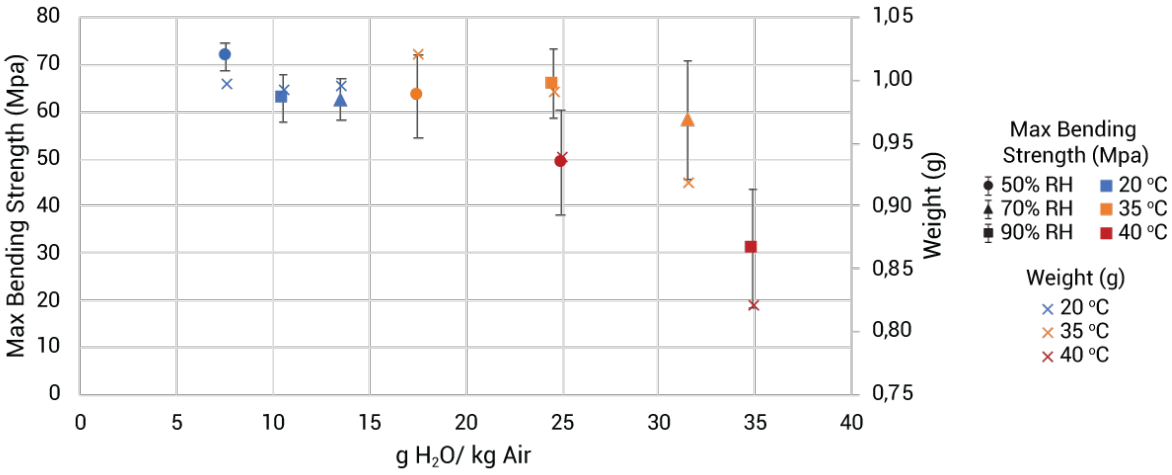


Figure 3.11: Bending strength of the specimen for different storage conditions of the specimens produced with material stored for 24 hours at these absolute humidity conditions and produced under the same humidity conditions (left axis) compared to the corresponding weight (x) of the specimen (right axis). The error bars show the standard deviation.

Since the dimensional deviations in the specimens are minimal, the trends observed in in maximum bending strength at varying temperature and humidity are similar to $F_{max}$. As visible, the maximum bending strength varies between 75 and 55 Mpa at a humidity between 7.5 and 31.5 g $H_2O$/ kg air, at temperature 20 and 35$^o$C. It seems that an increasing humidity at constant temperature (20 or 35$^o$C) leads to a lower maximum bending strength, but when looking at the absolute humidity in the air, the influence of increasing humidity at lower temperatures seems moderate. At a temperature of 40$^o$C however, the decrease in maximum bending strength is substantial with increasing humidity. Also the increase in temperature of 35 to 40$^o$C, with similar absolute humidity (around 20 g $H_2O$/ kg air) seems to have a substantial decreasing effect on the maximum bending strength. Similar to $F_max$, the weight of the specimen does not perfectly predict the bending strength of the specimen, but it can be used as an indicator since it does follow a similar trend.

*Elastic Modulus*

$F_{max}$ and the maximum bending strength however, indicate how the specimen performs in the plastic region. When a piece is reused, it is preferred to use the object only in the elastic region. Therefore, it is interesting how the specimens perform in the elastic region and so the elastic moduli of the specimens are examined. As visible in figure 3.12. For the specimen produced at 20$^o$C and at 40$^o$C, increasing RH seems to negatively affect the elastic modulus of the specimen. This trend is less observed at 35$^o$C. Furthermore, the standard deviation within the batches is higher when only looking at the elastic modulus, compared to for example $F_max$ and bending strength. This means that greater variations within the print batches exist when comparing for elastic modulus. And so, if elastic modulus is the most important mechanical factor, a greater safety factor needs to be considered in order to guarantee the print quality. As visible, the elastic modulus is especially influenced by temperature. Increasing RH has a great effect, but mostly for the specimen made at 40$^o$C. Similar to $F_max$ and bending strength, the weight of the specimen does not perfectly predict the elastic modulus of the specimen, but it can be used as an indicator since it does follow a similar trend.

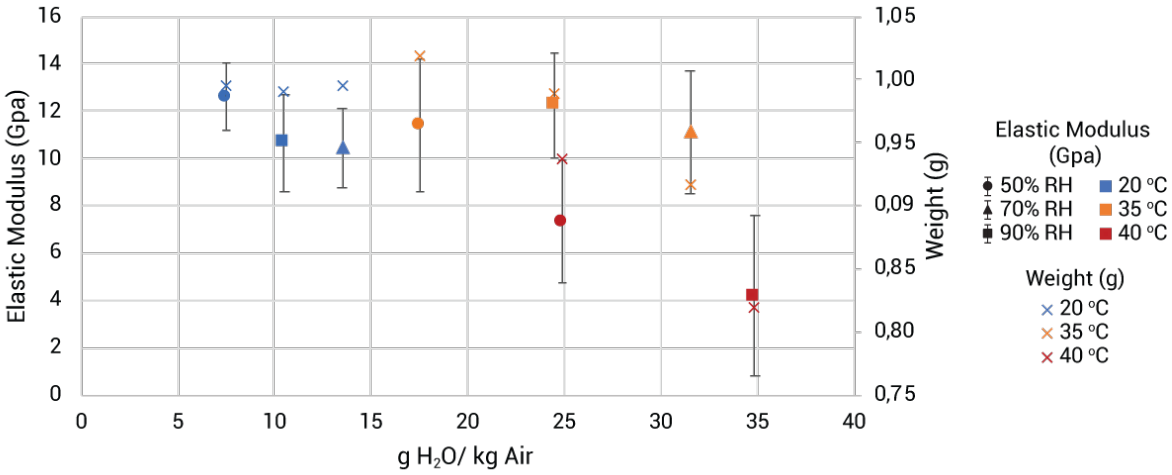


Figure 3.12: Elastic modulus of the specimen for different storage conditions of the specimens produced with material stored for 24 hours at these absolute humidity conditions and produced under the same humidity conditions. The error bars show the standard deviation.

### 3.1.3. Conclusion

As described above, 24 hour storage of the filament in combination with printing the specimen at specific temperatures and RH ranging from 20, 35 and 40 $^{o}$C and 50, 70 and 90 % can heavily influence the final print quality.

#### Adhesion to build plate

The adhesion to the build plate is heavily influenced by temperature and RH. Lower temperature and RH result in better adhesion to the build plate. The adhesion to the build plate is very poor at 35$^{o}$C and 90% RH and at 40$^{o}$C and 50, 70 and 90% RH.

#### Under extrusion

Increasing temperature and RH can cause under extrusion. This effect is only noticeable when both temperature and RH are high. At 20$^{o}$C, the increase of RH does not influence the specimen weight. Increasing the RH at 35 of 40 $^{o}$C however greatly influences the specimens weight. Under extrusion is mostly caused by the combination of high temperature and high RH.

#### Bending properties

The mechanical properties of the specimen go hand-in-hand with weight. Although weight cannot be used to exactly predict the mechanical properties of the specimen, the mechanical properties are similarly influenced by increasing temperature and relative humidity. It seems evident that the $F_{max}$ and maximum bending strength decrease due to under extrusion. Same goes for elastic bending modulus. The mechanical properties especially seem to decrease when going from 35$^{o}$C to 40$^{o}$C. The negative influence of increasing RH on the mechanical properties also seem to be highest at 40$^{o}$C. Furthermore, a higher standard deviation is observed for the samples produced at higher temperature. This means that when printing at higher temperatures, a bigger safety factor needs to be considered in the design for final quality assurance.

## 3.2. Influence of increasing temperature and relative humidity on print quality during storage of the final print prior to and while testing the print quality

Widely used test instructions, such as ISO ASTM, do not prescribe accurate conditions for testing in Kenya. Most ASTM and ISO test instructions instruct to perform tests at room temperature, around 20$^o$C and 50% RH. However, the temperatures in Kenya can fluctuate between 0 and 40$^o$C with a corresponding RH of 50 - 90%. Testing at varying temperatures and humidity might influence your test results, resulting in a non-consistent, non-reliable test result. Even more so, when the test results are influenced by the temperature and humidity this indicates that the performance of the printed parts also varies under varying temperature and humidity. This is a factor which should be taken into account when designing and producing specific parts.

### 3.2.1. Method

In order to validate whether the test results are influenced by temperature and RH several specimens are produced using 3D printing. Silver metallic PLA of the Ultimaker brand is used to produce the specimens. Before printing, the material is stored on the 3D printer for 24 hours under a specific temperature and humidity. Hereafter, the print is made under the same conditions. An Espec humidity oven is used to control the temperature and humidity of the environment. The filament is stored and printed at 20$^oC$ and 35$^oC$ at relative humidity of 50%, 70% and 90%. In the table 3.1 the corresponding absolute humidity to these conditions is shown.

The geometry of the 3D printed specimens was modelled in Rhinoceros, saved as an STL file and opened in the open source software Cura. Cura software was used to generate the G-code file and to command and control the printer parameters. The ASTM D790 test dimensions were used for the production of the small specimens as shown in figure 3.1.

Per condition (temperature and relative humidity combination) two batches of 7 specimens were created. The Ultimaker 2Go 3D printer is used to created the specimens. Due to the small dimensions of the printer, it fits in the humidity oven. Furthermore, Ultimaker is known as a reliable 3D printer, therefore deviations caused by an unreliable printer are minimized. The Ultimaker to Go printer is upgraded with a heating bed, which makes it possible to heat the build plate. Before printing, blue Ultimaker tape is applied to the build plate. Except for the humidity and temperature at which the filament is stored before printing and at which the printer is operated during printer, all printer parameters are similar for all the print batches. The constant print parameters used can be found in table 3.2.

After production of the specimens with the 3D printer, the print is removed from the build plate. Hereafter, the printed brim is removed and the specimens are detached from each other and stored for at room temperature at low RH. 24 hours before testing, the specimens are placed in the Espec humidity oven at either 20$^o$C and 50% RH or at 40$^o$C and 90% RH. After 24 hours, the specimens are taken out of the humidity oven, weighted and directly after weighting tested for their bending properties. A precision scale of KERN with a deviation of 0.01 mg/0.1 is used to weigh, to test the bending properties a Zwick//Roell testing machine is used.

### 3.2.2. Results

After printing and conditioning the printed parts, the specimen are weighted and tested for their mechanical properties.

#### Weight

All specimen were weighted immediately before they are tested for their bending properties. Although in previous experiments a higher weight corresponded to better bending properties, it was expected that in this experiment higher weight would result in poorer bending properties. This is because it was expected that the specimen which were placed in the humidity oven at $40^oC$ and 90% had absorbed more water than the specimen placed in the humidity oven at $20^oC$ and 50%. The absorption of water might decrease the specimens Tg, according to Passerini and Craig [79] the change in Tg followed the Gordon-Taylore relationship [88], as described in equation 3.1.

$$Tg_{mix} = \frac{w_1 * Tg_1 + k * w_2 * Tg_2}{w_1 + k * w_2} \tag{3.1}$$

With k being a constant value;

$$k = \frac{\rho_1 * Tg_1}{\rho_2 * Tg_2} \tag{3.2}$$

For PLA and water this results in a value of 0.415 for k. Passerini and Craig furthermore state that totally dry PLA has a Tg of around $52^oC$.

A flaw in the performed experiment is that the specimen are not dried and weighted when dry, therefore it is not possible to exactly determine the amount of water present in the specimen. It is however possible to look at the difference in weight between the specimen placed at $20^oC$ and 50% RH and the specimen placed at $40^oC$ and 90% RH 24 hours before testing. This enables us to make a rough estimate about the water uptake and potential related decrease in Tg. Although this is not correct, the weight of the specimens at $20^oC$ and 50% RH is considered as the 'dry weight'. Table 3.3 displays the weight of the specimens placed at $20^oC$ and 50% RH and $40^oC$ and 90% RH 24 hours before testing, with the corresponding Tg according to equation 3.1, considering the specimens placed at $20^oC$ and 50% RH as the dry specimens and using 325K as the Tg for the dry PLA and 135K as the Tg for water.

Table 3.3: 'Dry' and wet weight, with corresponding estimated Tg for the wet specimen.

| Filament & Print Conditions | | Weight (g) of specimen after 24 hours at: | | | | Weight Difference | Corresponding Tg |
|---|---|---|---|---|---|---|---|
| Temp. $^oC$ | Hum. % RH | Temp. 20 $^oC$ | Hum. 50% RH | Temp. 40 $^oC$ | Hum. 90% RH | Δ g | $^oC$ |
| 20 | 50 | 0,9967 | | 1,0013 | | 0,0045 | 51,6 |
| 20 | 70 | 0,9914 | | 0,9990 | | 0,0075 | 51,4 |
| 20 | 90 | 0,9952 | | 0,9980 | | 0,0028 | 51,7 |
| 35 | 50 | 1,0172 | | 1,0193 | | 0,0021 | 51,8 |
| 35 | 70 | 0,9897 | | 1,0287 | | 0,0391 | 48,9 |
| 35 | 90 | 0,9178 | | 1,0223 | | 0,1045 | 43,4 |

Remarkable is that the difference in weight is small for all specimens which are manufactured with material stored at, and a printer operating at a temperature of $20^oC$. Also for the specimens which are printed at and with material stored at $35^oC$ and 50% RH, the difference in weight is small. However, the increase in weight for the specimens produced at $35^oC$ and 70/90% RH shows a substantial difference in weight. Figures 3.5, 3.6 and 3.7 demonstrate that the surface quality of these prints is relatively good for low temperature and humidity. However, when increasing the temperature or humidity of filament storage and printing, the adhesion to the build plate resulting in poor surface print quality. During

the manufacturing process, water evaporates when reaching the nozzle. At higher temperature and humidity this causes the material to form larger voids. This more open structure might absorb more water then the specimens produced at lower temperature and humidity, resulting in a higher decrease in Tg when stored under humid conditions.

**Bending properties**

*$F_{max}$*
When looking at the weight for the specimens stored at 20$^o$C and 50% RH and 40$^o$C and 90% RH, all specimens produced at 20$^o$C show a minimal increase in weight. Therefore, it is expected that the changes in the material are minimal and the $F_{max}$ values to be similar. The same accounts for the specimens produced at 35$^o$C and 50% RH. The rough estimates of Tg for the specimens stored at these conditions also show a minimal difference in Tg. The specimens produced at 35$^o$C and 70/90% RH however result in a greater difference in weight when stored at 20$^o$C and 50% RH compared to storing conditions of 40$^o$C and 90% RH. The Tg of these specimens is lower, while the storage temperature is higher. Therefore, a substantial difference in $F_{max}$ is expected for these specimens. The test results are shown in figure 3.13.

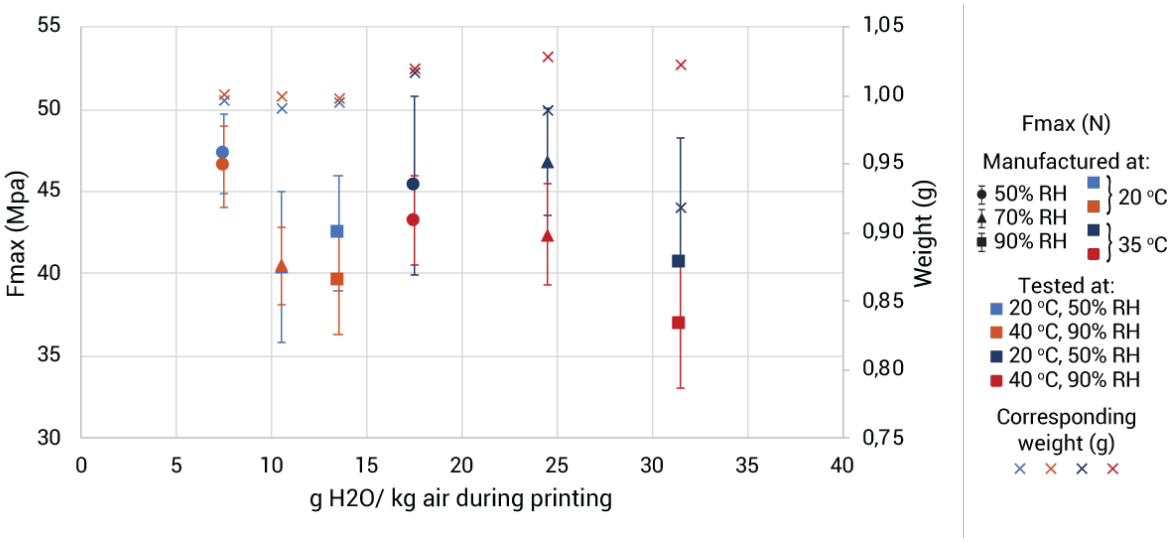


Figure 3.13: $F_{max}$ of the specimens for different testing conditions of the specimens placed at specific temperature and humidity 24 hours before testing. The error bars show the standard deviation.

As visible in figure 3.13, the $F_{max}$ decreases when it is stored 24 hours at increased temperature and humidity prior to testing. The largest difference in $F_{max}$ is noticed for the samples printed at 35$^o$C. The increase in weight does not seem to be a good indicator on how $F_{max}$ is influenced. The largest difference in weight is measured for the samples stored at different temperature and humidity which are produced at 35$^o$C and 90% RH, but the difference in $F_{max}$ is relatively low for these samples. This while nearly any weight difference is measured for the batch of samples stored at different temperature and humidity which are produced at 35$^o$C and 50% RH, while these samples resemble one of the largest differences in $F_{max}$.

*Bending Strength*
For bending strength similar results are expected as for $F_{max}$. The higher storage temperature is closer to the specimens' Tg. Furthermore, the higher RH at higher temperature results in more water uptake, which lowers the Tg. It is expected that this negatively influences the bending properties. The results of the tests are showed in figure 3.13

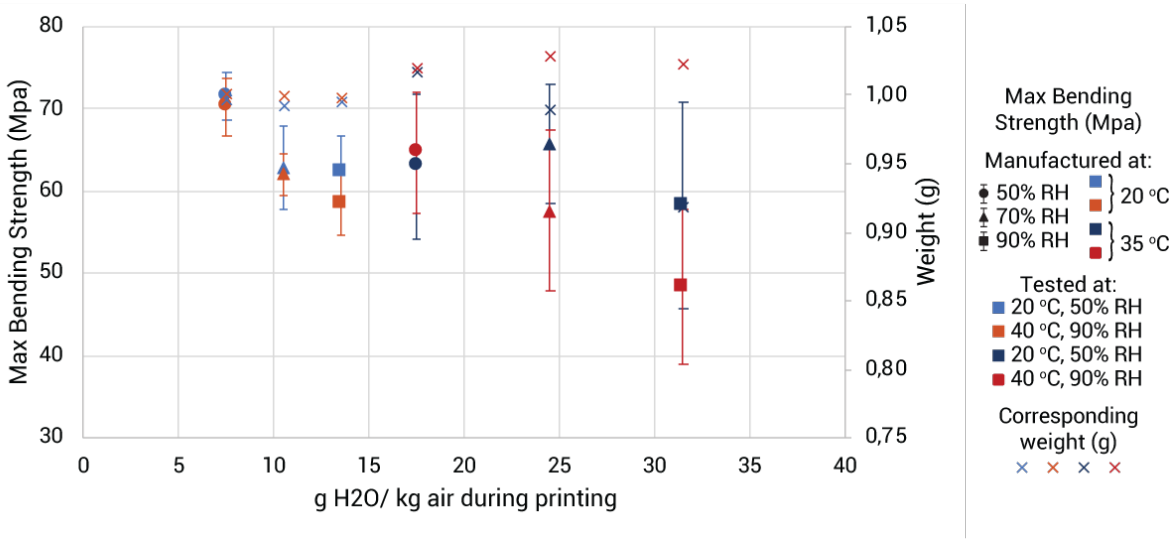


Figure 3.14: Bending strength of the specimens for different testing conditions of the specimens placed at specific temperature and humidity 24 hours before testing. The error bars show the standard deviation.

As visible in figure 3.14, the maximum bending strength decreases when it is stored 24 hours under increasing temperature and humidity prior to testing. Remarkably this difference is especially seen for the samples produced at 35$^o$C and 50 and 90 %RH. The samples which are produced at lower temperatures or RH, already approach the Tg when stored at 40$^o$C and 90% RH. The Tg of these samples is around 51.4 - 51.8 $^o$C, while the Tg of the sample produced at 35$^o$C and 70% RH is around 48.9 $^o$C. This difference is only 0.5 - 0.9 $^o$C, but seems to have a great influence. This might be explained by the weight difference, the weight difference for the two samples produced at 35$^o$C and 50 and 90 %RH. These are the only two samples at which the weight difference is higher than 1% (4% and 11.4%).

*Elastic modulus*

Similar to $F_{max}$ and maximum bending strength, it is expected that the elastic modulus will decrease when storing 24 hours at higher temperature and RH, due to the fact that the Tg is closer to the storage temperature. The test results are shown in figure 3.15.

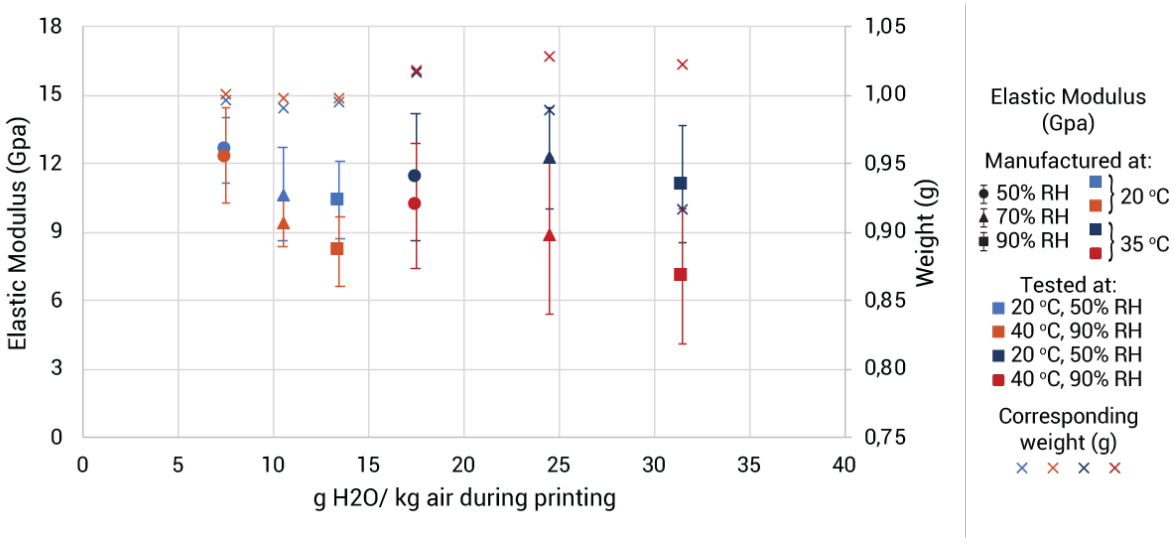


Figure 3.15: Elastic modulus of the specimens for different testing conditions of the specimens placed at specific temperature and humidity 24 hours before testing. The error bars show the standard deviation.

As visible in figure 3.14, the elastic modulus decreases when the specimens are stored under increased temperature and humidity 24 hours prior to testing. Similar to the maximum bending strength, the

largest difference is seen for the samples produced at 35$^{o}$C and 50 and 90 %RH. This might be explained by the water uptake of these samples. The weight difference for these two samples is higher than 1% (4% and 11.4%), due to which the Tg decreases which might influence the mechanical properties of the specimen.

### 3.2.3. Conclusion

As described above, storing the specimens at increasing temperature and RH ranging 24 hours prior to testing can negatively influence the measured bending properties.

When looking at the mechanical bending properties of the printed specimens;

- The mechanical bending properties of the final prints are poorer when stored at increased temperature and relative humidity 24 hours prior to testing.
- The effect of increasing storage temperature and RH is largest on the prints which are created with filament stored and a printer operating at higher temperature and RH.
- The biggest weight difference between storage at increased temperature and RH was measured for the specimens which are created with filament stored and a printer operating at higher temperature and RH. The high weight difference indicates that these specimens can absorb more water than the specimens created at lower temperature.

## 3.3. Discussion

When designing, testing, and manufacturing a 3D printed device, it is important to keep in mind that room temperature and RH might influence the performance of the 3D printed device. It is important to understand in what environmental conditions the final print will be used. It is wise closely monitor the environmental temperature and RH during storage of the print material, during printing, and during testing. A QA process could be set up to cancel printing when temperature and RH are too high. Extra research is needed to define at what exact temperature and RH it should be advised to stop printing. Furthermore, when validating the print, it would be best to test the final print under the warmest and most humid conditions which can be expected for usage. This simulates the 'worst-case' scenario for usage. When it is not possible to create this test environment an extra safety factor should be taken into mind when testing the print.

# 4

# Discussion

This report studied and investigated the quality assurance of 3D prints. First, a low-cost homemade set-up was designed and built. Hereafter, the influence of varying temperatures and humidity on print quality was investigated.
Initially, the results of the homemade set-up were validated and compared with the Zwick/Roell test set-up. For this purpose, 3D printing was employed to create PLA specimens. The dimensions of the specimen were set according to the ASTM D790 standard. The samples were tested under varying temperatures and 50% RH conditions. The results showed no significant difference between the bending properties measured by the homemade and conventional Zwick/Roell test set-up except for the the $F_{max}$ measured with specimen batch 1. All the results measured with the homemade test set-up showed a higher value than the results measured with the Zwick/Roell test set-up, indicating the possibility that the homemade test set-up is wrongly calibrated at the beginning. Therefore, calibrating the load cell might result in lower results and a non-significant difference between all the results measured by the homemade test set-up and the Zwick/Roell test set-up
Furthermore, detailed tests were performed in temperatures ranging from $20^oC$, $35^oC$ and $40^oC$ at a relative humidity of 50%, 70%, and 90%. It was noted that higher temperature and humidity negatively affected the print's bending properties. An increasing humidity at $20^oC$ has a minimal effect on the final print. Increasing humidity at $35^oC$, however, negatively impacts the bending properties of the print. Hence, for storing filament and manufacturing a product, the temperature, and relative humidity should be kept at low temperature and humidity to ensure good print quality. The mechanical bending properties of the final prints are lower when placed in warmer and more humid conditions (24 hours prior to testing). The effect of increasing storage temperature and %RH is most significant on the prints created with filament stored and a printer operating at a higher temperature and %RH. Increased temperature and humidity before testing also increased weight, indicating water uptake. These bending properties strongly correlate with the printed product's weight. For this case, heavier weight means poorer bending properties. The final weight gives a reasonable estimation of the print properties; a lower weight indicates under-extrusion or hampering of material feeder, which results in poorer bending properties.

## 4.1. Limitations

The test-set up is now built to test bending properties, however, changing the grips should enable the test set-up to also test for other mechanical properties. These grips should be created and also validate for their reliability.
Furthermore, the test set-up has not yet been optimized to withstand power outages. It could be necessary that extra protections should be build in, to protect the test set-up from power outages.
Lastly, the test set-up should be locally built by end-users to verify whether these end-users can indeed locally obtain the components for the test, build and operate the test, and validate whether the step-by-step instructions are effective, especially for local end-users with limited knowledge of the open-source

software Arduino.

To measure the influence of temperature and RH, different test methods are designed. However, there are some limitations;
In the current method, the influence of temperature and RH is only measured for bending strength, while many prints will be created in which other mechanical properties are more critical. Therefore, the influence of temperature and RH on other mechanical properties should also be measured.
The dimensions of the printed specimen are very small. Therefore, if the adhesion to the build plate is poor, this has a big influence on the print quality. Increasing temperature and RH result in poorer adhesion to the build plate. Therefore, When creating bigger specimens, the influence of increased temperature and RH might decrease.
In order to investigate the influence of increased temperature and RH during the testing of the mechanical properties, the printed specimens were placed in a humidity oven 24 hours prior to testing. However, since the Zwick/Roell test set-up did not fit into the Espec humidity oven, the specimen are taken out of the oven and (directly) tested for their properties at room temperature. The results might have differed if the specimen were also tested in the humidity oven.
By storing the 3D printer filament 24 hours prior to printing at set conditions in the Espec humidity oven, it is not possible to solely investigate the influence of temperature and humidity on the printing process. Therefore, it is not possible to conclude whether the decreased bending properties are a result of the material stored in the oven prior to printing, due to the printing process taking place at higher temperature and RH or due to a combination of both.

## 4.2. Recommendations

Further research is needed to ensure that the correlation in continuity in mechanical properties of a test strip and the mechanical properties of the final product, which were produced simultaneously, is strong enough to guarantee the continuity in mechanical properties of the final product solely by testing the test strip. When this seems to be the fact, the following steps can be taken to ensure the mechanical properties of the product.

- Design process
  - Design and optimise the product while validating for simulated use. When printing the product, simultaneously print a test-strip.
  - Validate the final product for the worst possible user conditions; at high temperature and high relative humidity.
  - When the final product passes the simulated user tests, weigh the test strip and test for mechanical properties using the homemade test set-up.
- Prior to printing
  - Store filament under dry conditions at low temperature.
  - Measure temperature and humidity prior to printing, only print when temperature is between 20-35 degrees. When temperature is around 35 degrees, do not print if relative humidity is higher than 50%.
- While printing
  - Measure temperature and humidity during the print process. If the temperature becomes higher than 35 degrees, thoroughly inspect the print, especially when relative humidity becomes higher than 50%.
- After printing
  - Visually inspect the print for abnormalities.
  - Weigh the print after production. When the print's weight is lower than expected, pay extra attention in the next step.
  - Test the printed test strip with the homemade test set-up for mechanical properties. When the mechanical properties of the printed test strip are insufficient, the printed product needs to be rejected.

# A

# Building the test

## A.1. Part list

Table A.1: The parts used in this test set-up with corresponding price and webshop

| | Item | # | Price/ Piece | Total Price | Source (Click for link) |
|---|---|---|---|---|---|
| Electronics | Load cell | 1 | $23,60 | $23,60 | AliExpress |
| | Arduino Leonardo | 1 | $8,60 | $8,60 | Jumia |
| | Motor driver A4988 | 2 | $1,22 | $2,44 | Jumia |
| | Wire male & male | 1 | $3,91 | $3,91 | Jumia |
| | Wire female & male | 1 | $3,91 | $3,91 | Jumia |
| | Breadboard | 1 | $3,67 | $3,67 | Jumia |
| | Power supply | 1 | $7,37 | $7,37 | Jumia |
| | | | | | |
| Actuator & Sensor | LoadCell amplifier HX711 | 1 | $4,83 | $4,83 | Jumia |
| | Stepper motor | 2 | $14,11 | $28,22 | Jumia |
| | Lead screw & nut TR8 x 0.5 | 2 | $5,46 | $10,92 | Jumia |
| | Flange 8 mm | 2 | $1,68 | $3,35 | Jumia |
| | Motor coupling 8/8 | 2 | $1,16 | $2,32 | Jumia |
| | | | | | |
| Frame | Alu4040 500 mm | 2 | $3,02 | $6,04 | Jumia |
| | Alu4040 100 mm | 4 | $0,76 | $3,02 | Jumia |
| | Alu4040 300 mm | 2 | $3,02 | $6,04 | Jumia |
| | Alu4040 210 mm | 1 | $3,02 | $3,02 | Jumia |
| | Nuts & bolts | | $7,54 | $7,54 | Jumia |
| | $90^o$ Angle profile | 8 | $3,69 | $29,52 | Jumia |
| | | | | | |
| | **Total** | | | **$158,32** | |

## A.2. Tool list

Table A.2: Required tools for making the test set-up

| | |
|---|---|
| **Minimal required** | Drill<br>Drill bits<br>Pencil<br>Center punch<br>Hammer<br>Ruler<br>Wrench |
| **Recommended** | Drill press<br>Engineer square/<br>Spirit level |

## A.3. Assembly

### A.3.1. 3D printing

While it is possible to buy most necessary items, it is harder to find suitable grips for the bending test. Therefor, the required grips are printed. The STL files for the grips can be found here. These are the grips for 3-point bending tests. For tensile tests, one can use the grips designed by [3] which can be found here. It is recommended to print the grips with printer parameters which result in a high quality print. So 100% infill, zero (or negative) air gap, low printer speed and small layer height.

### A.3.2. Drilling the holes

In order to secure the stepper motor, the digital caliper and the middle bar with lead screw and nut, several holes have to be drilled into the bars of the frame before assembling the frame.

As a first step the holes for the lead screw and nut have to be drilled in the middle bar (210 mm). First, the hole for the lead screw is made;

(a) Measure a distance of 16 mm from the end and a distance of 20 mm from the edge of the middle bar.

(b) Indicate with a pencil where the holes have to be drilled.

(c) Use a center punch and hammer to make a small hole where the holes for the nut have to be placed.

(d) Drill the hole using a drill bit suitable to drill metal with a diameter slightly bigger than the 8mm of the lead screw, if necessary first use a drill with a smaller diameter.

(e) Repeat the above steps for the other side of the middle bar.

(f) When the holes are drilled, check whether the lead screw easily passes through the holes. If not, repeat step 2d using a slightly bigger drill.

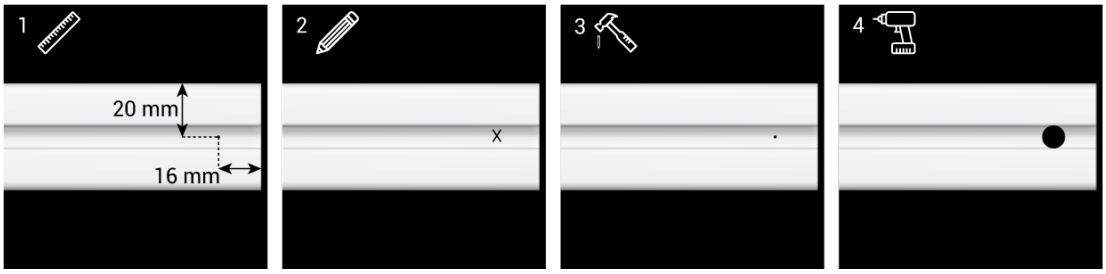

When the holes for the lead screw are drilled, the holes for the lead nut have to be drilled;

(a) Place the lead nut at the middle bar in such a way that the drilled hole for the lead screw is exactly in the middle of the nut.

(b) Indicate with a pencil where the holes have to be placed.

(c) Use a center punch and hammer to make a small hole where the holes for the nut have to be placed.

(d) Drill the holes using a drill bit suitable to drill metal with a diameter suitable for the bolts used to ensure the lead nut. Drill the holes through the entire middle bar.

(e) Repeat the above steps for the other side of the middle bar.

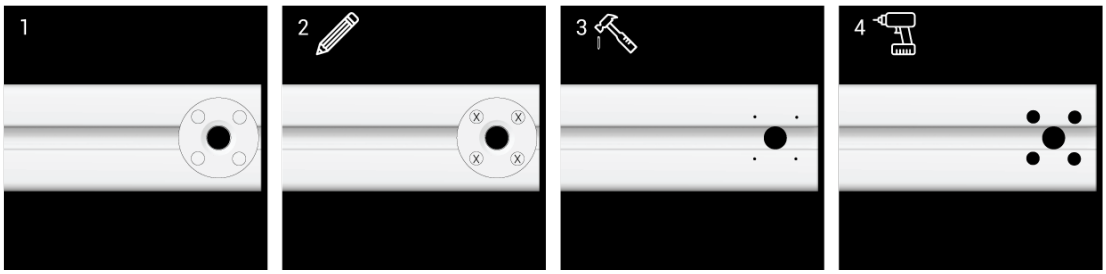

### A.3.3. Lower bar

In order to assemble the lower bar, perform the following steps;

(a) Take the lower bar (300 mm).

(b) Place 8 bolts in the slot of on side of the lower bar and place 4 bolts in the two slots of the adjacent sides as displayed.

(c) Screw the two vertical bars (500 mm) on the first and the $8^{th}$ bolts placed on the lower bar, such that they are placed on the two ends of the lower bar

(d) Your set-up should look like this.

(e) Screw the four little bars (100 mm) on the first and the $4^{th}$ bolts placed on the two sides on the lower bar, such that they are placed on the two ends of the lower bar.

(f) Your set-up should look like this.

(g) Slide 2 bolts in the slots of every little bar, one facing the 'ceiling' and one facing the opposite little bar. Slide two bolts in the slots of both the vertical bars facing the same direction as the little bar.

(h) Place 8 angle profiles, using the bolts placed in the slots.

(i) Attach the angle profiles using nuts.

(j) Your set-up should look like this.

(k) Place the two flanges on the bolts two most outer bolts of the lower bar, such that the end of each flange touches the vertical bar and attach using nuts.

(l) Both corners of the lower bar should look like this.

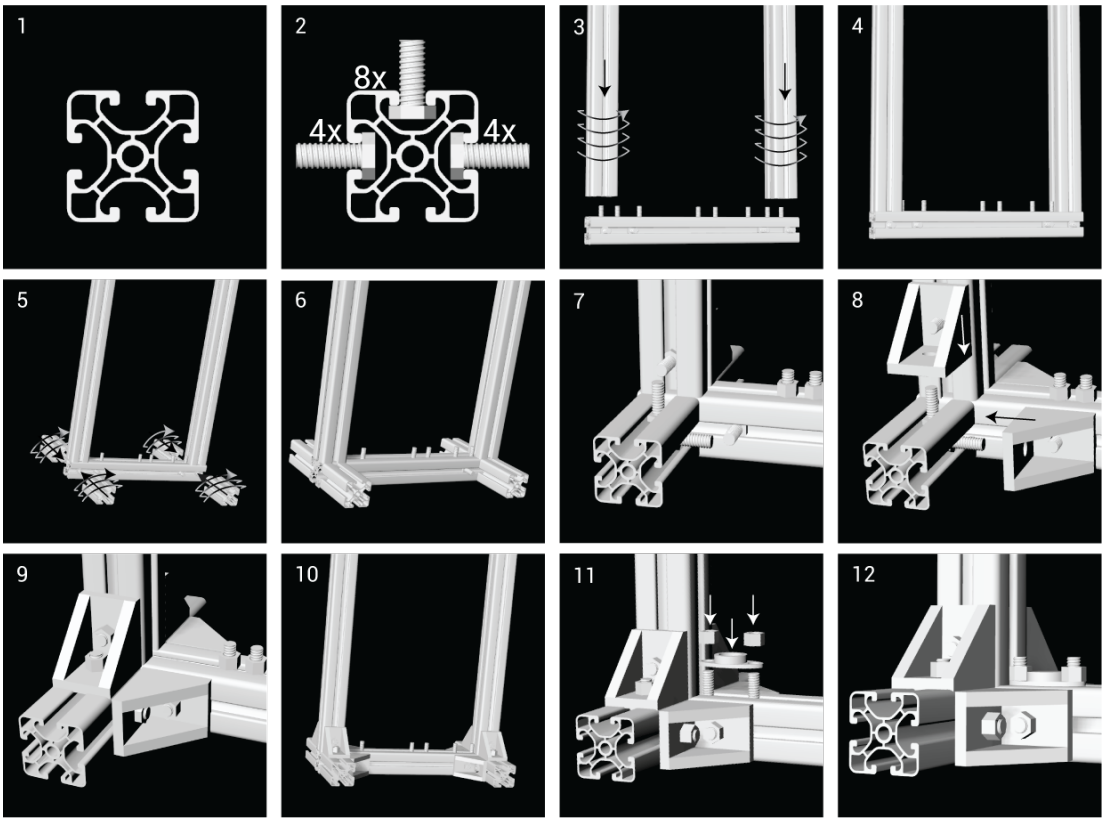

### A.3.4. Middle bar

In order to assemble the middle bar, take the bar middle bar in which the holes are drilled and perform the following steps;

(a) Place a bolt in the slot of on side of the middle bar such that the bolt stick out at one side at which the holes are also visible.

(b) Place the long bolts through the four holes which are drilled for the lead nut and place the lead nut on the four holes.

(c) Attach the lead nut using nuts. And repeat for the other end of the middle bar.

(d) Your set-up should look like this.

(e) Attach the load cell by screwing it onto the bolt placed in step 2a, if necessary use an extra nut to attach the load cell extra firm.

(f) Your set-up should look like this.

(g) Place the printed loading 'nose' by placing the sawed bolt and nut and screwing the printed nose onto it.

(h) Your set-up should look like this.

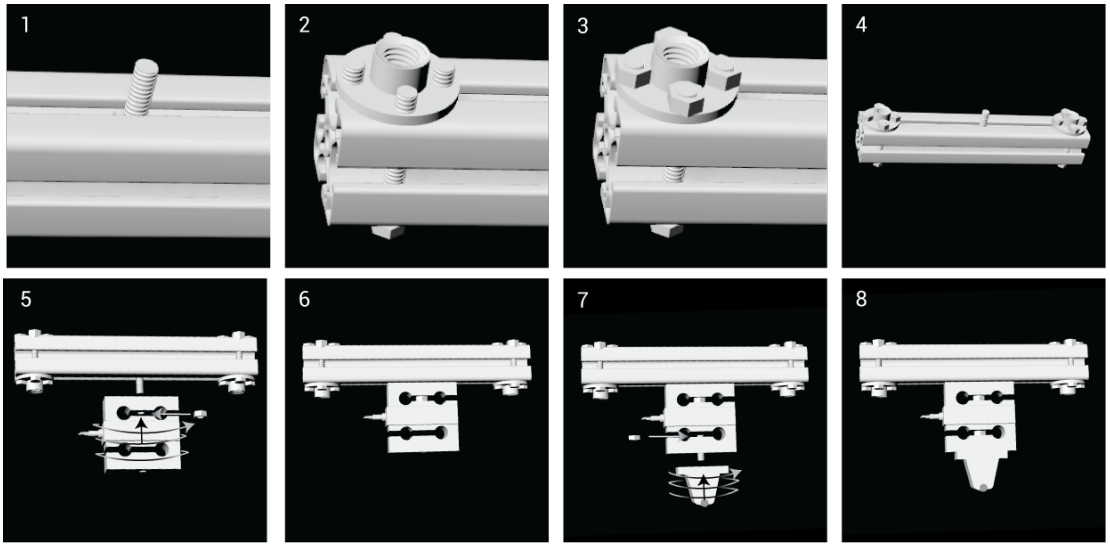

### A.3.5. Assembly

For the final assembly, the upper bar is placed, motor is coupled to the lead screw and the lead screw is placed.

(a) Place four bolts in the slot of on side of the upper bar such that the bolt stick out at one side at which the holes are also visible.

(b) Place two angle profiles on the two inner bolts which are placed on the upper bar. Attach with nuts.

(c) Place the upper bar on the two vertical bars (placed on the lower bar), such that the angle profiles face down.

(d) Place the lead screws on the middle bar, by driving them into the lead nuts. Make sure the lead screws are just as much driven into the left as into the right lead nut.

(e) Attach the motors to the lead screws using the motor coupling.

(f) Place the lead screw on the bearing flanges of the lower bar.

(g) Secure the motors to the upper bar using the angle profiles (of step 2)

(h) Your test set-up is finished, it should look like this.

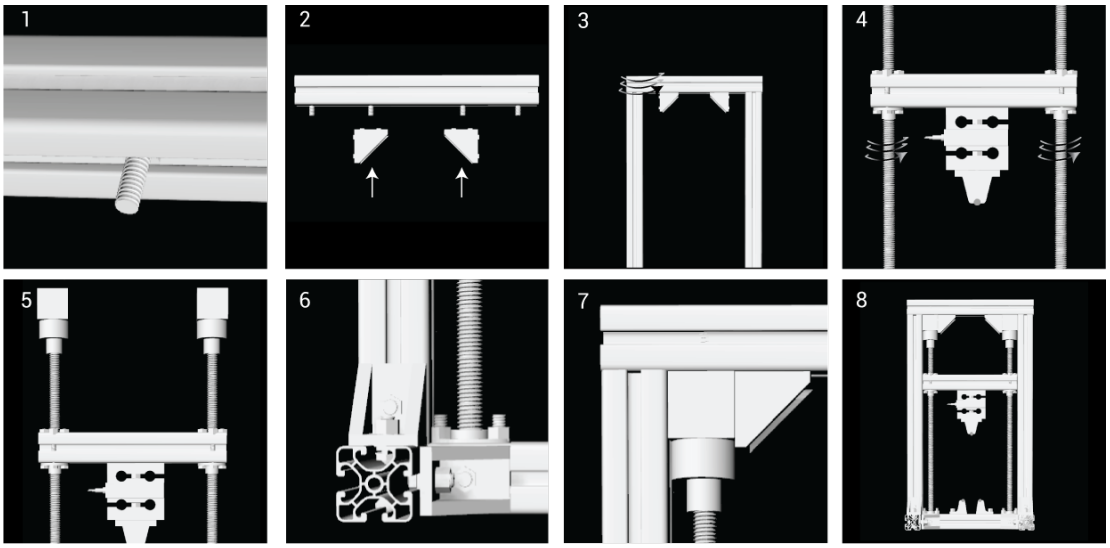

## A.4. Electronics

Now the electronic part needs to be assembled. Herefore, the following electronic schematic has to be build:

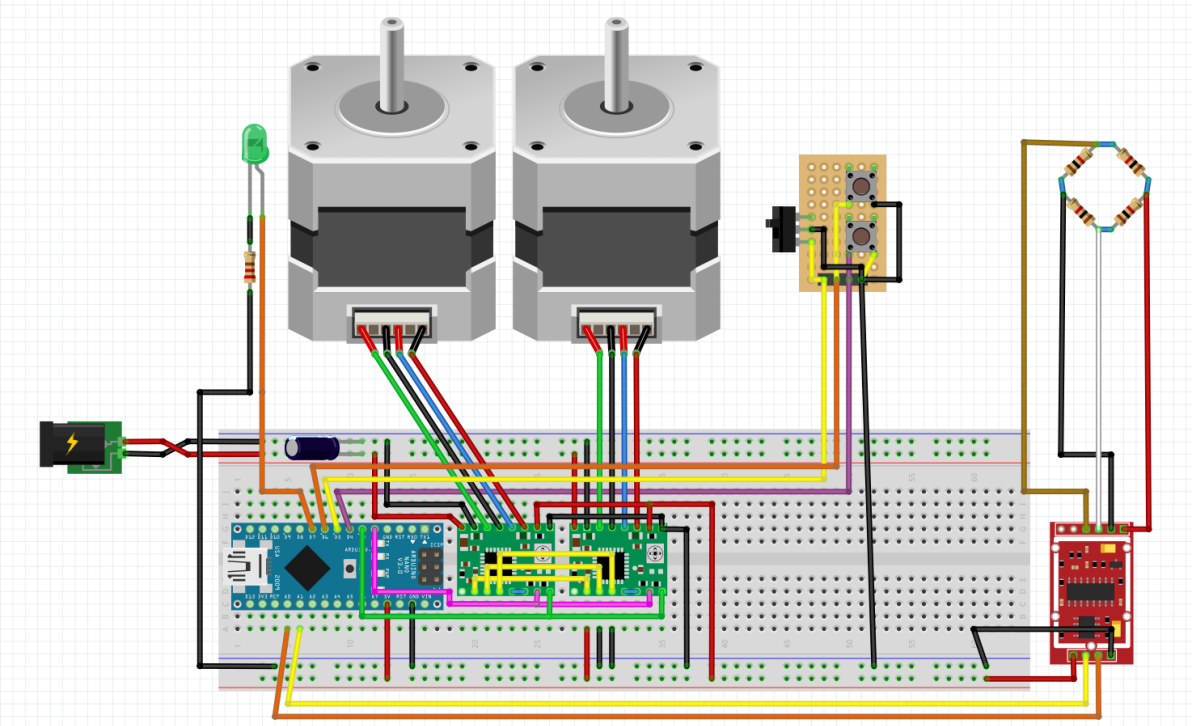

Figure A.1: Schematics Electronics

Blue is the arduino nano, the green parts are the stepper motor drivers and the red part resembles the load cell amplifier. Their ports are placed on the breadboard as listed below:

| D12 | D11 | D10 | D9 | D8 | D7 | D6 | D5 | D4 | D3 | D2 | GND | RST | RXO | TX1 |
|---|---|---|---|---|---|---|---|---|---|---|---|---|---|---|
| ARDUINO NANO | | | | | | | | | | | | | | |
| D13 | 3V3 | REF | A0 | A1 | A2 | A3 | A4 | A5 | A6 | A7 | 5V | RST | GND | VIN |

| VMOT | GND | 2B | 2A | 1B | 1A | VVD | GND |
|---|---|---|---|---|---|---|---|
| MOTOR DRIVER 14988 | | | | | | | |
| ENABLE | MS1 | MS2 | MS3 | RESET | SLEEP | STEP | DIRECTION |

| YLW | GRN | WHT | BLK | RED |
|---|---|---|---|---|
| LOAD CELL AMPLIFIER HX711 | | | | |
| GND | CLK | DAT | VCC | VDD |

## A.5. Software

In order to use the test set-up, the required software needs to be installed and implemented.

### A.5.1. Installing the software

(a) Go to https://www.arduino.cc/en/software and choose the correct software for your computer/tablet.

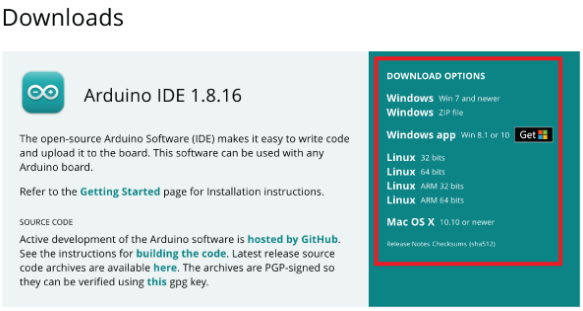


(b) Download the software. Choose 'just download' if you want to download it for free, choose a amount and 'contribute and download' if you want to contribute to the Arduino community.

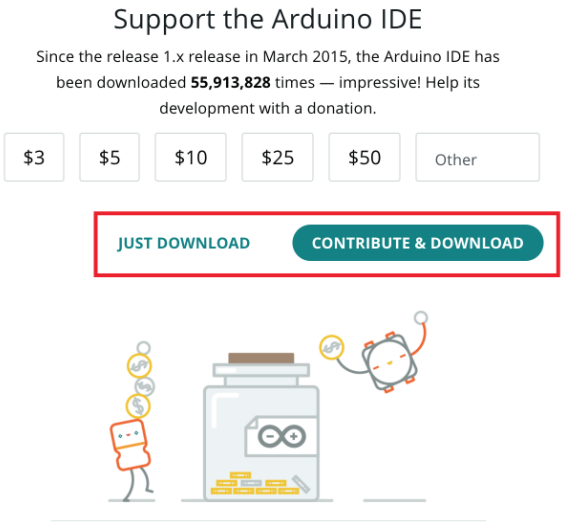


(c) Unpack the zip in your downloads and place the 'Arduino' program in the folder with programs.

### A.5.2. Installing software packages

Hereafter, some software packages need to be installed:

(a) Open Arduino.

(b) Go to sketch -> Include Library -> Manage Libraries

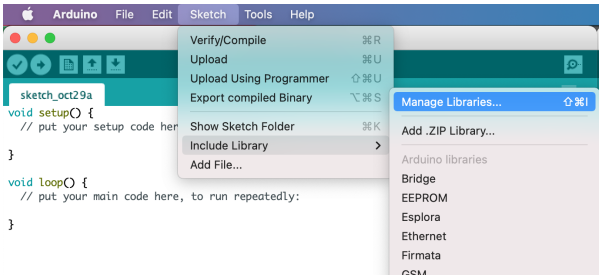


(c) Search for 'hx711' -> select in HX711 Arduino Library the latest version and click 'Install'.

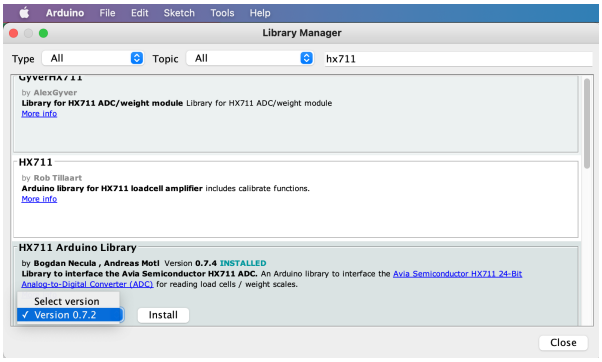


(d) Go to Tools -> Board -> Boards Manager

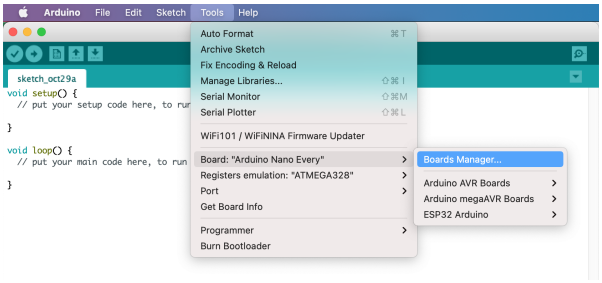


(e) Search for 'nano every' -> select in the latest version and click 'Install'.

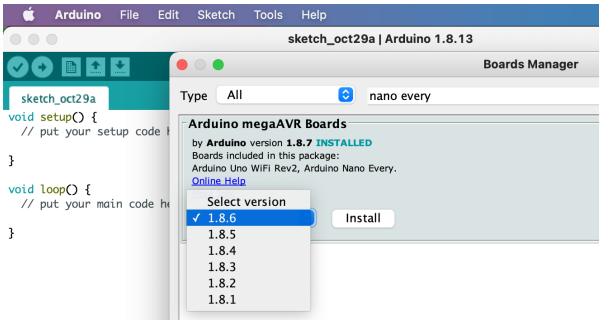

### A.5.3. Writing the code

The code can now be copy pasted into Arduino. if copied, click 'upload'. There are two things which needs to be done (inidcated in red in the code). First of all the correct serial number needs to be selected. Click on the magnifying glass on the top right corner to go to the serial monitor. On the right bottom, one can select the serial number. It is set at 38400, so this needs to be selected.
Hereafter, the load cell needs to be calibrated. Place a known weight to the load cell and look at the serial monitor what value the load cell returns. It is not necessary to purchase an expensive weight, one can use items such as a cola can or water bottle to calibrate. This might slightly influence the accuracy of the test set-up, but this should not be a problem. Change 8800 in the scale.set_scale(8800) such that the returned value corresponds with the known weight. Put another weight and check if the returned value still corresponds with the new weight.

**CODE**

```
// Load Cell

#include "HX711.h"
const int LOADCELL_DOUT_PIN = A0;
const int LOADCELL_SCK_PIN = A1;

void setup() {
Serial.begin(38400);

Serial.println("Initializing the scale");

scale.begin(LOADCELL_DOUT_PIN, LOADCELL_SCK_PIN);

Serial.println("Before setting up the scale:");
Serial.print("read: \ t\t");
Serial.println(scale.read()); // print a raw reading from the ADC

Serial.print("read average:\t\t");
Serial.println(scale.read_average(20)); // print the average of 20 readings from the ADC

Serial.print("get value:\t\t");
Serial.println(scale.get_value(5)); // print the average of 5 readings from the ADC minus the tare weight
(not set yet)

Serial.print("get units:\t\t");
Serial.println(scale.get_units(5), 1); // print the average of 5 readings from the ADC minus tare weight
(not set) divided
// by the SCALE parameter (not set yet)

scale.set_scale(8800); // this value is obtained by calibrating the scale with known weights
scale.tare(); // reset the scale to 0

Serial.println("After setting up the scale:");

Serial.print("read:\t\t");
Serial.println(scale.read()); // print a raw reading from the ADC
```

```
Serial.print("read average:\t\t");
Serial.println(scale.read_average(20)); // print the average of 20 readings from the ADC

Serial.print("get value:\t\t");
Serial.println(scale.get_value(5)); // print the average of 5 readings from the ADC minus the tare weight,
set with tare()

Serial.print("get units:\t\t");
Serial.println(scale.get_units(5), 1); // print the average of 5 readings from the ADC minus tare weight,
divided
// by the SCALE parameter set with set_scale

Serial.println("Readings:");
}

void loop() {
Serial.print("one reading:\t");
Serial.print(scale.get_units(), 1);
Serial.print("\t| average:\t");
Serial.println(scale.get_units(10), 1);

scale.power_down(); // put the ADC in sleep mode
delay(1000);
scale.power_up();
}

float measuringIntervall = 2; //Measuring interval when IDLE
float measuringIntervallTest = .5; //Measuring interval during SLOW test
float measuringIntervallTestFast = .15; ///Measuring interval during FAST test

long tareValue;

// Stepper Variables

int pulseLength = 10;
float stepsPerMM = 200 * 2 * (13 + 212.0 / 289.0) / 2; // Steps per rev * Microstepping * Gear reduction
ratio / Pitch
float stepsPerSecond = stepsPerMM / 60; //1mm/min
int slowSpeedDelay = 3000; //Time delay between steps for jogging slowly
int fastSpeedDelay = 300; ////Time delay between steps for jogging fast
boolean dir = 0;

// PIN definitions
int directionPin = 3;
int stepPin = 2;
int speedPin = 5;
int upPin = 4;
int downPin = 6;
int led1Pin = 7;

// Variables
byte mode = 2;
byte modeAddition = 0;
```

```
float currentSpeed = stepsPerSecond; //SLOW Test speed
float fastSpeed = 25 * stepsPerSecond; //FAST Test speed (x25 = 25mm/min)
long currentMicros = micros();
long lastLoadValue = 0;
long lastStep = 0;
String inputString;
float maxForce = 0;
float loweringCounter = 0;
long startTime = 0;
long yMTestTime = 30 * 1000; //Modulus Test time for SLOW speed (=30s)
bool debug = false; //debug mode to test the remote

void setup() {
// Serial
Serial.begin(38400);

// Load Cell
tareValue = loadCell.averageValue(32);

// Stepper
pinMode(directionPin, OUTPUT);
pinMode(stepPin, OUTPUT);
digitalWrite(directionPin, dir);
digitalWrite(stepPin, LOW);

//Up Button
pinMode(upPin, INPUT);
digitalWrite(upPin, HIGH);

//Down Button
pinMode(downPin, INPUT);
digitalWrite(downPin, HIGH);

//Speed Switch
pinMode(speedPin, INPUT);
digitalWrite(speedPin, HIGH);

//LED Pin
pinMode(led1Pin, OUTPUT);
digitalWrite(led1Pin, LOW);

}

void loop() {
int stringRead = 0;
//Serial COmmunication
inputString = "";
while (Serial.available())
{
inputString = Serial.readString();
stringRead = 1;
}
if (stringRead == 1) {
```

```
String taskPart;
String rest;
taskPart = inputString.substring(0, inputString.indexOf(" "));
rest = inputString.substring(inputString.indexOf(" ") + 1);
if (taskPart == "M10") {  //Start SLOW test
mode = 1;
if (rest == "S1") {
modeAddition = 1;
}
measuringIntervall = measuringIntervallTest;
maxForce = 0;
loweringCounter = 0;
digitalWrite(directionPin, LOW);
printSpaces(5);
Serial.println("Tare");
tareValue = loadCell.averageValue(32); //Tare
Serial.println("Start Test");
digitalWrite(led1Pin, HIGH);
delay(500);
digitalWrite(led1Pin, LOW);
delay(200);
digitalWrite(led1Pin, HIGH);
delay(500);
digitalWrite(led1Pin, LOW);
}  else if (taskPart == "M11") {  //manual Mode (not implemented yet)
Serial.println("Manual Mode");
measuringIntervall = 2;
mode = 2;
}  else if (taskPart == "M12") {  //tare
measuringIntervall = 2;
Serial.println("Tare");
tareValue = loadCell.averageValue(32);
}  else if (taskPart == "M13") {  //Youngs Modulus Test Mode
mode = 4;
measuringIntervall = measuringIntervallTest;
maxForce = 0;
loweringCounter = 0;
digitalWrite(directionPin, LOW);
printSpaces(5);
Serial.println("Tare");
tareValue = loadCell.averageValue(32);
Serial.println("Start Test");
digitalWrite(led1Pin, HIGH);
delay(500);
digitalWrite(led1Pin, LOW);
delay(200);
digitalWrite(led1Pin, HIGH);
delay(500);
digitalWrite(led1Pin, LOW);
startTime = millis();
}  else if (taskPart == "M14") {  //Start FAST test
mode = 3;
measuringIntervall = measuringIntervallTestFast;
maxForce = 0;
loweringCounter = 0;
digitalWrite(directionPin, LOW);
```

```
printSpaces(5);
Serial.println("Tare");
tareValue = loadCell.averageValue(32);
Serial.println("Start Fast Test");
digitalWrite(led1Pin, HIGH);
delay(500);
digitalWrite(led1Pin, LOW);
delay(200);
digitalWrite(led1Pin, HIGH);
delay(500);
digitalWrite(led1Pin, LOW);
} else {
Serial.println("ERROR: Command not found!");
}
}

// Bending Test Mode
if (mode == 1) {
currentMicros = micros();
if ((currentMicros - lastStep) >= 1000000. / currentSpeed) {
digitalWrite(stepPin, HIGH);
delayMicroseconds(pulseLength);
digitalWrite(stepPin, LOW);
lastStep = currentMicros;
} if (!digitalRead(downPin)) { //Stop test if DOWN Button is pressed
Serial.println("Test aborted - entering manual mode");
printSpaces(5);
mode = 2;
modeAddition = 0;
measuringIntervall = 2;
currentSpeed = stepsPerSecond;
}

// Manual Test Mode
} else if (mode == 2) {
boolean performStep = 0;
if (!digitalRead(upPin)) {
digitalWrite(directionPin, LOW);
performStep = 1;
if(debug){ Serial.println("UP"); }
} else if (!digitalRead(downPin)) {
digitalWrite(directionPin, HIGH);
performStep = 1;
if(debug){ Serial.println("DOWN"); }
}
//Perform Step
if (performStep) {
digitalWrite(stepPin, HIGH);
delayMicroseconds(pulseLength);
digitalWrite(stepPin, LOW);
}
if (digitalRead(speedPin)) {
delayMicroseconds(slowSpeedDelay);
if(debug){ Serial.println("Slow Speed");}
} else {
delayMicroseconds(fastSpeedDelay);
```

```
if(debug){ Serial.println("Fast Speed");}
}

// Fast Test Mode
}  else if (mode == 3) {
currentMicros = micros();
if ((currentMicros - lastStep) >= 1000000. / fastSpeed) {
digitalWrite(stepPin, HIGH);
delayMicroseconds(pulseLength);
digitalWrite(stepPin, LOW);
lastStep = currentMicros;
}
if (!digitalRead(downPin)) {
Serial.println("Test aborted - entering manual mode");
printSpaces(5);
mode = 2;
modeAddition = 0;
measuringIntervall = 2;
currentSpeed = stepsPerSecond;
}
// Youngs Modulus Test
}  else if (mode == 4) {
currentMicros = micros();
if ((currentMicros - lastStep) >= 1000000. / currentSpeed) {
digitalWrite(stepPin, HIGH);
delayMicroseconds(pulseLength);
digitalWrite(stepPin, LOW);
lastStep = currentMicros;
}
if (millis() - startTime >= yMTestTime) {
mode = 3;
measuringIntervall = measuringIntervallTestFast;
}
if (!digitalRead(downPin)) {
Serial.println("Test aborted - entering manual mode");
printSpaces(5);
mode = 2;
modeAddition = 0;
measuringIntervall = 2;
currentSpeed = stepsPerSecond;
}
}

// Get load value
currentMicros = micros();
if ((micros() - lastLoadValue) >= measuringIntervall * 1000000) {
digitalWrite(led1Pin, HIGH);
float loadValue = (loadCell.averageValue(1) - tareValue) / gainValue;
Serial.println(loadValue);
//Serial.println((loadCell.averageValue(1)-tareValue));
digitalWrite(led1Pin, LOW);
lastLoadValue = currentMicros;
if (mode == 1 && modeAddition == 1) {
if (loadValue >= maxForce) {
maxForce = loadValue;
loweringCounter = 0;
```

```
} else {
loweringCounter++;
}
if (loweringCounter >= 20) {
currentSpeed = currentSpeed * 4;
modeAddition = 0;
}
}
}
}

void printSpaces(int numberOfSpaces) { //This function will print a given amount of empty lines
for (int i = numberOfSpaces; i > 0; i–) {
Serial.println("");
}
}
```

# B

# Fused deposition modeling

The most common used 3D printing technology is material extrusion (ME) [89]. There are different ME techniques, the most accessible, affordable and therefor suitable ME technique for LMICs is fused deposition modeling (FDM).

## B.1. Fused deposition modeling technique

### B.1.1. The print process

The FDM technique uses a heated nozzle to extrude a bead of material. The material is supplied as continuous filament. The filament is pushed to the nozzle by a tractor-feed system. When the filament reaches the nozzle, it is heated and extruded through the nozzle in a semisolid state. The nozzle moves in the x-y plane. After the deposition of one layer, the build plate is lowered in the z-direction, and a new layer is added to the previous layer. The newly deposited material binds to the already extruded layer. This process continues until the print is completed. Constant pressure used to push the filament through the nozzle, constant nozzle temperature and constant print speed result in a product with a more continuous layer thickness. After extrusion through the nozzle, the product cools and solidifies. The nozzle temperature should be high enough to liquefy the material to enable extrusion. Overheating the material, however, deteriorates the product quality since the filament polymers tend to degrade at high temperatures. [90]

### B.1.2. Dimensional deviations

Extrusion of the material through the nozzle is related to applied pressure, nozzle geometry and material viscosity, which is primarily dependent on temperature. After material extrusion, the material ideally solidifies in the same shape and size. Gravity and surface tension, however, may cause the material to change shape, influencing the dimensional accuracy of the FDM fabricated product. Cooling of the material may cause the material to shrink. Shrinking of the material is minimal when the temperature difference between the surrounding and the extruded filament is minimal, and when the cooling process has a gradual and slow profile. For the layers to bind appropriately, sufficient residual heat energy is required. Insufficient residual heat energy generates a distinct boundary between new and previously deposited material, increasing the chance on fracture at this surface (fracture surface). Excessive heat energy, however, may cause the material to flow, resulting in low dimensional accuracy. Therefore, extruding temperature is a crucial factor for product quality in FDM [90].

### B.1.3. Printing with support

FDM builds products layer-by-layer, depositing extruded material on earlier extruded material. Printing with an overhang, therefore, requires support material. This support can either be printed with the

same product filament material or with support material. When printing with the same material, the removal of the support material is hard, and parts and supports must be carefully designed and placed with respect to each other. Adjusting the temperature may help in generating a fracture surface. Increasing the layer thickness might also affect the energy transfer and contribute to the generation of a fracture surface. Printing with support material, however, is the easiest way to remove the support material. Printers capable of printing with an overhang have two nozzles, one to extrude the product material and one to print the support material. The support material is soluble in water. When the product is printed, it is placed in a bath of water, the support material dissolves, and the product is ready. Printing with support gives the user more freedom, but requires extra material and enlarges the build time, which results in a higher cost price [90].

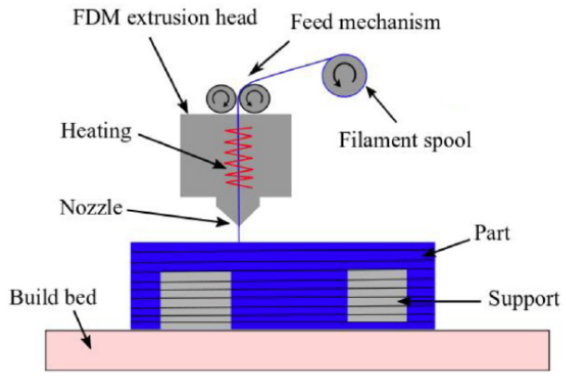


Figure B.1: A schematic visualization of the fused deposition modeling setup. This image is derived from [91]

Unlike many other 3D printers, a FDM printer is mainly composed of standard, widely available components. No expensive lasers are used, and the material does not have to be cured using light. Therefore, low-cost FDM printers are available on the market, and spare parts are easily obtained. Furthermore, FDM is extremely user-friendly with regards to mechanical output and software setup [92]. These factors make the FDM technique perfectly suitable for LMICs.

## B.2. Bond Formation

When using FDM, the final product is the result of many raster layers bonded together (see figure B.2.C. The mechanical properties of the printed product depend on several factors. According to Akhoundi and Behravesh [93] the maximum achievable strength of FDM printed products depends mainly on three factors;

(a) The strength of the used filament

(b) The binding quality between the deposited rasters and layers

(c) The size and population of voids

The mechanical properties of the product at the interference (neck) between the deposited roads is inferior to the properties within the roads [54]. The neck growth between the rasters and layers occurs when the filament is in the semi-melted state, promoted by thermal energy. Bonding occurs through the sintering process, starting with (1) surface contact, (2) neck growth, (3) diffusion of the material at the interface and randomisation. This process is shown in figure B.2.D [55]. The higher the neck growth, the better the binding quality and the lower the density of the voids, which results in higher strength.

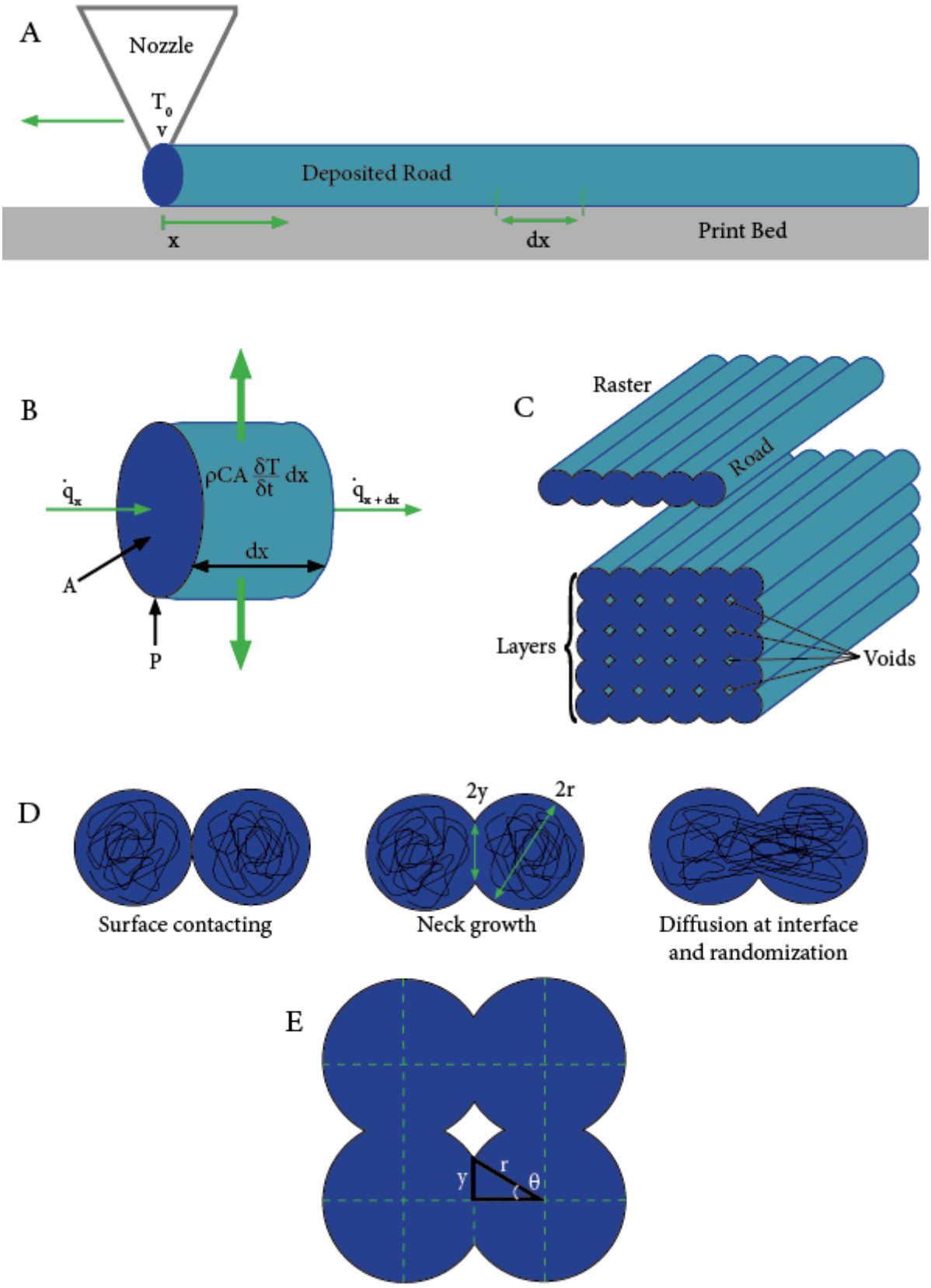


Figure B.2:
A: Schematic review of the deposition of filament by a FDM extrusion head [94]
B: Energy interaction on the finite element dx [94].
C: Structure of FDM printed product [55].
D: Bond formation process between two deposited roads [55].
E: The ratio between neck length and radius of the road [95].

The sintering process depends on the temperature of the material. Therefore, the thermal history of the polymeric raster plays a crucial role in the quality of the bonds. The products temperature history depends on the processing parameters and on the filaments thermal properties [55, 96].

The neck growth over time and temperature can be estimated. First, the temperature in the filament is estimated using the lumped-capacity model [54]. Defining the origin of the coordinate at the nozzle output (figure B.2.A) and assuming that the heat is transferred through conduction trough the filament (k) and convection with the air and conduction with the foundation (h) (figure B.2.B). When assuming (1) uniform temperature distribution across the cross-sectional area of the filament, (2) semi-infinite filament length and (3) constant heat transfer/convection coefficients, it is possible to obtain an energy balance using the law of conservation of energy. [54, 55, 94, 96]

$$\rho c A \frac{dT}{dt} = A \frac{(k \frac{dT}{dx})}{dx} - hP(T - T_\infty) \tag{B.1}$$

With c is the specific heat of the material, A is the cross-sectional area of the filament and P is the perimeter of the filament. Considering the boundary conditions;

$$T = T_N \ \ at\, x = 0 \ \ and\, t \geq 0 \tag{B.2}$$

$$T = T_\infty \ \ at\, x = \infty \ \ and\, t \geq 0 \tag{B.3}$$

And realising;

$$\frac{dT}{dt} = \frac{dT}{dx}\frac{dx}{dt} = \frac{dT}{dx} v \tag{B.4}$$

Enables you to rewrite the equation into;

$$T(t) = T_\infty + (T_N - T_\infty) * exp[\frac{\rho V c}{k} - \sqrt{(\frac{\rho V c}{k})^2 + 4 * \frac{hP}{kA}}] * \frac{vt}{2} \tag{B.5}$$

With $T_\infty$ is the environment temperature and $T_N$ is the extrusion temperature of the nozzle.

Define;

$$m = \frac{\sqrt{1 + 4\alpha\beta} - 1}{2\alpha} \tag{B.6}$$

With;

$$\alpha = \frac{k}{\rho V c} \tag{B.7}$$

and

$$\beta = \frac{hP}{\rho A V c} \tag{B.8}$$

Equation B.5 can be written as;

$$T(t) = T_\infty + (T_N - T_\infty) * e^{-mvt} \tag{B.9}$$

To describe the neck growth, the method described by Gurrala and Regalla [95] is used. When looking at figure B.2.E it can be seen that the half-length of the neck can be described as;

$$y = r sin\theta \tag{B.10}$$

And so

$$\theta = sin^{-1} y/r \tag{B.11}$$

When neck growth between two adjacent roads occurs, the volume does not change and the radius at time t of the roads can be described in terms of $r_0$ and $\theta$;

$$r = \frac{r_0\sqrt{\pi}}{\sqrt{\pi - \theta + sin\theta cos\theta}} \tag{B.12}$$

When necking between the two roads has begun, the net cross-sectional area (S) can be described as;

$$S = 2lr sin\theta \tag{B.13}$$

Next, the work of viscous forces ($W_v$) and work of surface tension ($W_s$) can be described as [95];

$$W_s = -\Gamma \frac{dS}{dt} \tag{B.14}$$

With $\Gamma$ = the surface tension coefficient. Combining and rewriting equations B.12, B.13 and B.14 gives;

$$W_s = \Gamma 2\sqrt{\pi} l r_o \frac{(\pi - \theta)cos\theta + sin\theta}{[(\pi - \theta) + sin\theta cos\theta]^{3/2}} \dot{\theta} \tag{B.15}$$

With;

$$\dot{\theta} = \frac{d\theta}{dt}$$

When it is assumed that the flow of the material between the filaments is a Newton flow, the following equation can be used for $W_v$;

$$W_v = \int\int\int_v 3\eta\dot{\epsilon}^2 dV \tag{B.16}$$

With $\eta$ = viscosity, V = volume and $\dot{\epsilon}$ = strain rate [95]. For $\dot{\epsilon}$ the following equation is used;

$$\dot{\epsilon} = \frac{(\theta - \pi)sin\theta}{[(\pi - \theta) + sin\theta cos\theta]} \tag{B.17}$$

Combining and integrating equations B.16 and B.17 gives;

$$W_v = 6\pi r_0^2 l\eta \frac{(\pi - \theta)^2 sin^2\theta}{[(\pi - \theta) + sin\theta cos\theta]^2} \dot{\theta}^2 \tag{B.18}$$

Assuming that all other forces (like gravity) are negligible, it is assumed that $W_s$ and $W_v$ are equal. Therefore, equations B.15 and B.18 are combined and rewritten, which gives the equation for dimensionless neck growth with time;

$$\dot{\theta} = \frac{d\theta}{dt} = \frac{\Gamma}{3\sqrt{\pi} r_0 \eta} \frac{[(\pi - \theta)cos\theta + sin\theta][(\pi - \theta) + sin\theta cos\theta]^{1/2}}{(\pi - \theta)^2 sin^2\theta} \tag{B.19}$$

As described by Bhalodi et al. [94], $\frac{d\theta}{dt}$ can be rewritten;

$$\frac{d\theta}{dt} = \frac{d\theta}{dT}\frac{dT}{dt} \tag{B.20}$$

Differentiating equation B.9 gives;

$$\frac{dT}{dt} = -m\upsilon(T - T_\infty) \tag{B.21}$$

Combining equations B.20 and B.21 gives [54, 55, 94, 96];

$$\frac{d\theta}{dt} = \frac{d\theta}{dT} * (-m\upsilon(T - T_\infty)) \tag{B.22}$$

Combining and rewriting equations B.19 and B.22 gives the equation for dimensionless neck growth with temperature [94];

$$\frac{d\theta}{dT} = \frac{\Gamma}{3\sqrt{\pi} r_0 \eta m v (T - T_\infty)} \frac{[(\pi-\theta)cos\theta + sin\theta][(\pi-\theta) + sin\theta cos\theta]^{1/2}}{(\pi-\theta)^2 sin^2\theta} \tag{B.23}$$

Equation B.19 gives the equation for dimensionless neck growth with time and equation B.23 gives the equation for dimensionless neck growth with temperature. As visible, the neck growth depends on several material properties such as c, k, $\eta$ etc and on several printer parameters such as $r_0$, v, $T_\infty$ etc.

Sun [97] performed a stress sweep at different frequencies in order to obtain the viscoelastic properties of ABS P400. The values of zero-shear viscosity were estimated by fitting the modified Cross model [98] according to equation B.24 [98];

$$\eta = \frac{\eta_0}{1 + (C\omega)^m} \tag{B.24}$$

The tests results of the viscosity of ABS P400 are shown in table B.1.

Table B.1: Viscosity values for ABS P400 [97]

| Temperature ($^oC$) | $\eta_0$ (Pa.s) | C | m |
|---|---|---|---|
| 200 | 48000 | 1.49 | 0.77 |
| 220 | 14000 | 0.546 | 0.66 |
| 240 | 5100 | 0.158 | 0.73 |

Using equation B.25 for zero shear viscosity was used to fit the data in table B.1.

$$\eta_0 = \eta_{0ref} * e^{-b_0(T - T_{ref})} \tag{B.25}$$

Which resulted in $\eta_{0ref}$ to be 48000 Pa.s, with a corresponding temperature of $T_{ref}$ to be 200 $^oC$ and $b_0$ to be 0.056. Giving the following equation for viscosity;

$$\eta_0 = 48000 * e^{-0.056(T - 200(^oC))} \tag{B.26}$$

Using this equation for viscosity, Sun [97] conducted a sintering neck growth test and fitted the data to equation B.19 to obtain values for the surface tension. The obtained values for surface tension were hereafter fitted to the equation B.27.

$$\Gamma = \Gamma_{ref} + c_{ref} * (T - T_{ref}) \tag{B.27}$$

The test resulted in $\Gamma_{ref}$ to be 0.029 and the constant, $c_{ref}$ to be -0.000345 at a temperature of 240 $^oC$. Which resulted in the following equation for surface tension;

$$\Gamma = 0.029 - 0.000345 * (T - 240) \tag{B.28}$$

# C

# What should be tested?

When testing the manufactured product, it is essential to define what property should be tested. This can vary greatly per manufactured product. A double ended hose connector will be exposed to totally different types and magnitudes of forces than a face shield or a prosthesis.

The to be tested properties of the 3D printed parts depend on the expected forces applied on the printed parts during intended use in combination with the expected frequency at which these forces are applied and the corresponding risk. Also, incorrect usage of the product should be taken into account. While it should be possible to advice/warn the end-user to only use the product as intended, one has to consider the possible risks attached to incorrect usage.

## C.1. Compare with existing products

Since estimating the required mechanical properties for quality assurance might be difficult, one can also compare the product to already existing products. The 3D print lab Kijabe noticed that many hospitals lack spare parts, due to which an entire machine is inoperative. By printing spare parts this problem can be solved. When these printed parts are an alternative for other parts on the market, it is reasonable to assume a reliable manufacturer has already tested similar parts. In this case the 3D print lab can search for the requirements for the mechanical properties the reliable manufacturer uses for the production of the similar parts. If these requirements can be found, the 3D print lab can use these same requirements.

When it is not possible to find the mechanical requirements used by a reliable producer, but the 3D print lab does have some of the parts produced by this manufacturer (or it is easy to gather some of these parts), it is possible to test the mechanical properties of these parts. In this case, the lab first has to define the intended use and possible misuse of the product. Second, the engineers have to estimate due to which force(s) the product is most likely to fail and estimate the corresponding risk. Hereafter, the test can be performed. The force(s) which is(/are) most likely to cause failure is(/are) applied to the parts produced by the other manufacturer upon fealure of the part. The force at which the product failed can be used as a requirement for the newly printed product.

The following flow chart can be used;

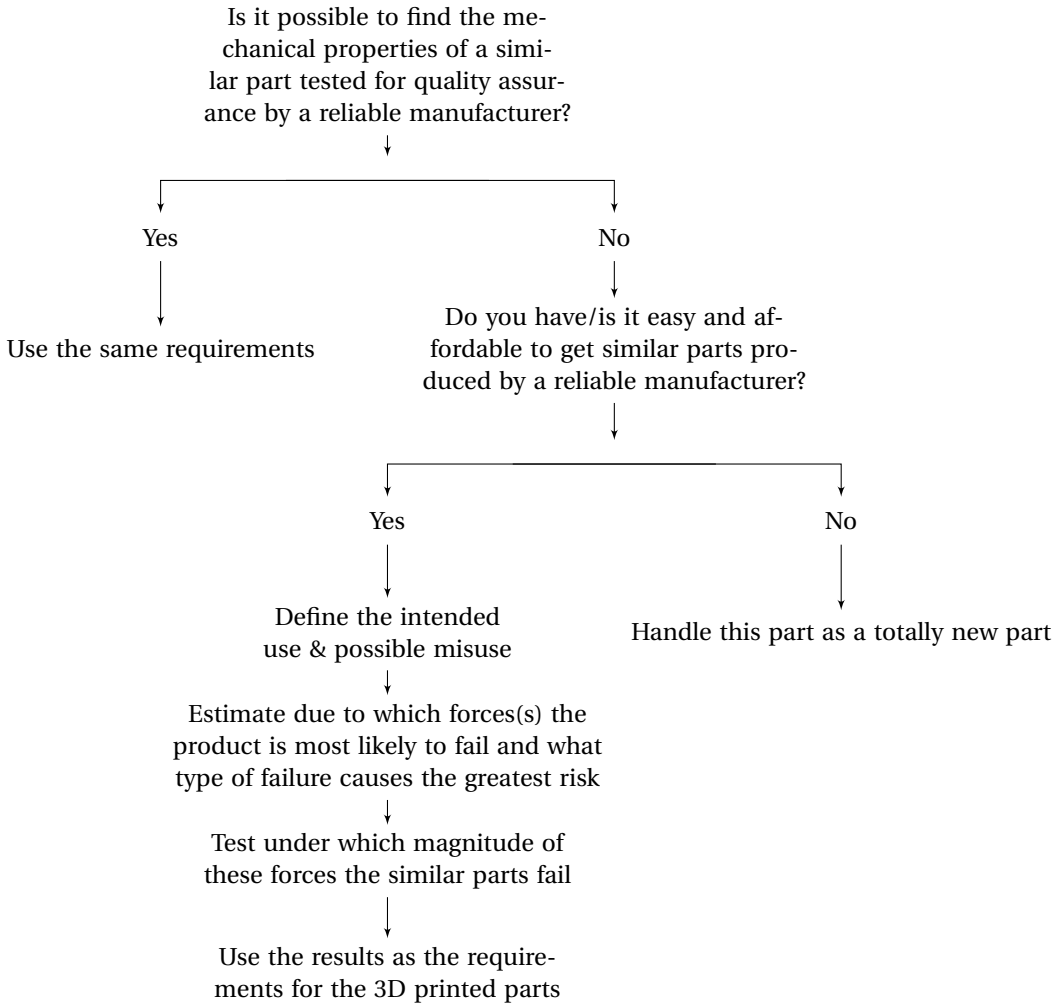


## C.2. New design

When it is not possible to compare the mechanical requirements with similar products produced by a reliable manufacturer, or when the lab creates a totally new device, the 3D print lab has to define the requirements for the mechanical properties itself. This is a difficult task which can be split into several steps.

First of all one has to estimate to what kind of forces the printed product will be exposed during intended usage;

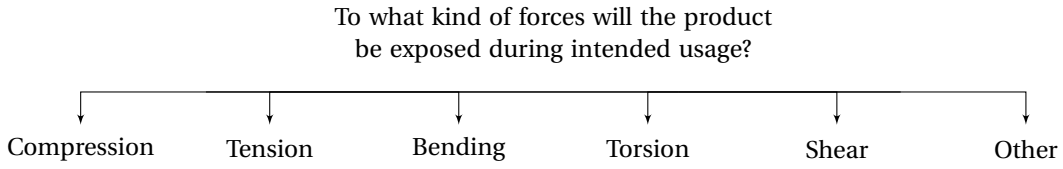

Secondly it is estimated to what kind of forces the printed product will be exposed during wrong usage, this only accounts for wrong usage which is likely to occur or might have a catastrophic impact;

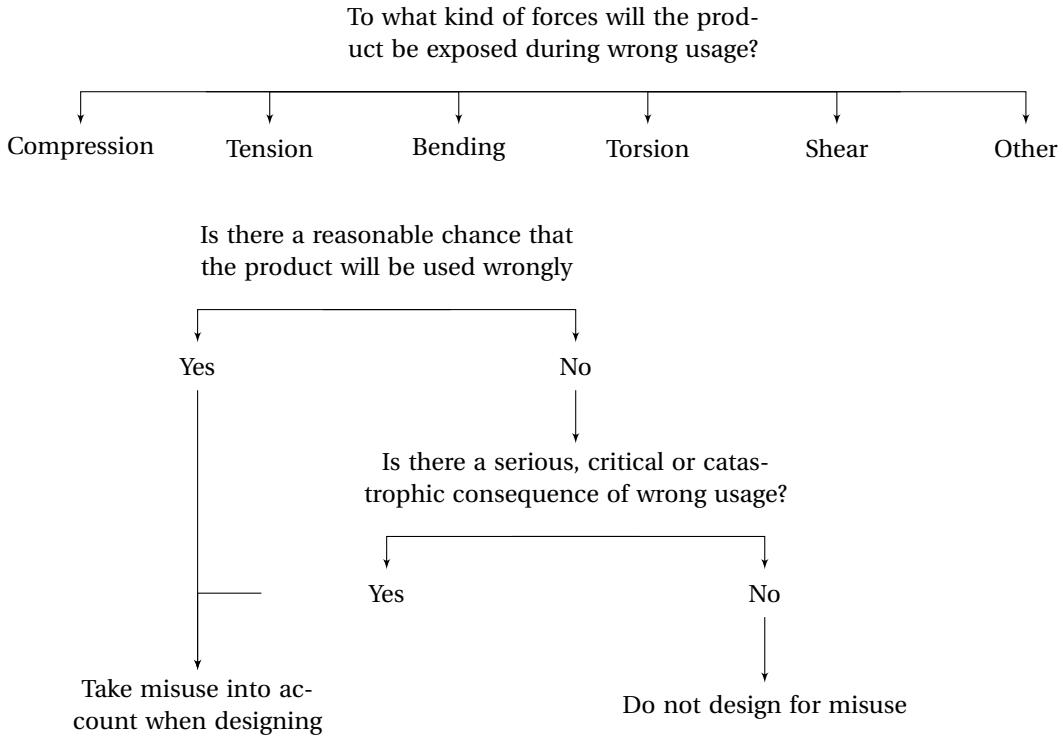


When an estimation of the kind of expected applied forces to the product is made, one has to determine how these forces might cause the product to fail. This depends on the duration at which the force will be applied, the frequency at which the force will be applied and the magnitude of the force. For each expected force, one can ask the following questions;

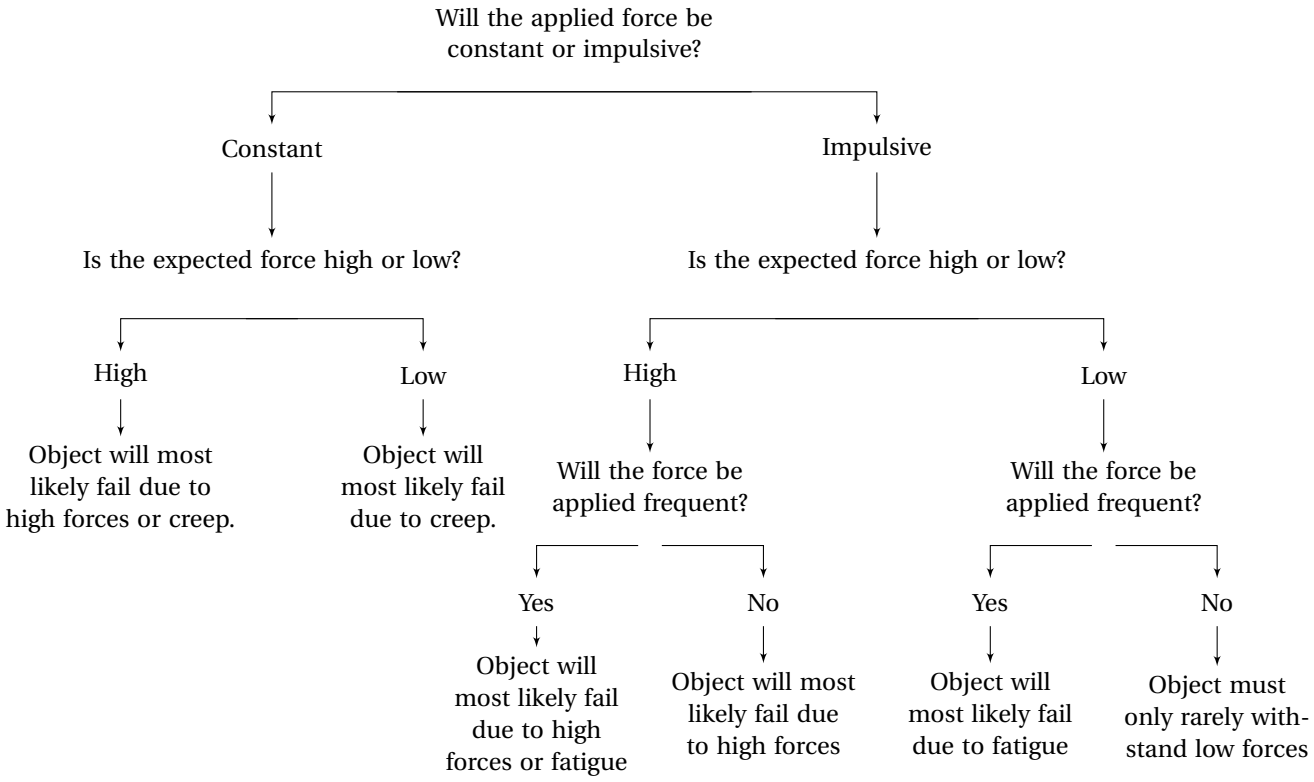


## C.3. Probability and consequences of failure with corresponding risk

When the possible failure modes have been determined, one should estimate the likelihood of the product failing due to these failure modes and the risks attached to these kinds of failure. Therefor, the ISO standard: *ISO 13971 Medical devices — Application of risk management to medical devices* can be used. Both the likelihood of failure and the consequences of this failure are categorized, according to the following classification in table C.1

Table C.1: The likelihood and consequences of failure

| **Probability of Failure** | | **Consequences of Failure** | |
|---|---|---|---|
| Frequent | 1/10 | Catastrophic | Results in patient death. |
| Probable | 1/100 | Critical | Results in permanent impairment or life-threatening injury. |
| Occasional | 1/1000 | Serious | Results in injury or impairment requiring professional medical intervention. |
| Remote | 1/10.000 | Minor | Slight customer inconvenience; little to no effect on product performance, non-vital fault. |
| Improbable | 1/100.000 | Negligible | No or negligible risk to patient or customer. |

Combining the probability of failure with the magnitude of the consequence this failure might cause, will give the risk factor, as shown in table C.2.

Risks have to mitigated in such a way that they can be reduced to a medium risk at maximum. There are three main possibilities to mitigate high risks. Preferable, the design is changed to mitigate the risk. If this is not possible, protective measures in the medical device itself or in the manufacturing process can be used and lastly information can be provided for safety [99].

Table C.2: Risk factor

| | | | | | |
|---|---|---|---|---|---|
| **Frequent** | Medium risk | High risk | High risk | High risk | High risk |
| **Probable** | Medium risk | Medium risk | High risk | High risk | High risk |
| **Occasional** | No risk | Medium risk | Medium risk | High risk | High risk |
| **Remote** | No risk | No risk | Medium risk | Medium risk | High risk |
| **Improbable** | No risk | No risk | No risk | Medium risk | Medium risk |
| | **Negligible** | **Minor** | **Serious** | **Critical** | **Catastrophic** |

- *Adapting the Design*; Changing the design is the most obvious thing to do to reduce risks. When a product is likely to fail due to certain forces, one can reinforce the product to these kind of forces, lowering the probability of failure. However, caution is required. When adapting a design the changes might result in weaknesses in other parts of the design.
- *Protective measures in the medical device itself or in the manufacturing process*; Risks can also be mitigated using protective measures in the medical device itself, such as adding an alarm or visually indicating where the user should apply pressure and where not. Another way is to take protective measures in the manufacturing process, if it is known for example that the print quality worsens when printing under humid conditions, humidity extractor methods can be used to increase print quality.
- *Provide information for safety*; Another way to reduce risk is to apply user instructions, such that the probability of failure will decrease. Giving the end-user specific instructions on how to properly use the product will reduce the risk of failure. It should however be considered how these instructions can be properly communicated to the end-user. While user instructions must always be put on paper, it is uncertain whether the end-user will always read and understand the instructions. Training assures that the user will get the instructions and it gives the end-user the possibility to ask questions straight-away. Therefor, it is preferred to provide training on correct usage next to the written user instructions. If, for some reason, it is not possible to provide training, the likelihood of the end-users carefully reading the user-instructions should be considered. When it is not possible to further adapt the design to reduce the risk, neither to provide user training next to the written user instructions, it should be considered whether this product is the best option for this specific problem. Other products with a similar purpose may be less risky.

# Bibliography


[1] HJ Schindler and M Veidt. Low-cost dynamic tensile testing. *Le Journal de Physique IV*, 4(C8): C8–135, 1994.

[2] JJ Momoh, ONA Ajueyitsi, and AIM Onipede. Tensile and creep testing machine. *J. Eng. Applied Sell*, 3(6):491–495, 2008.

[3] Stefan Hermann. Fully open source universal test machine!, 2019. https://github.com/CNCKitchen/Open-Pull.

[4] John R Amend Jr and Hod Lipson. freeloader: An open source universal testing machine for high-throughput experimentation. In *International Design Engineering Technical Conferences and Computers and Information in Engineering Conference*, volume 54839, pages 685–693, 2011.

[5] Kijenzi. Catalog. https://www.kijenzi.com/catalog/.

[6] Charles N Mock, Peter Donkor, Atul Gawande, Dean T Jamison, Margaret E Kruk, and Haile T Debas. Essential surgery: key messages from disease control priorities. *The Lancet*, 385(9983): 2209–2219, 2015.

[7] Max Roser and Hannah Ritchie. Burden of disease. *Our World in Data*, 2021. https://ourworldindata.org/burden-of-disease.

[8] Renae E Stafford, Catherine A Morrison, Godwin Godfrey, and William Mahalu. Challenges to the provision of emergency services and critical care in resource-constrained settings. *Global heart*, 9 (3):319–323, 2014.

[9] J.G. Meara, A.J. Leather, L. Hagander, B.C. Alkire, N. Alonso, E.A. Ameh, S.W. Bickler, L. Conteh, A.J. Dare, and J. Davies. Global surgery 2030: evidence and solutions for achieving health, welfare, and economic development. *The Lancet*, 386(9993):569–624, 2015.

[10] Haile T Debas, Peter Donkor, Atul Gawande, Dean T Jamison, Margaret E Kruk, and Charles N Mock. *Disease control priorities, (Volume 1): essential surgery*. The World Bank, 2015.

[11] Institute for Health Metrics and Evaluation (IHME). Health service provision in uganda: Assessing facility capacity, costs of care, and patient perspectives, 2014.

[12] World Health Organization et al. Guidelines for health care equipment donations. Technical report, World Health Organization, 1997.

[13] Queeneth Kalu, Teresa Abang Edentekhe, and Stella Eguma. Anesthesia equipment and their chain of survival. 2019.

[14] Peter Howitt, Ara Darzi, Guang-Zhong Yang, Hutan Ashrafian, Rifat Atun, James Barlow, Alex Blakemore, Anthony MJ Bull, Josip Car, Lesong Conteh, et al. Technologies for global health. *The Lancet*, 380(9840):507–535, 2012.

[15] Lora Perry and Robert Malkin. Effectiveness of medical equipment donations to improve health systems: how much medical equipment is broken in the developing world?, 2011.

[16] Karin Diaconu, Yen-Fu Chen, Semira Manaseki-Holland, Carole Cummins, and Richard Lilford. Medical device procurement in low-and middle-income settings: protocol for a systematic review. *Systematic reviews*, 3(1):118, 2014.

[17] Roberto Aufieri, Simonetta Picone, and Piermichele Paolillo. Collaborative development of open source-appropriate technologies: a way to reduce the global access gap? *BMJ Innovations*, 1(2): 37–38, 2015.

[18] The World Bank. Cost to import, border compliance (us$)., 2019. https://data.worldbank.org/.

[19] The World Bank. Cost to import, documentary compliance (us$)., 2019. https://data.worldbank.org/.

[20] The World Bank. Time to import, border compliance (h)., 2019. https://data.worldbank.org/.

[21] The World Bank. Time to import, documentary compliance (h)., 2019. https://data.worldbank.org/.

[22] Thomas Birtchnell and William Hoyle. *3D printing for development in the global south: The 3D4D challenge*. Springer, 2014.

[23] Shayne Kondor, CAPT Gerald Grant, Peter Liacouras, MAJ James R Schmid, LTC Michael Parsons, Vipin K Rastogi, Lisa S Smith, Bill Macy, Brian Sabart, and Christian Macedonia. On demand additive manufacturing of a basic surgical kit. *Journal of Medical Devices*, 7(3):030916, 2013.

[24] Daniel Kats, Lucy Spicher, Ben Savonen, and John Gershenson. Paper 3d printing to supplement rural healthcare supplies—what do healthcare facilities want? In *2018 IEEE Global Humanitarian Technology Conference (GHTC)*, pages 1–8. IEEE, 2018.

[25] World Health Organization. *Medical devices: managing the mismatch: an outcome of the priority medical devices project*. World Health Organization, 2010.

[26] Karin Diaconu, Yen-Fu Chen, Carole Cummins, Gabriela Jimenez Moyao, Semira Manaseki-Holland, and Richard Lilford. Methods for medical device and equipment procurement and prioritization within low-and middle-income countries: findings of a systematic literature review. *Globalization and health*, 13(1):59, 2017.

[27] Helen McGuire and Bernhard H Weigl. Medical devices and diagnostics for cardiovascular diseases in low-resource settings. *Journal of cardiovascular translational research*, 7(8):737–748, 2014.

[28] Silvia Hostettler. *Technologies for development*. Springer, 2015.

[29] Tiffany E Chao, Ketan Sharma, Morgan Mandigo, Lars Hagander, Stephen C Resch, Thomas G Weiser, and John G Meara. Cost-effectiveness of surgery and its policy implications for global health: a systematic review and analysis. *The Lancet Global Health*, 2(6):e334–e345, 2014.

[30] Sujata K Bhatia and Krish W Ramadurai. 3d printing and bio-based materials in global health. *SpringerBriefs in Materials. Google Scholar*, 2017.

[31] Benjamin L Savonen. Criteria for sustainable product design with 3d printing in the developing world. Master's thesis, Michigan Technological University, 2015.

[32] Thomas Campbell, Christopher Williams, Olga Ivanova, and Banning Garrett. Could 3d printing change the world. *Technologies, Potential, and Implications of Additive Manufacturing, Atlantic Council, Washington, DC*, page 3, 2011.

[33] Clara B Aranda-Jan, Santosh Jagtap, and James Moultrie. Towards a framework for holistic contextual design for low-resource settings. *International Journal of Design*, 10(3):43–63, 2016.

[34] Tatjana Leblanc et al. Design vs. re-design and how to innovate. In *11th Engineering and Product Design Education Conference; Creating a better world*, pages 10–11, 2009.

[35] Yutaro Nemoto, Kentaro Uei, Keita Sato, and Yoshiki Shimomura. A context-based requirements analysis method for pss design. *Procedia CIRP*, 30:42–47, 2015.

[36] Pieter Jan Stappers, Paul Hekkert, David Keyson, et al. Design for interaction: consolidating the user-centred focus in industrial design engineering. In *DS 43: Proceedings of E&PDE 2007, the 9th International Conference on Engineering and Product Design Education, University of Northumbria, Newcastle, UK, 13.-14.09. 2007*, pages 69–74, 2007.

[37] Tom Oluoch, Xenophon Santas, Daniel Kwaro, Martin Were, Paul Biondich, Christopher Bailey, Ameen Abu-Hanna, and Nicolette de Keizer. The effect of electronic medical record-based clinical decision support on hiv care in resource-constrained settings: a systematic review. *International journal of medical informatics*, 81(10):e83–e92, 2012.

[38] Laaria Mingaine. Skill challenges in adoption and use of ict in public secondary schools, kenya. *International Journal of Humanities and Social Science*, 3(13):61–72, 2013.

[39] Ludo Hille Ris Lambers. Design of a 3d printer for healthcare in sub-saharan africa, 2019.

[40] Cecilia M Briceño-Garmendia and Maria Shkaratan. *Kenya's infrastructure: A continental perspective*. The World Bank, 2011.

[41] Ombara Isaac. Transport infrastructure development in kenya: How connectivity impacts eastern africa regional integration. *Insight on Africa*, 11(2):200–218, 2019.

[42] Hugh Lamarque. Profitable inefficiency: the politics of port infrastructure in mombasa, kenya. *The Journal of Modern African Studies*, 57(1):85–109, 2019.

[43] Adam Jaworski and Crispin Thurlow. The (de-) centering spaces of airports: Framing mobility and multilingualism. *Multilingualism and the periphery*, 154:198, 2013.

[44] Wanjiku Gacuru and K Kabare. Factors affecting efficiency in logistics performance of trading and distribution firms based in jomo kenyatta international airport area. *International Academic Journal of Procurement and Supply Chain Management*, 1(5):50–71, 2015.

[45] Ismail M Mohammad. *Challenges of Strategy Implementation of Cargo Companies Operating at Jomo Kenyatta International Airport, Nairobi Kenya*. PhD thesis, University of Nairobi, 2017.

[46] Bonnyventure SARONGE. *A comparative analysis of vehicle traffic flow at Jomo Kenyatta and Julius Nyerere international airport*. PhD thesis, Maseno University, 2017.

[47] The World Bank. Access to electricity (% of population)., 2018. https://data.worldbank.org/.

[48] The World Bank. Access to electricity, rural (% of rural population))., 2018. https://data.worldbank.org/.

[49] Jay Taneja. Measuring electricity reliability in kenya. *STIMA Lab, Department of Electrical and Computer Engineering*, pages 1–6, 2017.

[50] Rabin Craig. 6 best apps to master 3d printing with your smartphone, 2015. https://www.business2community.com/mobile-apps/6-best-apps-master-3d-printing-smartphone-01308428.

[51] Darren Allan. This free 3d printer is powered by your smartphone – but it comes with a big caveat, 2020. https://www.techradar.com/news/this-free-3d-printer-is-powered-by-your-smartphone-but-it-comes-with-a-big-caveat.

[52] Mghiar. 3d printing from phones without using computer, 2018. https://www.instructables.com/.

[53] Hans Erik Grøthaug. A software roadmap for the fab lab network. *KTH Computer Science and Communications, Rpyal Institute of Technology, Stockholm, Sweden*, 2011.

[54] Longmei Li, Qian Sun, Celine Bellehumeur, and Peihua Gu. Investigation of bond formation in fdm process. *Solid Freeform Fabrication Proceedings,(403)*, 400407, 2002.

[55] Céline Bellehumeur, Longmei Li, Qian Sun, and Peihua Gu. Modeling of bond formation between polymer filaments in the fused deposition modeling process. *Journal of Manufacturing Processes*, 6(2):170–178, 2004.

[56] Muhammad Harris, Johan Potgieter, Richard Archer, and Khalid Mahmood Arif. In-process thermal treatment of polylactic acid in fused deposition modelling. *Materials and Manufacturing Processes*, 34(6):701–713, 2019.

[57] Biranchi N Panda, K Shankhwar, Akhil Garg, and Zhang Jian. Performance evaluation of warping characteristic of fused deposition modelling process. *The International Journal of Advanced Manufacturing Technology*, 88(5-8):1799–1811, 2017.

[58] Tian-Ming Wang, Jun-Tong Xi, and Ye Jin. A model research for prototype warp deformation in the fdm process. *The International Journal of Advanced Manufacturing Technology*, 33(11-12): 1087–1096, 2007.

[59] Climate in ..., kenya, 2019. https://weather-and-climate.com.

[60] Kenya climate, 2019. https://en.climate-data.org/africa/kenya-124/.

[61] The World Bank. Gpd per capita (current us$), 2019. https://data.worldbank.org/.

[62] The World Bank. Poverty headcount ratio at national poverty lines (% of population), 2015. https://data.worldbank.org/.

[63] Ministry of Health. Public health expenditure in kenya. a comparative analysis of nine deep-dive counties, 2019.

[64] Elvis OA Wambiya, Peter O Otieno, Martin Kavao Mutua, Hermann Pythagore Pierre Donfouet, and Shukri F Mohamed. Patterns and predictors of private and public health care utilization among residents of an informal settlement in nairobi, kenya: a cross-sectional study. *BMC Public Health*, 21(1):1–11, 2021.

[65] Fablabs. Fablab nairobi. https://www.fablabs.io/labs/fablabnairobi.

[66] Ishita Kapoor. Liquid penetrant testing – advantages, disadvantages alternatives, 2019. https://ircengg.com/liquid-penetrant-testing/.

[67] Ajay Kapadia. Non destructive testing of composite materials. *National Composites Network*, pages 1–4, 2007.

[68] Composites World. Low-cost ultrasonic ndt method yields real-time results., 2008. https://www.compositesworld.com/.

[69] S Gholizadeh. A review of non-destructive testing methods of composite materials. *Procedia Structural Integrity*, 1:50–57, 2016.

[70] Sandeep Kumar Dwivedi, Manish Vishwakarma, and Akhilesh Soni. Advances and researches on non destructive testing: A review. *Materials Today: Proceedings*, 5(2):3690–3698, 2018.

[71] Claudia Barile, Caterina Casavola, and Alberto Cazzato. Acoustic emissions in 3d printed parts under mode i delamination test. *Materials*, 11(9):1760, 2018.

[72] T Zappia. Inspection and quality control in friction stir welding. In *Friction Stir Welding*, pages 183–212. Elsevier, 2010.

[73] YY Hung, Yun Shen Chen, SP Ng, L Liu, YH Huang, BL Luk, RWL Ip, CML Wu, and PS Chung. Review and comparison of shearography and active thermography for nondestructive evaluation. *Materials Science and Engineering: R: Reports*, 64(5-6):73–112, 2009.

[74] NDTS. Magnetic flux leakage testing. https://www.ndts.co.in/magnetic-flux-leakage-testing/.

[75] Sung-Hoon Ahn, Michael Montero, Dan Odell, Shad Roundy, and Paul K Wright. Anisotropic material properties of fused deposition modeling abs. *Rapid prototyping journal*, 8(4):248–257, 2002.

[76] Ana Pilar Valerga, Moisés Batista, Jorge Salguero, and Frank Girot. Influence of pla filament conditions on characteristics of fdm parts. *Materials*, 11(8):1322, 2018.

[77] Paolo Blasi, Susan S D'Souza, Francesca Selmin, and Patrick P DeLuca. Plasticizing effect of water on poly (lactide-co-glycolide). *Journal of Controlled Release*, 108(1):1–9, 2005.

[78] Gregory L Baker, Erin B Vogel, and Milton R Smith III. Glass transitions in polylactides. *Polymer Reviews*, 48(1):64–84, 2008.

[79] N Passerini and DQM Craig. An investigation into the effects of residual water on the glass transition temperature of polylactide microspheres using modulated temperature dsc. *Journal of Controlled Release*, 73(1):111–115, 2001.

[80] Mehlika Karamanlioglu and Umit Alkan. Influence of time and room temperature on mechanical and thermal degradation of poly (lactic) acid. *Thermal Science*, 23(Suppl. 1):383–390, 2019.

[81] Alain Copinet, Celine Bertrand, Stephanie Govindin, Veronique Coma, and Yves Couturier. Effects of ultraviolet light (315 nm), temperature and relative humidity on the degradation of polylactic acid plastic films. *Chemosphere*, 55(5):763–773, 2004.

[82] Humidity... a silent killer of pla 3d printer filament, 2019. https://www.filamently.com/blogs/all-blogs/humidity-a-silent-killer-of-pla-3d-printer-filament.

[83] Combating 3d printing problems: An ultimate troubleshooting guide. https://apm-designs.com/combating-the-most-common-3d-printing-problems-a-troubleshooting-guide/.

[84] 3dprinting. How do i know when filament is getting old, and what things can i do to correct for it?, 2018. https://3dprinting.stackexchange.com/questions/6784/how-do-i-know-when-filament-is-getting-old-and-what-things-can-i-do-to-correct.

[85] STANDARD PRINT CO. *PLA Printing Guide*, 2020. www.standardprintco.com.

[86] Symptoms of moisture saturated pla?, 2016. https://www.reddit.com/r/3Dprinting/.

[87] Anton Månsson. How moist filaments will screw up your 3d-printing, 2016. https://3dprinterchat.com/how-moist-filaments-will-screw-up-your-3d-printing/.

[88] Manfred Gordon and James S Taylor. Ideal copolymers and the second-order transitions of synthetic rubbers. i. non-crystalline copolymers. *Journal of Applied Chemistry*, 2(9):493–500, 1952.

[89] Ludmila Novakova-Marcincinova and Ivan Kuric. Basic and advanced materials for fused deposition modeling rapid prototyping technology. *Manuf. and Ind. Eng*, 11(1):24–27, 2012.

[90] Ian Gibson, David W Rosen, Brent Stucker, et al. *Additive manufacturing technologies*, volume 17. Springer, 2014.

[91] Ala Qattawi et al. Investigating the effect of fused deposition modeling processing parameters using taguchi design of experiment method. *Journal of Manufacturing Processes*, 36:164–174, 2018.

[92] Rhys Jones, Patrick Haufe, Edward Sells, Pejman Iravani, Vik Olliver, Chris Palmer, and Adrian Bowyer. Reprap–the replicating rapid prototyper. *Robotica*, 29(1):177–191, 2011.

[93] B Akhoundi and AH Behravesh. Effect of filling pattern on the tensile and flexural mechanical properties of fdm 3d printed products. *Experimental Mechanics*, pages 1–15, 2019.

[94] Deep Bhalodi, Karan Zalavadiya, and Pavan Kumar Gurrala. Influence of temperature on polymer parts manufactured by fused deposition modeling process. *Journal of the Brazilian Society of Mechanical Sciences and Engineering*, 41(3):113, 2019.

[95] Pavan Kumar Gurrala and Srinivasa Prakash Regalla. Part strength evolution with bonding between filaments in fused deposition modelling: This paper studies how coalescence of filaments contributes to the strength of final fdm part. *Virtual and Physical Prototyping*, 9(3):141–149, 2014.

[96] Longmei Li. *Analysis and fabrication of FDM prototypes with locally controlled properties*. PhD thesis, University of Calgary, 2004.

[97] Qian Sun. Bond formation between polymer filaments in fused deposition modeling process. Master's thesis, University of Calgary, 2005.

[98] Malcolm M Cross. Polymer rheology: influence of molecular weight and polydispersity. *Journal of Applied Polymer Science*, 13(4):765–774, 1969.

[99] Derek Flood, Fergal McCaffery, Valentine Casey, Ruth McKeever, and Peter Rust. A roadmap to iso 14971 implementation. *Journal of Software: Evolution and Process*, 27(5):319–336, 2015.